Agent-Based Optimal Energy Management for Distribution Grids with Industrial and Residential Flexibility

a thesis approved for the academic degree of

Doktor der Ingenieurwissenschaften (Dr.-Ing.)

at the

Faculty of Electrical Engineering and Information Technology
TU Dortmund University

by

Debopama Sen Sarma, M. Sc.

Supervisor:	Prof. Dr.-Ing. Christian Rehtanz
Co-Advisor:	Prof. Dr. Matti Lehtonen

Day of Oral Examination: 20. 11. 2024

Abstract

The ongoing energy transition has led to a paradigm shift in distribution power systems infrastructure and operations owing to the ever-increasing volume of intermittent renewable energy generation and electricity consumption across several recently developed sectors. Integrating previously separated energy sectors and electricity market liberalization transforms the distribution system environment into a complex system that includes several participants with conflicting interests. Therefore, innovative approaches to optimal and efficient energy management of available resources are paramount to achieving sustainability goals through economic, environmental, social, and technical factors. One way to test the feasibility and robustness of such new and improved solutions is through power system modeling and simulation.

This dissertation presents an agent-based hierarchical energy management architecture that draws from research and practically applies to the liberalized electricity market. The architecture is designed to solve a multi-objective optimization routine for distribution grid operation in a distributed way. An online feedback mechanism is a vital feature of the optimization algorithm, which is solved in collaboration with the agents representing the various participants in a distribution grid ecosystem. The distributed nature of computation ensures data privacy, as sensitive information is not shared with a central coordinator. A unique combination of Tchebycheff's decomposition and the Gradient projection method is used to solve the constrained and multi-objective optimal power flow problem. Adding penalty functions to the objective function effectively handles the system constraints. The formulation of industrial and residential demand profiles incorporates socio-behavioral aspects of the connected prosumers, reflecting their economic, behavioral, or environmental goals. The energy management architecture and its optimization function are then applied in a co-simulation framework to study the impact of industrial and residential flexibility on the connected distribution grid's economic, environmental, and technical aspects. The energy management architecture seamlessly integrates into the co-simulation framework with the help of a co-simulation platform, *mosaik*, that facilitates communication between various multi-disciplinary models. A preexisting agent-based grid simulation model, SIMONA, represents the distribution grid, calculating grid power flow and resulting system gradients. The results provide valuable indicators for distribution grid planning and operation under future renewable generation and flexible load integration scenarios.

Kurzfassung

Die Energiewende führt zu einem Paradigmenwechsel in Bezug auf die Infrastruktur der Verteilnetze und deren Betrieb, da sowohl die Stromerzeugung aus erneuerbaren Energien als auch der Stromverbrauch der neu entwickelten Sektoren zunehmen. Die Integration von zuvor getrennten Sektoren und die Liberalisierung des Strommarktes wandeln das Umfeld der Verteilnetze in ein komplexes System, das mehrere Teilnehmer mit gegensätzlichen Interessen umfasst. Daher sind innovative Ansätze für ein optimales und effizientes Management der verfügbaren Ressourcen von entscheidender Bedeutung, um die Nachhaltigkeitsziele über wirtschaftliche, ökologische, soziale und technische Einflussmöglichkeiten zu erreichen. Eine Möglichkeit, die Machbarkeit und Robustheit neuer und verbesserter Lösungen zu testen, ist die Modellierung und Simulation von Energiesystemen.

In dieser Dissertation wird eine agentenbasierte hierarchische Energiemanagementarchitektur vorgestellt, die aus der Forschung stammt und in der Praxis anwendbar ist. Die Architektur löst eine multikriterielle Optimierungsroutine auf dezentralisierte Weise. Ein Online-Feedback-Mechanismus findet die optimale Lösung in Zusammenarbeit mit den Agenten, welche die verschiedenen Teilnehmer in einem Verteilnetz-Ökosystem repräsentieren. Der verteilte Charakter der Berechnungen gewährleistet den Datenschutz, da sensible Informationen nicht an einen zentralen Koordinator weitergegeben werden. Eine einzigartige Kombination aus Tchebycheff-Dekomposition und der Gradientenprojektion wird verwendet, um das eingeschränkte und multikriterielle Problem des optimalen Energieflusses zu lösen. Die Formulierung von Lastprofilen für Industrie und privathaushalte berücksichtigt sozio-technische Aspekte der angeschlossenen Prosumer und reflektiert deren wirtschaftliche, soziale oder ökologische Ziele. Die Energiemanagementarchitektur wird dann in einem Co-Simulations-Framework angewendet, um die Auswirkungen der Flexibilität von Industrie und Haushalten auf die wirtschaftlichen, ökologischen und technischen Aspekte des angeschlossenen Verteilnetzes zu untersuchen. Die Energiemanagementarchitektur fügt sich mit Hilfe einer Co-Simulationsplattform, *mosaik*, die die Kommunikation zwischen verschiedenen multidisziplinären Modellen erleichtert, nahtlos in das Co-Simulation-Framework ein. Ein bereits vorhandenes agentenbasiertes Netzsimulationsmodell, SIMONA, stellt das Verteilnetz dar und berechnet den Netzleistungsfluss und die daraus resultierenden Systemgradienten. Die Ergebnisse liefern wertvolle Indikatoren für die Planung und den Betrieb von Verteilnetzen unter zukünftigen Szenarien der erneuerbaren Erzeugung und der flexiblen Lastintegration.

Acknowledgement

This thesis results from research activities conducted during my time as a research associate at the Institute of Energy Systems, Energy Efficiency and Energy Economics (ie^3) at TU Dortmund University.

I want to express my deepest gratitude to my supervisor, Univ.-Prof. Dr.-Ing. habil. Christian Rehtanz, for his support during my term as a scientific employee at the institute. He was always available to provide constructive feedback and a critical outlook on intermediate and final progress, questions, and results. I thank him for his trust in my vision and the freedom he granted me to continue working on the topic.

I am deeply grateful to Prof. Dr. Matti Lehtonen for his willingness to serve as my co-advisor and for allowing me to conduct a research stay at the esteemed Department of Electrical Engineering and Automation, Aalto University. This experience was invaluable, and his team, including Püvi Verner, Samar Fatima, and Ilkka Jokinen, played a crucial role in enhancing the quality of this thesis.

I also sincerely thank my peers and superiors who cooperated to make the MoMeEnT project successful. I am exceedingly obliged to Tom Warendorf and Matteo Barsanti for the favorable discussions and output on integrating the prosumer side into the energy management architecture.

Thanks to my colleagues at ie^3 for the pleasant work atmosphere and great moments during various workshops, seminars, and coffee room discussions. The SIMONA team members have been incredibly supportive in brainstorming and implementing challenging ideas.

I want to thank everyone who worked through this manuscript and made valuable contributions to its improvement.

Lastly, I want to express my gratitude to my parents and husband for their constant encouragement and support from conception to the delivery of my dissertation.

"All our knowledge begins with the senses, proceeds then to the understanding, and ends with reason. There is nothing higher than reason." - Immanuel Kant

Contents

1 Introduction

1.1 Motivation and Research Question

The energy transition aims to realize a secure and sustainable electricity supply while restricting the global temperature increase to 1.5°C from pre-industrial levels [1]. Realizing a sustainable supply involves adapting diverse and global transformation avenues in the power system supply chain. Increasing penetration of renewable sources, such as hydropower, solar, wind, and biothermal, in the supply mix combined with the electrification of newly identified sectors; heat, gas, and mobility are the key drivers of the energy transition. Advancements in storage technologies are making it a dependable answer to the intermittent renewable generation problem [2]. Integrating these new elements into the power system infrastructure permanently changes the structure of energy supply, demand, and prices. Increasing energy efficiency is significant following the expansion of renewable energies and controllable loads. Possible solutions range from modernization of power systems, energy-saving industrial processes, energy-efficient buildings, and household technologies [3]. *Distributed Energy Resources* (DER) umbrella term encompasses these contemporary participants in the holistic power system environment. Owing to the geographic dispersion of DERs, they promote traditionally passive distribution networks into active participants that can support bidirectional power flow. Figure 1.1 demonstrates the change in the distribution system structure to accommodate new efficient and ecological technologies.

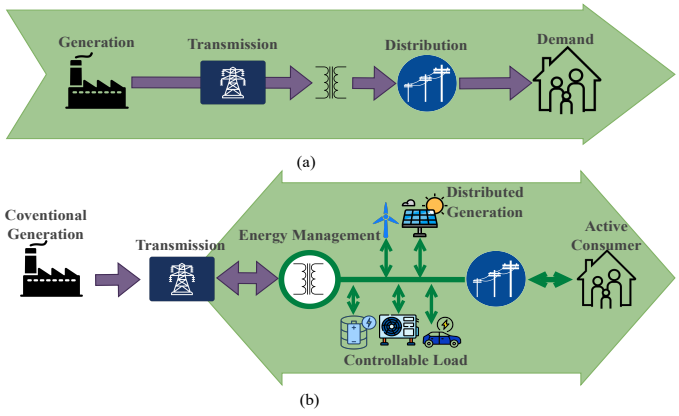

Figure 1.1: (a) Traditional Passive Distribution Network; (b) Modern Active Distribution Network [4]

Distribution Grid Energy Management

As seen in Figure 1.1, the modern distribution grid is connected to *distributed generation* (DG) units in the form of wind and solar, responsive load, such as charging stations for electric vehicles and storage technologies, and end users who are associated with energy-intensive processes, rooftop *photovoltaic* (PV) installations, electric heat pumps and so on [5]. DERs can also represent units participating in energy-efficient or demand-side programs. The integration of DERs poses several challenges to distribution grid planning and operation. Under scenarios of unplanned operation, the distribution network might witness congestion, voltage overloads, reverse power flow, failure of protective equipment, and increased investments in grid expansion measures. Therefore, intelligent management techniques should be included to monitor, control, and optimize the available resources while respecting system constraints. On the other hand, consumers adopting sustainable technologies should see a return on their investment in terms of economic or energy-saving benefits. Therefore, an energy management solution aims to benefit all involved participants in a distribution grid ecosystem.

The IEEE Standard Association coined a blanket term *Distributed Energy Resources Management Systems* (DERMS) to define the scope and application for such energy management software solutions for distribution grids [6]. The idea is to modularize the scope of intelligent management techniques to target specific goals. The essential functions of a DERMS are categorized into:

- **Aggregate**: Bundle smaller DERs, i.e., DGs and *demand response* (DR) participants, and present them as manageable profiles to the electricity market or the *distribution system operator* (DSO).
- **Simplify**: Control granular details for the distributed components and provide easily quantifiable grid-related services.
- **Optimize**: Compute optimal control signals for connected DG units and prosumers to produce the desired output, namely minimal operational costs and optimal power quality.
- **Translate**: Individual participants may speak different languages according to their time resolution and scale. Thus, a DERMS should enable cohesive and compatible communication between all components.

Regarding aggregation and optimization, DERMS solutions can be categorized into DER aggregators or utility DERMS, commonly operated by the DSO [7]. A DER

aggregator bundles smaller DG units or controllable loads such as charging stations, storage facilities, and heat pumps to optimally manage their operation and participate in energy-saving schemes, provision of ancillary services, and market trading. A utility DERMS uses the DER aggregators, among other resources, to manage the connected DER units efficiently while respecting the technical constraints of the network related to operational voltage limits and power balance. The utility DERMS can also optimize distribution grid operation by controlling the available resources to reduce operational costs, address congestion issues, and improve voltage profiles.

Consequently, DER aggregators and utility DERMS exist hierarchically, where DER aggregators are unaware of the grid model and utility DERMS are grid-aware. Therefore, if these two solutions are properly integrated, they can provide efficient customer and grid-related services in the liberalized electricity market at the distribution grid level. Several players' involvement, roles, and responsibilities in the electricity market and economic, environmental, social, and technical goals make the modern distribution grid ecosystem a highly complex model to render.

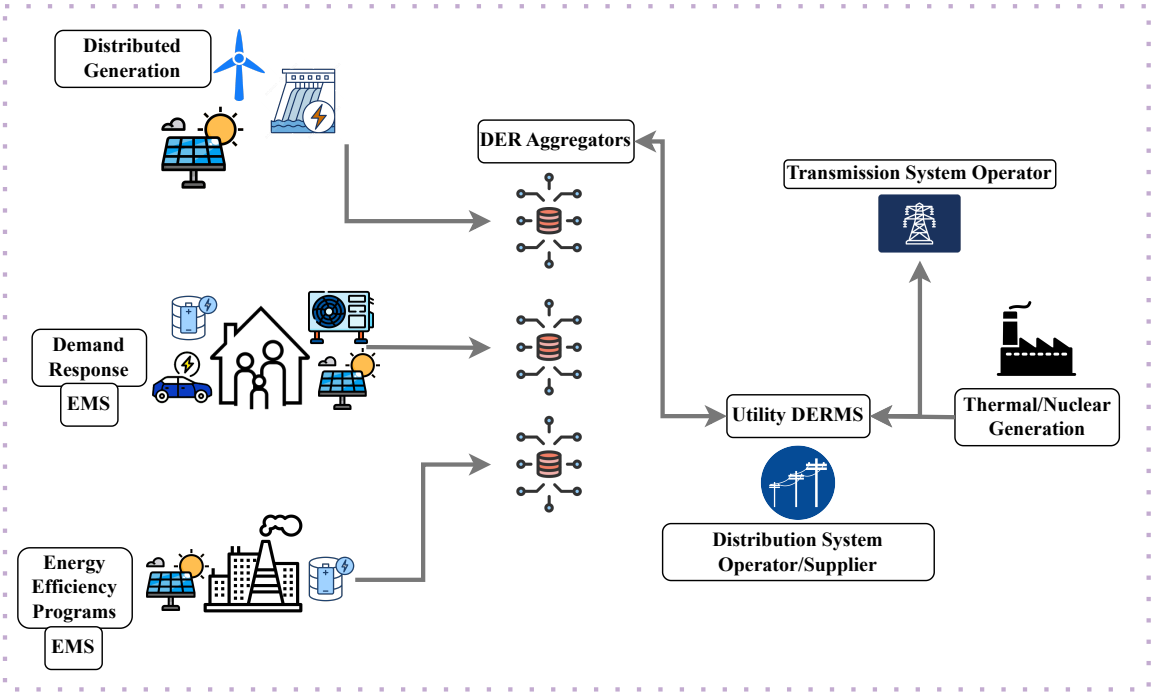

Figure 1.2: Future Energy Management Systems [8]

The term *Energy Management System* (EMS) encompasses all solutions for efficiently managing distributed resources following grid-aware, customer-favoring, or market-

aware schemes. Therefore, both DER aggregators and utility DERMS provide energy management solutions. The differences lie in EMS objectives, the surrounding environment, and specific monitoring and control tasks. Figure 1.2 shows the envisioned architecture of an EMS in a future smart grid environment connected to smart homes, innovative industries, and several DERs, which can be sources of generation or responsive load. Although the full impact of this development is yet to be foreseeable today, it raises many important questions. For example, how can one design and integrate a large number of complex technical systems into existing frameworks and regulatory structures? What essential considerations help define communication channels and data interaction protocols between participants? How do increasing electrification and active consumers in industrial and residential sectors impact distribution grid objectives and parameters? How significant is the impact of human behavior and government regulations in adopting and operating advanced technologies? To operate a secure and sustainable distribution system, one must analyze control options available to the DSO to be minimally invasive yet efficient. Moreover, translating software solutions in the field requires investments in improving the infrastructure with metering and measurement devices capable of communication. The *Information and Communication Technologies* (ICT) prerequisites and associated costs to implement an EMS within the distribution system environment are also essential.

Note: This thesis uses the inclusive term energy management to describe the proposed solution, even though the EMS model executes tasks of a DERMS by combining the functionalities of a DER aggregator and a utility DERMS. The specific name depends on the regulatory roles of an aggregator and the DSO when applied to a specific real-world market scenario.

Paragraph 14a EnWG

Highlighting the importance of incorporating these resources, the German government introduced Paragraph 14a in their Energy Industry Act (EnWG) [9], which came into force in the year 2024. In this act, the government policy allows the grid operators to issue emergency control over flexible energy-consuming assets such as heat pumps, batteries, etc., and reduce their output to avoid overloading while offering relaxations in grid fees to the targeted consumer. Another benefit of this policy is that it avoids delays in approving connection requests for controllable assets into the grid due to insufficient grid capacity [10]. Thus, with government regulations imposing a mandate on increasing power demand, especially in low-voltage distribution grids, through new

connections, finding solutions to optimally manage the available resources without breaking the security of supply has become imperative in power systems research.

Research Question

In academic and industrial research, modeling and simulation are powerful methods for designing and evaluating complex systems and processes [11]. Recent developments in the distribution grid environment have facilitated the necessity to model the holistic system with accurate, granular details of all its participants and evaluate their impact on grid performance's economic, environmental, and technical parameters. It is essential to produce grid-aware solutions to reach climate change goals effectively. The electricity grid model should encompass the laws of physics that drive the network such that the solutions respect physical and operational constraints on the distribution grid. The variation in these parameters under specific integration scenarios helps in several application cases, such as determining the grid's hosting capacity, constraint management, voltage regulation, demand forecasting, and participation in customer-related services in the electricity market.

To this purpose, the development of versatile energy management models that can perform one or more tasks from aggregation, simplification, optimization, and translation is requisite. The software solution can target individual smart homes, industries, DG groups, aggregators, or the utility grid. The energy management model should tackle an influx of renewable generation and flexible load profiles from various categories of end users, where the modeling of end users is realistic and considers their socio-behavioral aspects. Consideration of socio-behavioral aspects of end users helps improve the designing of efficient and non-invasive incentive mechanisms for future smart grids. The final output of the model should be optimal operating points for all involved participants that ensure sustained and cost-efficient electricity supply without harming the environment. Therefore, the main research question this thesis attempts to solve is:

Research Question

How do we design and model an energy management architecture for low/medium-voltage distribution grids that can optimally address the grid's economic, environmental, and technical aspects under intensive electrification and flexibility practices by industrial and residential consumers?

1.2 Thesis Outline

This section outlines the upcoming chapters in this thesis, highlighting the contributions.

Chapter 2 - Research Trends in Energy Management and Optimization Methods

Chapter 2 presents a comprehensive literature review of energy management and optimization research trends in distribution grids, focusing on the multifaceted elements addressed by energy management systems and the fundamental characteristics expected of an EMS. It is essential to ascertain the implementation technique of proposed solutions and their advantages and disadvantages. The second half of the chapter carefully examines the evolving landscape of distributed grid optimization, offering insights into emerging technologies and methodologies. It briefly reviews existing methods to solve multi-objective and distributed optimal power flow problems to justify the selection of the solution algorithm. Furthermore, it highlights the contributions of the thesis within the context of available literature, clarifying the rationale behind the proposed solution architecture and algorithm selection. Through an in-depth examination of existing literature and ongoing research, this chapter lays the groundwork for the subsequent chapters, providing a solid foundation for the study's contributions and methodologies.

Chapter 3 - Agent-Based Energy Management Architecture

Chapter 3 introduces this thesis's proposed agent-based energy management architecture. It begins by explaining the fundamental concepts of the liberalized electricity market in Germany. The suitability of agent-based modeling and the practical applicability of the proposed model are established after identifying the essential players and their specific roles and responsibilities in a real-world electricity market example. It describes the core concepts of multi-agent systems and discusses the advantages and limitations of employing agent-based simulation techniques. Furthermore, the chapter provides a comprehensive overview of the SIMONA ecosystem, the grid simulation platform that furnishes agents for the distribution grid operator and distributed wind and solar generation units. After applying the optimization algorithm's solution, SIMONA calculates power flow to assess the grid state. Within a co-simulation

environment, the energy management agents and SIMONA interact alongside various multi-agent systems representing industrial and residential prosumers and governance regulations, among other factors. The development of this co-simulation environment was supported by the *DeutscheForschungsgemeinschaft* (DFG) under the MoMeEnT[1] project in collaboration with other project members. The chapter further details the utilization of daily demand profiles from short-term socio-technical models for industrial (*alien*) and residential (*demod*) prosumers, developed by Tom Warendorf and Matteo Barsanti, respectively. It briefly explains the modeling techniques employed in these systems to derive final load profiles, while the co-simulation software, *mosaik*, facilitates communication among the various multi-agent systems. The contributions of this thesis to the energy management architecture encompass:

- a hierarchical energy management architecture enabling distributed grid operational optimization that integrates the properties of a DER aggregator and a utility DERMS,
- a closed-loop feedback interaction between the energy management model and the distribution grid to solve the optimization problem,
- applying the developed architecture in a co-simulation framework, i.e., connecting SIMONA, the energy management model, and the prosumer agents using the co-simulation platform *mosaik* via software *application program interfaces* (API)s and
- design and conception of two application case studies with industrial and residential prosumers considering their socio-technical behavior.

Chapter 4 - Multi-Objective Distributed Optimal Power Flow

Chapter 4 delves into the intricate mathematical implementation of a *multi-objective distributed optimal power flow* (MO-DOPF) algorithm designed to address multiple grid-oriented objectives about economic, environmental, and technical aspects. This chapter focuses on developing a novel two-fold approach, combining Tchebycheff's decomposition method with a distributed *online* Gradient projection algorithm. It explores the theoretical underpinnings of both methods, highlighting their respective strengths and applicability to the problem. Furthermore, it explains the complexities

[1] https://gepris.dfg.de/gepris/projekt/409620273

of adapting these methods to the distributed nature of power flow optimization, emphasizing the need for efficient coordination and communication among distributed agents. The chapter presents mathematical formulations and algorithmic procedures, providing a detailed roadmap for the implementation process. The contributions of this thesis are:

- a distributed solution to the multi-objective problem in an agent-based energy management architecture,
- application to arbitrary grid topologies using two alternative gradient computation methods,
- consideration of an operational curtailment penalty to the grid operator under renewable generation curtailment and
- addition of reference node generation limits to operational constraints for the distribution grid to prevent power flow failures.

Chapter 5 - Performance Evaluation and Application

Chapter 5 evaluates the performance of the proposed gradient projection algorithm with a state-of-the-art centralized *optimal power flow* (OPF) algorithm. It verifies the optimality of the algorithm and explores the differences in computational complexities and scalability considerations, comparing the two alternative methods of gradient computation. These results help assess the applicability of the algorithm to real-world scenarios. After that, the chapter presents two application cases where the developed EMS model is validated to solve the multi-objective OPF problem for the distribution grid with connected DG units and flexible consumers from the industrial and residential sectors:

- two different types of industrial prosumers simulating real-world small-scale industries: profit-seeking self-optimization using a peak-shaving strategy, optimized production processes with the help of storage.
- residential prosumers clustered into socio-behavioral groups and modeled to generate daily load profiles accounting for heat pump control, PV generation, and types of buildings.

Chapter 6 concludes this thesis by summarizing the research objective and the proposed solution, critically reviewing the model, and providing a future outlook.

2 Research Trends in Energy Management and Optimization Methods

This chapter delves deep into the ongoing practices in academia following the transformation in the power system industry and related policies regarding energy management and optimization methodologies, which aim to achieve climate change goals. A comprehensive literature review is essential to understanding the requirements for the proposed thesis topic. The preliminary advent of the relevant methods and their application is stated in centralized power systems and mostly exclusive electricity markets, with the transmission grid operators enjoying complete control and ownership over generation and distribution. After this, fundamental characteristics of EMS and power system optimization are presented and supported by contemporary research. This portion highlights the crucial properties to consider when modeling an efficient EMS to address the challenges in modern distribution grids to improve operation, planning, and analysis. While assessing available literature, this chapter highlights the advantages of using one technique over the other, critical research gaps, and the justification of the proposed solution in the given context. This chapter builds a theoretical answer to this thesis's research question before explaining the methodologies in depth.

The chapter is divided into two sections: **Section 2.1** describes energy management fundamentals in power systems, their conception, application, and transformation to support applicability to distribution systems. It also justifies using agent-based systems to develop a simulation equivalent of the real-world framework involving energy management schemes with many participants in the liberalized electricity market; **Section 2.2** similarly treats the topic of optimization. After discussing the fundamental use of optimization algorithms in an electricity network, broad classifications of methods to solve distributed optimization problems are presented. Proceeding, the suitability of available mathematical algorithms for the proposed agent-based set-up is examined, justifying the choice of the proposed solution.

2.1 Energy Management in Power Systems

The advent of EMS concepts and tools dates back to the 1990s when they formed a critical entity being deployed at the centralized control centers for transmission systems to ensure operational security and reliability [12]. The development of *Supervisory Control and Data Acquisition* (SCADA) systems made the field implementation possible. Finally, they evolved into real-time solutions offering load control, dispatch scheduling, and distribution system management [13].

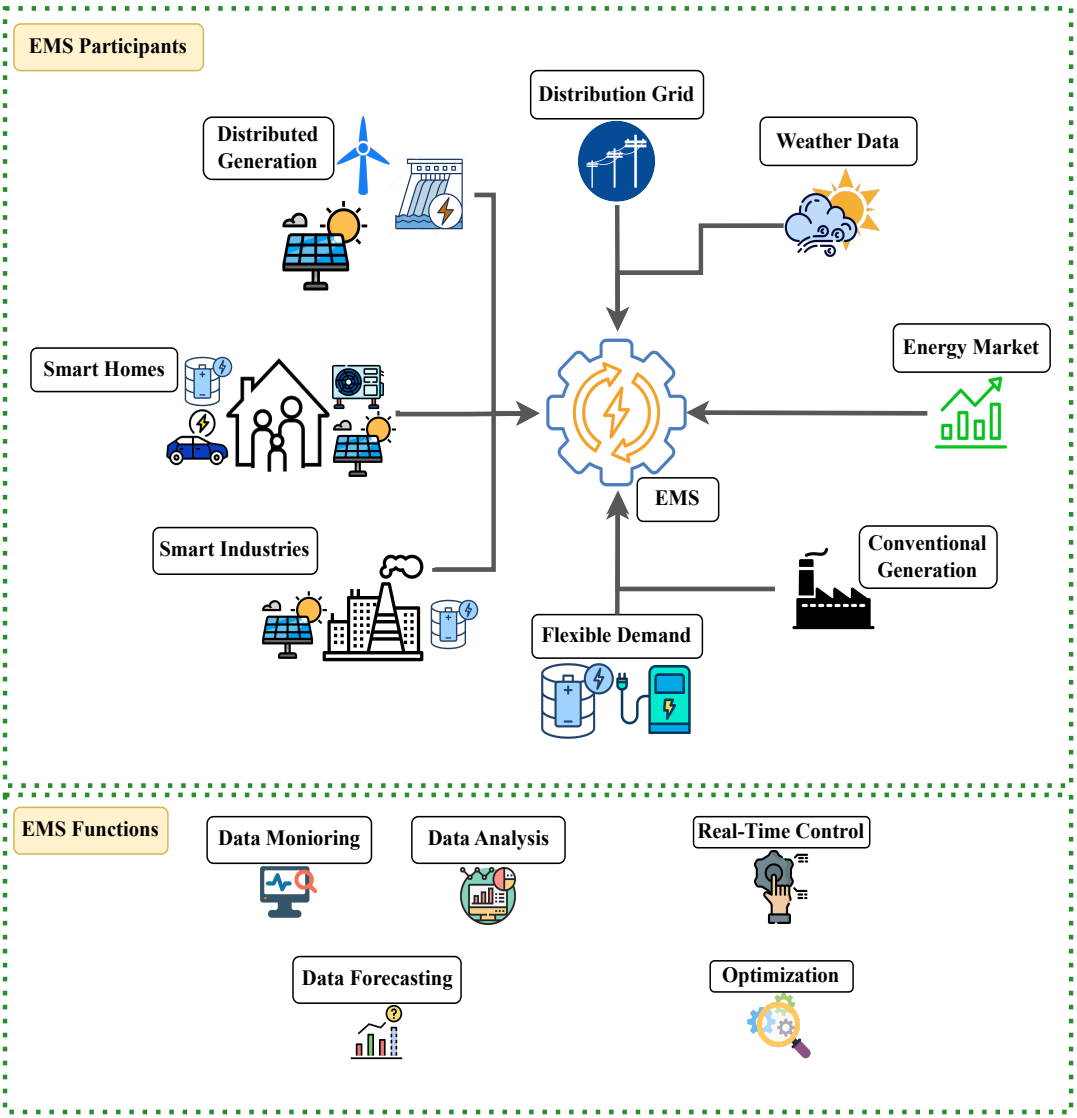

Figure 2.1: EMS Participants and Functions in Distribution Grids [14]

In recent years, energy transition pathways have led to a dramatic transformation at the distribution grid level, which results in the need for similar tools formulated for active distribution networks with diverse connected participants. Stressing the urgency of the topic, academic institutions are creating standardized definitions for DERs, EMS, and DERMS, industrial companies are supporting the development of efficient and robust tools and solutions, and regulatory bodies are introducing policies to aid in the application of *energy management* (EM) initiated control in the distribution network. The function of such an EMS is to optimally allocate required units of available generation to the end-users while promoting the use of renewable resources without compromising the power system's reliability, security, and safety [15]. The primary functions of an EMS are to monitor, supervise, optimize, and control the operation of all involved participants in the electricity network [16].

With increasing complexities due to the influx of renewable sources of generation, responsive loads such as storage and electric vehicles, and complicated DR strategies, improvement in EM modeling can ensure a cost-effective and sustainable supply of energy that respects the technical constraints of the system while considering weather, market and behavioral uncertainties [17]. To successfully model and implement an efficient EMS, one must adequately define the associated characteristics regarding the EM type, objectives, stakeholders, architecture, and communication infrastructure [18]. Figure 2.1 shows the possible participants involved within an EMS solution and lists the typical functions an EMS model performs. The following sections examine the literature to quantify the various EM solutions and their benefits and limitations to justify the choice of the proposed architecture.

Objectives of EMS

An EMS's goal can be single or multi-objective, covering the integrated distribution system's economic, technical, social, and environmental aspects. Most available research deals with economic objectives where the EMS aims to minimize system operational costs. The word "system" signifies the user of the EMS method, which can be smart homes, smart industries, a group of DG units, or the physical power system. System costs can be minimized by avoiding using expensive generation units during peak load hours or grid reconfiguration principles. In [19], the authors propose a multi-agent transactive EMS that handles high levels of renewable sources and electric vehicles in the system. Multifarious strategies are introduced to solve the EMS problem for microgrids in grid-connected or islanded modes to reduce fuel

consumption and thus save on energy prices [20–23]. The importance of optimally managing grid reconfiguration to minimize operational costs is highlighted in [24, 25]. However, the utilities pay the price for incurred power losses in the transportation of electricity, which can be minimized by optimally allocating DG units in the distribution grid [26]. Optimization of costs is studied under the influence of integrated PV-battery systems in [27]. The EMS framework is expanded to deliver cost-effective solutions for hybrid AC/DC grids in [28]. EMS systems are also applied to minimize carbon emissions from fossil-fuel-based generation units [29, 30]. Technical objectives might include power quality [31], equipment performance [32], transformer degradation [33], improvement of voltage profiles [34], etc. Recently, there has been a surge in multi-objective EMS solutions because optimizing costs is not enough to guarantee a sustainable and secure electricity value chain [35, 36] under the ongoing power system transformation.

Architecture of EMS

There are three distinct architectures to build an EMS for distribution power systems:

- **Centralized**: This type of architecture has a central controller equipped with a high-performing computation unit and a reliable communication infrastructure to manage energy utilization. The central controller collects all relevant data from the distribution grid, the DERs, consumers, and other relevant units to solve an optimization routine for concerned objectives [37]. However, centralized architecture comes with a high computational burden, extensive data sharing, and a single point of failure, making it unsuitable for distribution grid ecosystems with dispersed active participants with conflicting interests. Therefore, data sharing is limited among the stakeholders involved.
- **Distributed**: This structure is characterized by intelligent agents with control authority and peer-to-peer communication capabilities representing the various participants in the network [38]. They share relevant information and coordinate with each other to solve the global optimization problem. Distributed architecture offers low computational and communication burden and faster response time while compromising on the global optimality of the solution as compared to its centralized counterparts [39]. They are well suited for modern distribution systems.

- **Hierarchical**: Following from decentralized approaches, hierarchical architecture constructs multiple levels of control among the involved participants where the distributed agents can communicate with an agent from a higher or lower level but not with an agent from the same level. This structure is comparatively easier to model than the fully distributed option because of fewer communication channels [40, 41].

However, the specific market structure affects the choice of the architecture. In the case of local energy communities organized by multiple aggregators, several agents operating on the same level will communicate and trade with other local agents in the energy community. A purely hierarchical architecture restricts peer-to-peer communication, which is a limitation. However, worldwide electricity market structures must still be ready to handle electricity trading between neighbors. Therefore, a hierarchical architecture with a few distributed modes of communication is the most practical EMS solution for most liberalized electricity markets in the world.

Selecting a modeling tool for EMS is closely tied to the chosen architecture. In the case of integrated distribution grids with diverse, active sources of generation and consumption, a distributed, hierarchical, or combined architecture is often preferred. Therefore, the inherent architecture of the distribution grid ecosystem makes an agent-based modeling approach a suitable choice. Agent-based modeling supports distributed and parallel communication between intelligent agents following predefined communication protocols and data exchange to solve a given objective.

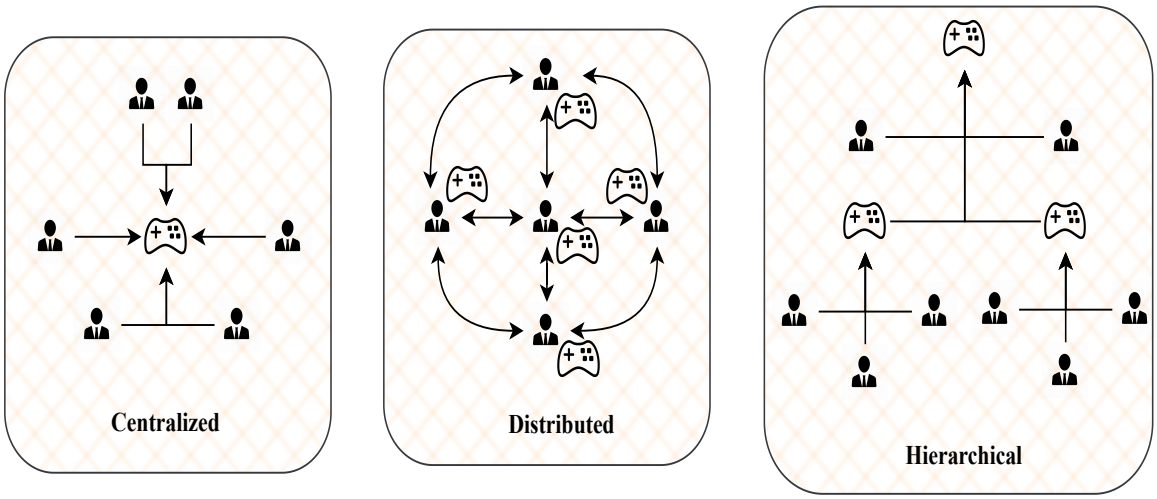

Figure 2.2: Types of EMS Architecture

Types of EMS

EMS can be employed at the transmission, distribution, or end-user levels. Until now, the role of an EMS at the distribution grid level has been discussed. In contrast, the EMS at the end-user level is exclusively concerned with reducing energy usage on the consumer premises to achieve energy price savings. However, active prosumers can participate in the electricity market to trade their excess generation if available or provide ancillary services to the connected utility grid to support secure operation. Therefore, the EMS at end-user levels should also facilitate market participation or DR activities in coordination with the distribution-level EMS. Different categories of end-user EMS systems are as follows:

- *Home Energy Management Systems* (HEMS) [42–45] allow the user to monitor and control the energy usage of a single household.
- *Building Energy Management Systems* (BEMS) [46–48] monitors and controls the energy needs of a building following customer comfort.
- *Plant Energy management Systems* (PEMS) [49] controls the power output and consumption of a *virtual power plant* (VPP) or aggregated DG units.

The abovementioned classification types of EMS are not binding or all-encompassing. Several kinds of EMS deal with clusters of similar entities and their power management, such as energy communities, charging stations, storage systems, microgrids, and even distribution grids (i.e., utility DERMS) [50].

EMS Participants

Significant participants of EMS are the regulators, small-scale prosumers (consumers and producers), DSOs, suppliers, transmission grids, and aggregators. The selected EMS models predefine each participant's functional boundaries, i.e., roles and responsibilities, according to the regulatory structure of the concerned electricity market. The majority of information flows between the participants are bidirectional to provide decision support to DERs, consumers, DG owners, aggregators, and agents, especially for DR programs, which enables consumers to actively participate and offer services for the flexible and efficient operation of the grid. The more complicated sector includes DG units and prosumers from the residential and industrial sections. There is plenty of literature available that looks into the complex mechanisms of DR in the residential sector and proposes efficient strategies to control their load for

grid-oriented benefits optimally [51, 52]. Similarly, EM concepts are applied to industrial consumers to optimally manage their consumption and improve the potential for grid-oriented ancillary services [53, 54]. However, compared to the research found on the residential sector, literature associated with the industrial sector is still relatively sparse. Therefore, this thesis concentrated on including industrial prosumers in distribution grids with various flexible practices that consider the impact of governance policies on industrial technology adoption.

On the electricity grid side, an existing hierarchy between transmission grids, DSOs, suppliers, and balancing market operators dictates the information exchange and control flow. Generally, the transmission grid operates and manages high-voltage transmission networks with cross-border capacities. They are also responsible for balancing services in coordination with the balancing operators after the market closes. The DSOs enjoy similar monitoring and control over medium- and low-voltage distribution networks, which involve managing and coordinating connected DERs while maintaining network constraints related to voltages, line flows, and power balance. Suppliers are responsible for providing electricity to end-users based on bilateral contracts. In specific scenarios, the DSO can take over the responsibilities of a supplier. In [55], the authors expand the scope of EMS to multi-energy systems, including heat and gas networks, into the fold. In [56], the hosting capacity of hydrogen DGs is determined for a connected distribution grid under EM strategies. Similar literature is available to help integrate PV units, storage systems, wind generators, and charging stations. Figure 2.3 shows a generic representation of the main players in the electricity market and their interaction.

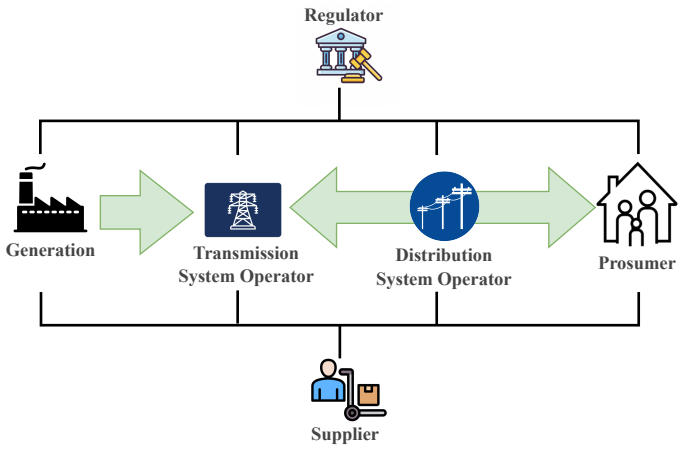

Figure 2.3: Roles and Responsibilities of EMS Participants

Communication Infrastructure for EMS implementation

The distribution grid participants are connected with communication links, enabling them to share necessary information. Critical monitoring, measurement, and control information is passed upstream and downstream to respective stakeholders of the EMS through ICT interfaces. Therefore, the growth of ICT tools is fundamental in supporting and accelerating the implementation of EMS in simulation and real-world scenarios. ICT infrastructure and communication protocols enable the sharing and use of critical information between the EMS and its participants to ensure the seamless functioning of the electric power systems. Communication technologies can be broadly classified into wired and wireless technologies. SCADA, *power line communication* (PLC), and optical fibers are established wired communication methods in centralized EMS architecture, which requires a secure and robust communication channel. For short-distance information flows, cost-effective wireless technologies such as Bluetooth, WLAN, ZigBee, etc., are preferred in HEMS, BEMS, etc. Table 2.1 summarizes the data transfer rates and coverage ranges for the most popularly used ICT protocols in power systems [57].

Protocols	**Transfer Rate**	**Range**
SCADA	51.8 Mbps to 2.48 Gbps	1000 miles or more
PLC	200 Mbps	200 miles or more
Optical Fiber	100 Mbps to 2.5 Gbps	100 km
WLAN	$54 - 900$ Mbps	100 m
Bluetooth	721 Kbps	100 m
Cellular	$14.4 - 100$ Mbps	$5 - 100$ km

Table 2.1: Transfer Rates And Ranges for Popular ICT Protocols

Note: This thesis develops an EMS architecture in a simulation environment, and therefore, the communication protocols between the different simulators are purely software algorithms.

Optimization as an EMS function

EM schemes include various subjects, such as optimal operation of renewable-sourced DG units, control of responsive loads in batteries and *electric vehicles* (EV)s, efficient DR programs, load control methods, etc. Several optimization algorithms and programming methods are developed to solve for the ultimate goal of maximizing

or minimizing the system's objective function. This objective function may include multiple objectives regarding system costs, carbon emissions, power quality, voltage stability, distribution losses, and reliability. Solutions available in literature use many *inexact* and *exact* algorithms to solve the optimization problem. The *exact* or numerical solutions guarantee optimality, whereas the *inexact* or heuristic methods deliver relatively faster computation. A quick survey of the literature will show that research tends to lean towards centralized *inexact* algorithms forming the class of heuristic or metaheuristic algorithms to solve the underlying optimization, especially in the case of multi-objective EM problems [58, 59]. Other approaches, such as *stochastic* or *robust* methods, are best suited to handle uncertainty [60]. However, in the current distribution grid set-up, there is a need to introduce suitable and efficient distributed optimization algorithms that fit the communication protocols of the framework and can deliver acceptable optimality and computational efficiency with limited information at individual agents.

This section highlights the primary characteristics of EMS and their applicability to modern distribution grids, using a literature review of recent research practices in the area.

2.2 Distributed Optimization Algorithms for Power Systems

Power system optimization was first conceptualized as a mathematical tool for calculating the instantaneous optimal point of operation for a power system under constraints that intend to meet operational feasibility and security [61]. Traditionally, *Independent System Operators* (ISO) aim to find a minimum cost-generation dispatch schedule for transmission systems by executing an optimization routine to solve the OPF problem [62–65]. A complete knowledge of the system state regarding network, generator, and load parameters is assumed at a central location with the ISO. Integrating DER technologies, including renewable generation, energy storage, and responsive loads, shifts the passive distribution systems to active participants in the electricity market [66]. New opportunities arise for diverse stakeholders such as retailers, policymakers, industrial and residential end-users [67]. Information and power flows are bidirectional, and supply and demand uncertainties are introduced.

Consequently, optimal management of dispersed resources becomes a prime necessity to efficiently maintain the security of supply in the distribution grid environment. Solving the OPF problem at a distribution level to control the connected DERs while considering network operation provides grid-aware optimal solutions. Therefore, distributed solutions well suited for active distribution networks with connected DERs, including DG units and DR participants, are formulated that offer the following potential advantages over centralized approaches:

- in an agent-based system where each agent has access to a specific set of data, a distributed solution can solve the OPF problem with limited information, reducing the requirement for elaborate communication infrastructure,
- they can mitigate scenarios related to communication or technical failure in agents,
- owing to parallel computing abilities, distributed solutions offer improvements in computational speed for larger problems as compared to centralized alternatives,
- they should respect the data privacy of involved participants and facilitate regulated information exchange

Before discussing the various methods available in the literature to solve the distributed OPF problem, a brief mathematical insight into the power flow formulation in distribution systems is required. Assumptions and relaxations adapted to aid the distributed algorithms in solving the power flow optimization routine are briefly introduced.

Power Flow Formulation

Consider an n bus distribution power system where $N = \{1,2,...,n\}$ denotes the set of buses. Let E denote the set of lines. The network admittance matrix holding the electrical parameters and topology information is denoted by $Y = G + jB$. Each bus has an associated voltage phasor, $|V|e^{j\theta} = V\angle\theta$, and active and reactive power injections, $P_i + jQ_i$.The power flow equations are:

$$P_i + jQ_i = V_i \sum_{k=1}^{n} \bar{Y_{ik}} \bar{V_k} \tag{2.1a}$$

with squared voltage magnitudes

$$v_i := V_i \bar{V_i} = |V_i|^2 \tag{2.1b}$$

Splitting real and imaginary parts of (2.1) and using polar coordinates, the power flow equations result in non-convex optimization problems that require linear approximations or convex relaxations for solution:

$$P_i = |V_i| \sum_{k=1}^{n} |V_k|(G_{ik}cos(\theta_i - \theta_k) + B_{ik}sin(\theta_i - \theta_k)) \tag{2.2a}$$

$$Q_i = |V_i| \sum_{k=1}^{n} |V_k|(G_{ik}sin(\theta_i - \theta_k) - B_{ik}cos(\theta_i - \theta_k)) \tag{2.2b}$$

An alternative *DistFlow* model represents the power flow equations for radial networks suited to predominantly radial distribution grids [68]. Use of (2.1) and (2.2) or the *DistFlow* model results in non-convex optimization problems, which leads to linear approximations and convex relaxation approaches to fit the equations to distributed solutions. The most commonly used linear approximation approach in the industry is the DC power flow model [67], which is unsuitable for distribution networks due to the following assumptions [69]:

- Reactive Power flows can be neglected,
- Shunt elements are neglected, and the lines are assumed lossless, i.e., $G \approx 0$,
- All nodal voltages are equal, i.e., $|V_i| = 1$ for $i \in N$, where N is the number of grid nodes
- angle differences between connected nodes are minor, i.e., $sin(\theta_i - \theta_k) \approx \delta_i - \delta_k$ for i,$k \in E$, where E is the number of connecting lines in the grid.

Therefore, alternate methods of linearization are proposed, such as linearization around the "no-load" voltage profile, assuming negligible shunt impedances and near-nominal voltage magnitudes [70, 71]. Neglecting losses in the *DistFlow* model can also linearize the problem. Linearization approximates the power flow equations. On the other hand, convex relaxations enclose the non-convex feasible spaces associated with the power flow equations in a larger space. It bounds the optimal objective value and provides sufficient conditions to certify problem infeasibility. Convex relaxation approaches can be further categorized into *semidefinite programming* (SDP) approaches [72, 73] and *second-order cone programming* (SOCP) relaxations [74, 75].

Note: All electrical parameters used in this thesis related to voltages, power flows, power injections, system matrices, etc., are expressed in *per unit* (p.u.) values for all calculations.

Distributed Optimization Techniques

A multitude of literature has been published on distributed optimization algorithms in the last decade. The available techniques can be roughly classified into the following groups:

- methods based on augmented Lagrangian decomposition including Dual Decomposition, the Alternating Direction Method of Multipliers (ADMM), Analytical Target Cascading, and the Auxilliary Problem Principle [76]
- methods based on the decentralized solution of the *Karush-Kuhn-Tucker* (KKT) necessary conditions for local optimality including Optimality Condition Decomposition and Consensus + Innovation [77]
- methods based on other approaches such as Gradient Dynamics and Dynamic Programming

These algorithms can be applied to solve linear, convex, non-linear, and non-convex OPF formulations with the help of modifications and extensions. The modeling of the distributed optimization techniques can be divided into *offline* or *online* methods. Offline algorithms, though distributed, need to iterate over all variables in the solution space until convergence is achieved before the solution can be applied to the physical grid. Therefore, the intermediate iterates do not satisfy the power flow equations, i.e., Kirchoff's laws or maintain operational constraints. Although favored for traditional power systems, volatile renewable generation and fluctuating loads deem offline methods inadequate to handle modern distribution systems with many connected DERs. Real-time or *online* algorithms only iterate on variables associated with controllable devices in a feedback interaction with the grid. Algebraic power flow equations represent the grid for slow timescale (steady-state) operations, and differential equations describe the grid for fast timescale (dynamic) operations in such algorithms. Figure 2.4 shows the general structure of an online algorithm.

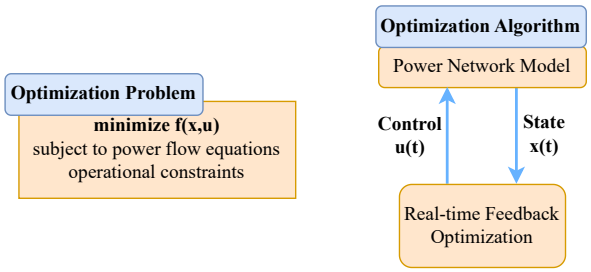

Figure 2.4: General Structure of Online Algorithms

The primary advantages of closed-loop feedback optimization are twofold: 1) It naturally tracks changing network conditions as they reflect in the state $x(t)$, which is used to calculate the control $u(t)$, promising robustness against uncertainties and disturbances; 2) Most algorithms implemented with the online approach are inherently decentralized due to the feedback mechanism involving at least two participants and model-free because the agent representing the model shares the updated state of the system masking model-specific information such as topology and operational limits. Online algorithms are prominently applied to solve real-time OPF, optimal frequency and voltage regulation, and optimal wide-area control. The class of online algorithms can also be termed gradient methods because the algorithms use the first or second-order gradients of the system to search for the optima as seen in Figure 2.5. The controller updates the control signal $u(t)$ for each time instant, t, and applies it to the physical grid that implicitly solves the power flow to obtain the updated state $x(t)$, which is measured to compute $u(t+1)$.

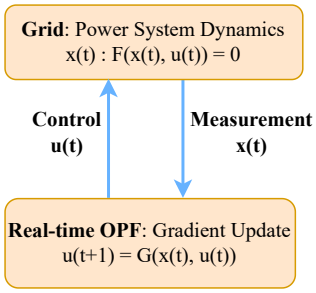

Figure 2.5: Online Algorithms with Gradient Update

In [78], the authors use the *DistFlow* equations and the first-order system gradients to compute the control signal at each iteration. Sufficient conditions for convergence to a local or global optimum of the non-convex OPF problem are established. A gradient-based extremum method is used to solve the OPF problem without knowing the network model by using a sinusoidal probing signal into the network to estimate the system gradients in [79]. The optimality conditions presented for this method also guarantee the global optimality attainment from [78]. A first-order subgradient algorithm for solving the SDP relaxation of the OPF problem is used for a general network model in [80]. These methods can be extended to multiphase unbalanced networks. In [81], the authors extend the methods to time-varying OPF models. Therefore, it is clear that the gradient-based techniques are highly versatile in their application and

can guarantee convergence to local or global optima with or without the knowledge of the physical network model. However, most proposed schemes in the literature provide a centralized scheme, with a few exceptions [82, 83].

2.3 Research Gap and Thesis Contribution

After a close survey of the ongoing transformations in the distribution grid ecosystem and the recent academic research trends, this thesis identifies the following areas as research gaps:

- Holistic models of energy management for the complete, integrated distribution system scenario to generate meaningful data for distribution grid planning and operation,
- a distributed implementation solution to the multi-objective optimization problem ensuring data privacy of involved participants
- accurate representations of involved participants and their behavior under electrification scenarios,

To this end, this thesis attempts to answer the research question by proposing an agent-based hierarchical EM architecture for an integrated distribution grid scenario containing several DG units and consumers adopting flexible technologies. Multi-agent representations of EM models are prevalent in research because they are characterized by autonomous decision-making ability and communication within a distributed network. The literature shows that the distribution grid environment and the associated market structure suggest an inherent hierarchical architecture. Therefore, this thesis exploits the same to design the proposed hierarchical architecture with possibilities of distributed communication. The agent representing the EMS imitates the roles of a theoretical DERMS for a real-world aggregator to execute a distributed OPF routine to assist in distribution grid planning and operation. However, using an online feedback mechanism to solve the optimization problem allows for coordination between the EMS agent and the DSO, which helps mask the actual network model from the aggregator. Therefore, the proposed architecture combines the functionalities of a DER aggregator and a utility DERMS and controls the connected DERs following grid-aware signals.

The multi-objective optimization problem is solved using a novel combination of Tchebycheff's decomposition method and the Gradient projection algorithm. On one

hand, the method preserves the benefits of meta-heuristic approaches of achieving high-resolution optimal solution points for the multi-objective problem. On the other hand, the numerical gradient-based method vouches for the accuracy of obtained solutions. The objectives of the OPF problem consider economic, environmental, and technical aspects of the connected distribution grid. Moreover, the system has physical and operational constraints regarding generation capacities and voltage limits. The unique qualities of *online* algorithms justify the selection of the method for an architecture where the agents representing the EMS and the distribution grid (DSO) will interact in the closed-loop feedback mechanism to ensure the satisfaction of power flow constraints.

Finally, the proposed architecture is implemented in a co-simulation framework to interact with other agent-based models representing industrial and residential consumers with flexible technologies. Various simulation scenarios are defined by varying the distribution grid environment, i.e., number of DGs, different topologies, etc., as well as by varying customer behavior, to study the impact of consumer flexibility practices on the connected distribution grid operational characteristics. The proposed architecture and the optimization routine are then validated in the co-simulation framework by simulating the predefined scenarios. Contemporary research articles suggesting similar solutions published during this thesis's development further stress the topic's importance [84, 85].

Chapter 2 Summary and Chapter 3 Preview

Key takeaways from this chapter:

2.1) Ongoing research trends on energy management practices in the distribution grid ecosystem,

2.2) Evaluation of theoretical concepts and implementation methods,

2.3) Motivation behind the proposed solution

Highlights for the next chapter:

a) Agent-based modeling fundamentals

b) Conceptual description of the proposed EM architecture

c) Implementation specifications in a co-simulation framework

3 Agent-Based Energy Management Architecture

This chapter introduces the proposed hierarchical EM architecture for modern distribution grids in a liberalized electricity market, mostly imitating the German market with a few assumptions. It is vital to understand the basic functioning of the wholesale and retail electricity market in a real-world scenario to properly envision the roles and responsibilities of involved participants, i.e., their level of autonomy, area of control, and access to information and communication with other participants. A generic understanding of possible participants in an EMS environment has been established in the previous chapters. This chapter uses the German electricity market to model the respective agents, considering the practical applicability of the design. For model validation, this thesis employs the EM architecture in a co-simulation framework with other agent-based models representing the various participants, where data sharing and communication follow the regulatory structure of the electricity market. The SIMONA ecosystem, an agent-based grid simulation platform written in SCALA and developed within a message-driven toolkit, AKKA [86], calculates the power flow routine and updates the grid state. The *Grid Agent* (GA) within SIMONA represents the network model and can communicate with the other agents in the grid network, which are aggregators or individual DER components. The primary *Energy Management Agent* (EMA) executes the multi-objective optimization routine in a feedback mechanism with the GA. The primary EMA can be classified as a DER aggregator or utility DERMS depending on the use of the software solution by aggregators, suppliers, or DSOs. The fundamental idea is to mask sensitive information such as grid topology and parameters, generation, or operational limits from concerned parties.

The chapter begins by describing the principles of the German electricity market and identifying the roles and responsibilities of primary players in Section 3.1. This section also talks about the ongoing changes in the market to accommodate the new players in the form of smaller DGs or DR participants. Section 3.2 provides fundamental concepts regarding agent-based simulation and its advantages and limitations. The following section, Section 3.3, lists essential concepts underlying the development of the SIMONA grid simulation platform with a particular focus on agent communication to solve the OPF routine in a distributed fashion and the backward-forward sweep power flow computation. Section 3.4 presents the conceptual design for the hi-

erarchical EM architecture. Finally, Section 3.5 supplies co-simulation fundamentals and describes the co-simulation framework used by this thesis to implement the EM architecture. This section briefly defines the model formulation for the industrial and residential prosumers used in the application case.

3.1 Liberalized Electricity Market - Germany

With over 180GW of installed capacity, Germany has the largest electricity market in Europe. In recent decades, the electricity market has undergone elemental changes owing to the continuous expansion of renewable energy generation and the abrupt decision to phase out nuclear power after 2011 [87]. The domestic electricity market was liberalized in 1998. Although there are currently over 900 DSOs operating the distribution grids and, in some instances, supplying electricity to end users in Germany, the four big *Transmission System Operators* (TSO), namely Amprion, Tenet, TransnetBW, and 50Hertz, control electricity transmission to the distribution grids and heavy industries. On top of that, the TSO is also responsible for managing balancing reserves for the entire ecosystem, i.e., the TSO decides the dispatch of balancing reserves after the market closes, considering forecasted demand. Energy trading can happen in two ways [88]:

- on organized energy exchanges where the market participants trade energy on public exchanges at transparent prices (double-blind auction)
- *over the counter* (OTC) approach where buyers and sellers interact using confidential bilateral contracts

Different components like energy, transmission capacity, and reserves/flexibility can be traded to match supply and demand. There are two different market mechanisms for electricity trading operated by a *market operator* (MO) in Germany [89]:

- ***Day Ahead*** markets operate on auctions with results calculated in 40 minutes for the next day. The required generation is scheduled according to forecasted demand, and the balancing reserves are set.
- ***Intraday*** markets are further distinguished into auction and continuous trading. The auction enables a 15-min optimization schedule for the market participants. Continuous trading is based on a "pay-as-bid" auction format for 5-minute time windows. Here, power supply and demand are matched in real time to handle deviations from the forecast.

The *market operator* is a passive participant that supplies the historical spot market prices for simulation. Ideally, the provision of aggregated, ancillary, or flexible services by prosumers at the distribution grid level should be organized by energy communities, peer-to-peer trading, and customized supplier contracts. Local market mechanisms are an emerging business model at the nascent stage of development. Therefore, there is a need for more suitable real or synthetic market data that reflects the current change in supply and demand in a fully integrated environment. Consequently, this thesis uses historical spot market prices from German retail markets in simulation case studies due to the lack of suitable market profiles tailored to meet distribution system requirements. In future extensions, adding a market simulator to organize local energy communities and peer-to-peer trading in the proposed EM architecture can significantly enhance the model. A real-world electricity supplier can take over this role and be included as a separate agent in the distribution grid ecosystem.

In this thesis, the market structure for distribution grids with the capacity to participate in energy exchange with connected consumers holds the following assumptions:

Assumption 3.1:

a. The TSO is responsible for balancing reserves settlement in the balancing market. Therefore, the boundary condition states that the conventional generator connected to the distribution grid has sufficient capacity to match current demand,

b. The distribution grid allows reverse power flow,

c. The renewable generation sourced DG units actively participate in the day-ahead spot markets to sell forecasted power,

d. Industrial or residential consumers can freely choose their electricity supplier in a liberalized market with bilateral contracts and

e. In cases of availability of consumer flexibility, they bid their services to the DSO or the supplier following historical spot market prices with the help of an *aggregator*

As is evident from the assumptions, the transmission level is treated as a predefined boundary condition and the market provides historical data.

Aggregators

The concept of aggregators is relatively new in the energy market. However, due to the increasing significance of procuring local short-term flexibility from dispersed units and consumers, aggregating smaller units capable of providing flexibility or grid-oriented services in the distribution grid control area is gaining traction [90]. An aggregator groups multiple agents in a power system (e.g., consumers, producers, prosumers, or a mix of all) to form a sizable capacity [91], such that they can provide aggregated and ancillary services to the distribution grid or the electricity supplier and trade flexibility in the market. An aggregator can be a third-party company that operates a *Virtual Power Plant* (VPP) where centralized software optimizes the operation of the participants of the VPP with the knowledge of weather forecasts and market profiles. The aggregator can help integrate renewable sources efficiently by optimizing demand and supply by optimally controlling the generation assets, DR resources, or storage units [92].

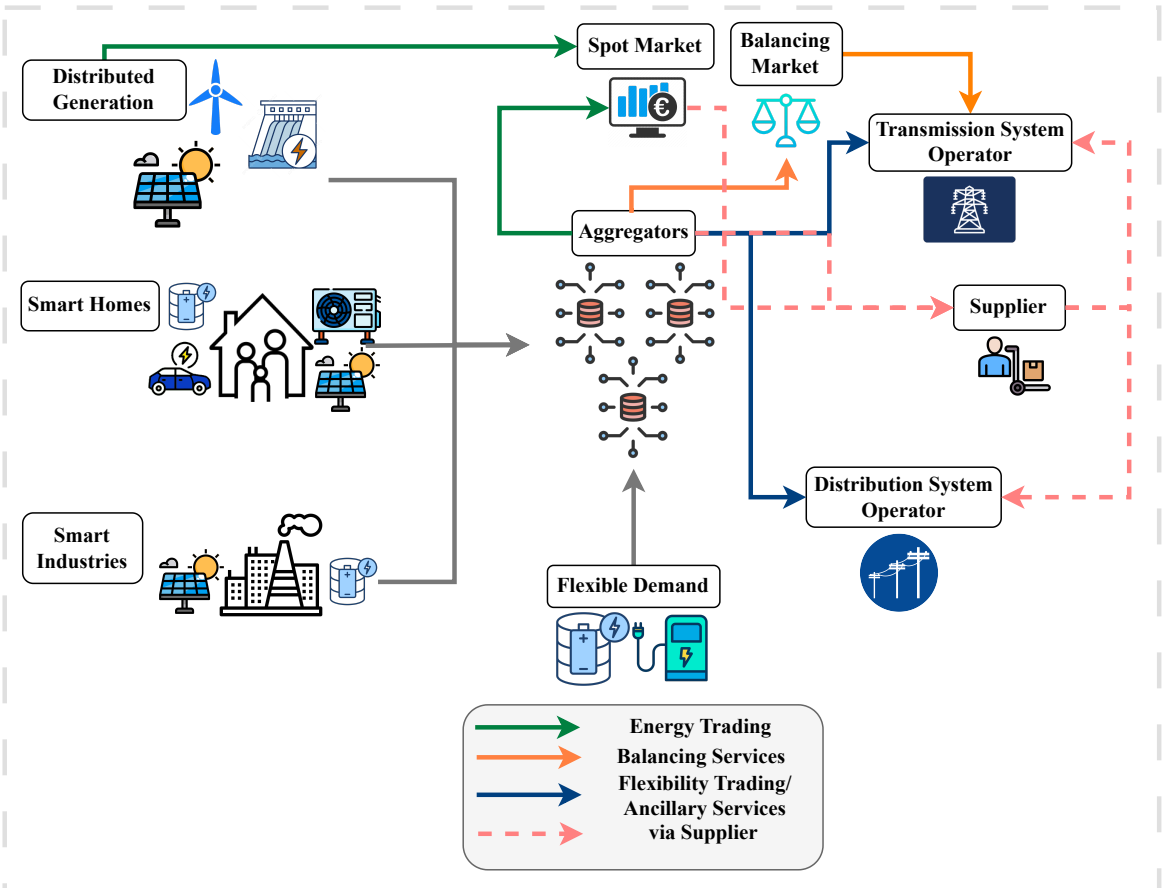

Figure 3.1: Aggregators in Power Systems [93]

Moreover, aggregators can provide several transmission-level services, such as frequency regulation and balancing services, to the balancing market. The data pooled at an aggregator can be extremely useful to study the impact of increasing consumer adoption of participating controllable assets on the connected utility grid. The benefits lie in reducing marginal costs for the utility grid and reduced investments in grid expansion methods owing to the optimal operation of available resources [94]. Several technical and regulatory requirements must be satisfied to integrate an aggregator in a real-world scenario. These requirements suggest changes to the hardware and software infrastructure accompanied by their communication protocols, wholesale and retail markets, and roles and responsibilities of a distribution grid operator. Therefore, an aggregator bridges the gap between relevant stakeholders in modern energy systems to deliver a smooth functioning ecosystem. Countries like Germany constantly strive to meet such requirements, adding weight to the research topic. *Energy and Meteo Systems* (Emsys) in Germany supports aggregators in controlling generation assets, scheduling, energy trading, etc. [95]. Figure 3.1 shows the general representation of aggregators, connected participants, and the various offered services in an electricity market.

After learning the basics of the German electricity market and exploring the ongoing transformation to accommodate local, flexible mechanisms in a DSO control area, three players can be envisioned to assume the role of energy management in the proposed architecture. The TSO, balancing, and spot markets are not considered active participants. In practical implementation, the choice will depend on the most cost-efficient and sustainable integration of an EM routine:

- The third-party ***Aggregator*** is instrumental in executing optimization routines for connected DERs and provides EM solutions in the form of energy and cost savings. It aggregates DERs and optimizes their performance based on grid-aware or market-aware schemes. As the aggregator already invests in developing optimal EM solutions for the DER units, extending the optimization routine to be grid-aware is relatively less invasive. However, the aggregator cannot access the accurate network model for the distribution grid. The feedback optimization mechanism helps solve grid-aware goals in collaboration with the DSO, which has network knowledge. In this case, the type of EM solution will be a grid-aware DER aggregator DERMS.
- The ***Electricity Supplier*** supplies electricity to end-users and handles bilateral contracts and market trading. It can take up the role of an EMA and execute

the multi-objective optimization routine by communicating with the DSO and the aggregators. However, in Germany, the roles of a supplier are merged into the roles of a DSO for distribution grids with less than 100,000 consumers.

- The ***DSO*** can function as an EMA and use the information derived from DER aggregators as input to the algorithm optimizing distribution grid operations. With accurate knowledge of the network model and authority to issue emergency control over connected, flexible units, the DSO becomes a suitable candidate to produce optimal set points and issue control action. In this case, the proposed EM solution will act as a utility DERMS.

This thesis proceeds with the first option of an aggregator to act as the EMA and optimally manage all available resources in the area by operating in a closed-loop feedback mechanism with the grid to achieve grid-aware economic, environmental, and technical benefits. Executing the optimization routine follows a distributed fashion where the DSO and DERs do not share sensitive information regarding grid topology, generator capacities, and operational limits with the EMA. Additionally, an aggregator has communication channels with DERs, DSO, the market, and electricity suppliers for daily operation.

The DSO, represented by the GA, can also be developed in the proposed architecture to act as an EMA with the help of minor modifications. SIMONA will use the optimization routine as an external library to solve the associated OPF problem. However, if the DSO acts as the EMA, the solution will essentially depend on a central coordinator, who will pool data from all participants. In the case of multi-voltage grid simulation, i.e., the presence of multiple agents representing the DSO, central coordination is helpful. In other scenarios, the aggregator or supplier (if existing as a separate role), acting as the EMA, can reduce data sharing and communication efforts with a suitable protocol design while maintaining a hierarchical architecture.

Note: In this work, the application cases could not provide the simulation data required for distribution grids connected to more than 100,000 customers. Therefore, the roles of a DSO and supplier are assumed to be merged into a single participant.

This section presents a simplified overview of the German electricity market and suggests an appropriate integration of the proposed EMA in the regulatory scenario. It clearly defines the market-related assumptions employed in this thesis.

3.2 Fundamentals of Agent-Based Simulation

3.2.1 Multi-Agent Systems

Multi-Agent Systems (MAS) allow for detailed representation of highly complex systems such as the distribution grid ecosystem using the decomposition principle [96]. They can be applied in terms of *Agent-Based Models* (ABM) and *Agent-Based Simulations* (ABS) to allow temporal dependencies and generate meaningful time series for further analysis. MAS is a subfield of distributed artificial intelligence defined as a network of individual computing entities, called agents, sharing knowledge and communicating with each other to solve a distributed problem beyond a single agent's scope [97]. Distributed problem solving enables the decomposition of a problem into smaller subproblems and their solution through efficient decentralized and parallel coordination [98]. In the case of power distribution systems and the related electricity market, distributed and parallel computation is essential to handle a large number of dispersed units and preserve their data privacy. ABMs have proven viable in academia and practice for studying complex, heterogeneous systems [99]. Their flexibility facilitates interdisciplinary use in the form of MAS in the field and ABS in simulation studies. The ability to capture granular details of a complex system by decomposing it into smaller subproblems is attractive in distribution grid modeling and simulation, where the granularity of the demand side is becoming increasingly important to consider. Figure 3.2 provides a schematic overview of general ABM components, including the environment, global properties and actions, and resource models.

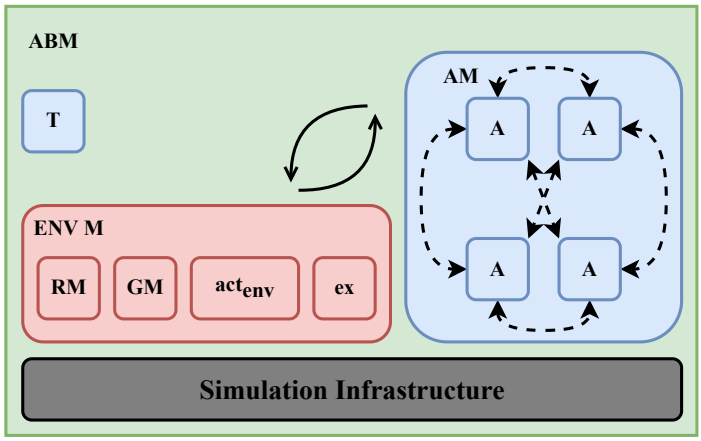

Figure 3.2: Overview of General ABM Components

Mathematically, an ABM is an invariant structure:

$$ABM = \langle T, ENV\ M, AM \rangle \tag{3.1}$$

where T represents time, $ENV\ M$ is the environment model and AM represents the actual model of the MAS. $ENV\ M$ is further decomposed into a model of all resources RM, global properties GM, a global action function act_{env}, and an execution function ex [100].

Agent-based approaches require careful consideration when formulating models regarding precise communication and behavior protocols for agents' interactions. They also need a valid balance between the granularity of model details and suitable abstractions. In improper modeling, the output is either inaccurate or requires extensive computational effort.

Despite the popularity of MAS in research and implementation, concrete definitions of individual components of MAS, such as *agents*, *environment*, and *agent perceptions and interactions* vary throughout literature [101]. That is to say that no universally accepted definition of an agent, MAS, or ABS exists, which is especially true when defining an agent's properties. However, a consensus exists on a broader understanding of the general components of an MAS. The three essential components of a MAS are briefly explained in this section. Please refer to [102, 103] for detailed insights into MAS theory and [104] for a history of ABS development throughout the past decades.

Agents

Agents are the constituent entity and primary ingredient of the MAS. By definition, a MAS consists of at least two, usually more agents. One of the most popular and general definitions of an agent is:

An agent is a computer system situated in some environment capable of autonomous action in this environment to meet its design objectives [102].

However, this definition does not account for specific requirements, such as what constitutes a computer system—hardware, software, or autonomous. Another definition classifies the agents based on their capabilities in terms of *individuality*, *behavior*, *interactions*, and *adaptability* [101]. Combining the two approaches, [100] defines an

agent as a hardware, software, or a combined entity equipped with sensors and actuators to perceive and influence its surrounding environment. Therefore, the essential properties of an agent are [105]:

- **Environment**: The agent exists within an environment and can observe with or without limitations. Moreover, the agent can interact with this environment with a degree of locality. Locality restricts the agent from interacting with all other agents in the system.
- **Autonomy**: The agent can determine its action to achieve desired targets according to the stimuli received from the environment.
- **Pro-Activity and Reactivity**: An agent might react flexibly to a signal received from another agent in the environment and handle the situation.
- **Rationality**: An agent, in pursuit of its objectives, tries to optimize its action to increase the probability of reaching the goal.
- **Sociality**: Communication between different agents in the MAS system is possible.

The multiple definitions of agents support their applicability to various problems. However, the features and limitations of an agent-based approach should be clearly defined in the context of its agents.

Environment

The environment is the space an agent can interact with, i.e., receive stimuli from other agents, which are part of the environment or influence the action of different agents. A high-level description or classification of environments is provided according to their characteristics in [103], defining the following properties:

- it can be *wholly* or *partially observable* to the agents in the system
- it may be *deterministic* or *non-deterministic* depending on the uncertainty of the impact of an agent's reaction
- it may be *episodic*, i.e., current time step does not affect any other, or *sequential*, i.e., present action can affect future decisions
- the environment can change while the agent updates itself, i.e., *dynamic*, or cannot change, i.e., *static*
- it may be *discrete* or *continuous* according to its number of states being finite

or otherwise

- the agents might know the "laws" of the environment (*known*) or not (*unknown*)
- it may be a *single-agent* environment with only two agent entities or a *multi-agent* environment with at least three agent entities

Interaction

The interaction between agents defines their communication and coordination protocols. Thus, it is vital to carefully construct their interaction protocols and design and record the information flow between respective agents. These protocols implicitly create a hierarchy that supports the structured and organized form of a MAS. It is also necessary to define the type of messages or information that an agent can perceive and their subsequent action. Several foundational protocols are provided in [106]. Figure 3.3 shows the general structure of a MAS.

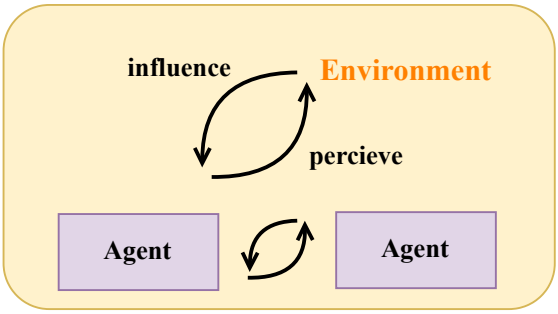

Figure 3.3: General Structure of a MAS

3.2.2 Agent-Based Simulation Model

A conceptual MAS can either be implemented to describe an existing complex system or to develop an artificial complex system to solve a specific task. Both approaches require system models, which they can use to simulate and observe the system or apply the model to a real-world field test. Depending on the specification of whether a model interacts with a real-world environment or a simulated environment classifies MAS systems into 1) *hardware or real-world MAS*, 2) *purely software MAS*. As hardware MAS, the system acts like autonomous components in a real-world scenario, which makes them applicable to power system problems [107]. In a pure software implementation, the simulation model withholds the basic structure of a MAS in a software

environment. The primary participants identify as agents and follow agent-related concepts and technologies in their behavior and interactions within the environment. Therefore, an ABS contains an agent system model, where each agent is autonomous and communicates with other agents using designed communication protocols. The environment model encloses the agents within a simulated space. Finally, the simulation infrastructure contains and provides all required components to facilitate the execution of the agent and environment models.

Agent-based simulation models can be implemented either using *agent-oriented programming* languages (APLs) [108] or generic programming languages, such as Python, Java, etc. However, APLs are not widely used, which makes generic languages more favorable. The first approach is to use *object-oriented programming* (OOP) [109] due to the apparent similarities between the definitions of an object and an agent. Objects are the main components of OOP, which encapsulates some state data and is active through its methods. However, an object does not enjoy authority over executing its method, i.e., to perform the designated action by an autonomous decision, unlike agents, which function on a request basis and can choose not to respond to a particular message.

Moreover, objects are not concurrent by nature, whereas MAS is inherently multi-threaded. The second approach uses the concept of *actors* [110] as a theoretical model of concurrent computation. The actor is the primary computational entity that can send or receive messages to and from other actors in the system. It can modify its state data and decide to respond to a message. An actor shares identity, autonomy, communication, and coordination with an agent. However, an actor is strictly guided by deterministic pre-programmed behavior, i.e., actors react to external stimuli, and agents optimize their actions to achieve desired targets. Actors are essentially the software counterparts of agents whose goals are strictly dependent on software performance issues. In contrast, agents determine their output on indicators related to solving a specific task with its own set of rules. However, from an implementation perspective, actor-based paradigms outperform APLs in terms of simulation performance.

3.2.3 Implementation Specifications

This thesis implements the proposed EM architecture in a co-simulation framework where multiple pure software MAS interact with each other following agent commu-

nication protocols using a co-simulation platform *mosaik*. Each MAS is treated like an agent model in the overall co-simulation environment. The MAS implements their respective models with OOP concepts and the actor paradigm. SIMONA, the grid simulation platform, uses the actor paradigm to model the distribution grid agents. Therefore, it can perform deterministic tasks such as power flow execution with high computational efficiency when triggered by a control signal from the EMA. However, it cannot execute an optimization routine due to its autonomy limitations. The agents act following the properties defined earlier. The simulation environment possesses the following properties:

- *partially observable* by the agents
- *deterministic* i.e., the result of an agent's action to the environment is not uncertain
- *episodic* meaning an agent's current decisions do not influence future actions
- *static* i.e., there are no changes in the system while an agent is updating itself
- *discrete*, i.e., there are finite states that the environment can reach
- the agents know the "laws" of the environment, meaning it is a *known* environment
- it is a *multi-agent* environment with more than three MAS interacting

The agents, playing a crucial role in the simulation environment, follow predefined communication protocols and interact via software APIs and message passing.

This section provides the theoretical background for developing ABS frameworks. It defines the characteristics of the proposed solution in context, which helps realize the design and modeling of the EMA architecture implemented in a co-simulation framework.

3.3 SIMONA - a Distribution Grid Simulation Platform

This section introduces SIMONA[2], a recently developed agent-based discrete-event, flexible, and holistic grid simulation model that generates grid and system participant time series to support active distribution system planning, operation, and analysis.

[2]https://simona.ie3.e-technik.tu-dortmund.de/

The most critical agent entities in SIMONA are the GA and the *System Participant Agents* (SPA) that represent the numerous DERs in the distribution grid environment. These agents follow the concept of *actors* and interact with each other to solve the power flow for multi-voltage level grids. The design of SIMONA follows a bottom-up architecture, and the operation is behavior-oriented, where the agent behavior is of utmost importance. Additionally, SIMONA provides a flexible and efficient interface that allows connection with other software models, MAS, or co-simulation frameworks. Figure 3.4 gives a schematic overview of the simulation architecture in SIMONA.

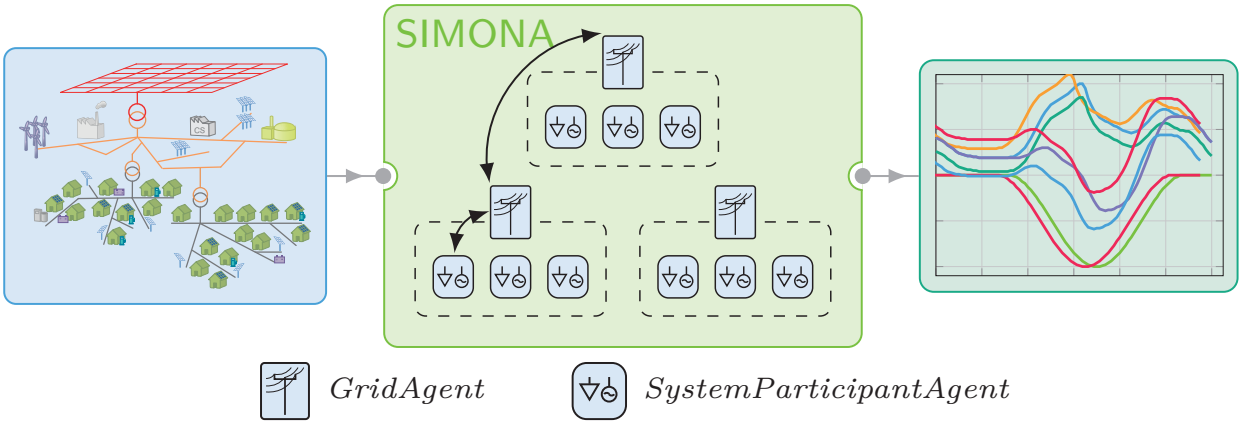

Figure 3.4: High-level Overview of the SIMONA Environment

SIMONA was first introduced in [111] and [112] as an agent-based simulator for pure distribution grid planning approaches. However, the current version stems from [100] and [113], where the authors introduce several agent concepts, such as scheduling services and time management schemes, to broaden the scope of the simulator. The DSOs and researchers in multi-energy systems at the distribution grid level are the primary target users for SIMONA. Potential future applications of SIMONA can study the impact of new technologies and entities or control and optimization algorithms on the distribution grid. Moreover, the application case can be extended to multiple coupled sectors in a multi-energy environment.

This thesis extends the application of SIMONA in a co-simulation environment to interact with several DERs with generation or demand capacities, offering grid-oriented flexibility services. The central components of SIMONA that are important to the development of the present work are the GA, the power flow computation, and the interface that allows communication with external agents or simulators. Therefore, the upcoming sections will briefly state the fundamentals of SIMONA modeling and

the interaction between the agents to concurrently solve the power flow equations. The EMA is not part of the SIMONA environment in this implementation because the third-party aggregator acts as the EMA, not the DSO. It interacts with SIMONA via the co-simulation platform as an external model or agent. However, the DSO could also function as the EMA under proper technical and regulatory requirements.

Conceptual Overview

SIMONA is a closed, self-contained system with core components of an *agent system model*, an *environment model*, and a *simulation architecture* following the general structure of an ABS. Figure 3.5 gives the conceptual overview of the primary components in SIMONA.

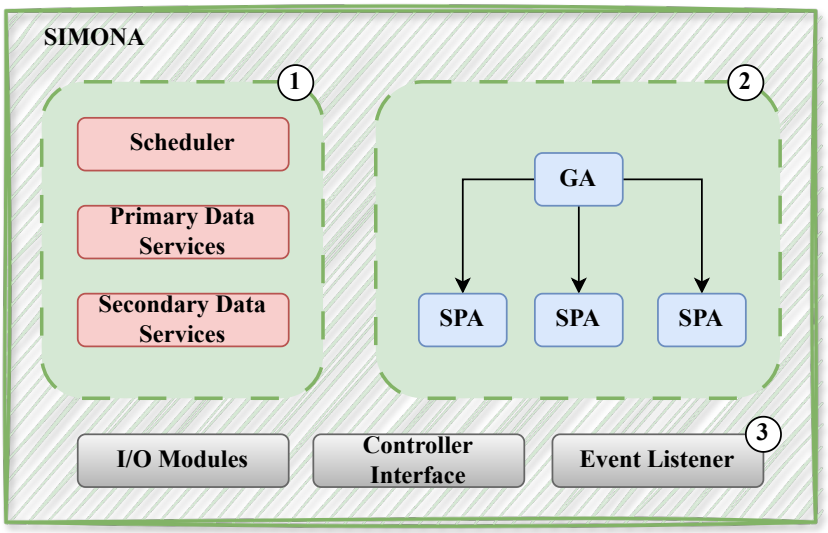

Figure 3.5: High-Level Aggregated Concept of the SIMONA Environment

Agent System Model (1)

This model constitutes the vital autonomous agent entities interacting with each other. There are two different agent entities and their instances, the GA and the SPAs. Each GA is responsible for a galvanically isolated subgrid, including the system participants connected to it. Therefore, the GA represents the underlying physical properties of the electricity grid and coordinates the interactions between the connected SPAs and itself. The SPAs are generally connected DG units with solar or wind generation. In this work, the concept of SPAs has been extended to include

flexible consumers who can inject power back into the distribution grid. SIMONA can simulate multiple voltage levels and calculate the total power flow from the high-voltage grid to low-voltage grids; hence, numerous instances exist of the GA and the SPAs. However, in the application case of this thesis, the environment consists of a single low/medium voltage distribution grid and consists of only one GA with several connected SPAs. To perform its primary function of solving the power flow equations to calculate or update the grid state, the GA should know or request the power generation or consumption from the SPAs, i.e., the generation or demand at the DER units. The underlying distribution grid is represented as a graph structure (N,E), where N is the number of nodes that could be power-regulated (pq), voltage-regulated (pv), or reference nodes. E is the number of lines connecting the grid nodes. Kirchoff's laws describe the power flow through such a grid as:

$$\vec{i} = [Y] \cdot \vec{v} \tag{3.2}$$

where, $\vec{i}$ are the nodal currents, $[Y]$ is the nodal admittance matrix, and $\vec{v}$ is the nodal voltages.

Environment Model (2)

This model provides the artificial representation of a real-world environment. It is also responsible for providing global state information, i.e., current simulation time step or synchronization protocols to the *agent system model*. It is composed of three main services:

- The **Scheduler** manages the chronological execution order of events, i.e., time synchronization between participating agents.
- **Primary Data Services** is responsible for providing model data for externally connected agents that is valuable during the power flow calculation, such as the active power generation values for the connected DG units represented as SPAs.
- **Secondary Data Services** help the SPA agents in SIMONA to calculate their model data, i.e., weather data helps compute the PV generation output of a single entity. This thesis does not use *secondary data services* as the model data for connected DERs are derived from externally connected MAS or agents who provide *primary data* to the SPA instances of SIMONA.

Simulation Architecture (3)

This component provides the platform to form physical connections to external agents such as the EMA or the DER units. It also provides the protocol to control the SIMONA simulation, i.e., request a power flow computation.

Power Flow Computation

A proper understanding of the GA's internal structure and operational characteristics will help comprehend the power flow computation algorithm employed within SIMONA.

Grid Agent

The internal structure of the GA consists of two parts - a physical model and a behavioral model. The physical model contains the grid topology (N,E) and associated parameters such as the nominal apparent power S_{nom} and the nominal voltages V_{nom}^{n} of all nodes $n \in N$, and references to the assets connected to its grid, which are also represented as agents by the SPAs. The GA uses the Newton-Rhapson (NR) method to solve its local power flow calculations, using additional configuration parameters such as convergence threshold ϵ_{sweep} for the outer loop, convergence criterion ϵ_{NR} for the local power flow calculation, and a maximum sweep counter $i_{sweep,max}$. The behavioral model follows the *Finite State Machine* (FSM) paradigm having respective agent states. The mathematical representation is given by:

$$GA = \langle \mathbf{X},\mathbf{A},\mathbf{S},\mathbf{M},\mathbf{Y},\delta_{int},\delta_{ext},\lambda,ta \rangle \tag{3.3}$$

where, $\mathbf{X}$ is the set of all input events, $\mathbf{Y}$ is the set of all output events, and $\mathbf{A} = \{(s,m)|s \in S,m \in M\}$ is the set of agent states. SIMONA defines the agent state as consisting of a basic state $\mathbf{S}$, the state the agent can be in, and a physical model state $\mathbf{M}$, the state an agent can achieve. Data or control signal events can interrupt the current agents' states to allow a transition to another state. The time advancement function $ta : \mathbf{A} \rightarrow \mathbb{R}^{+}_{0,\infty}$ of the agent entity defines the maximum time an agent stays in a specific state if no interruption, e.g., due to an external event, occurs. The internal and external transition functions describes state changes $\delta_{\text{int}} : \mathbf{A} \rightarrow \mathbf{A}$ and $\delta_{\text{ext}} : \mathbf{A} \times \mathbf{X} \rightarrow \mathbf{A}$. Lastly, $\lambda : \mathbf{A} \rightarrow \mathbf{Y}$ determines possible output events. Figure 3.6

visualizes the FSM structure of the GA.

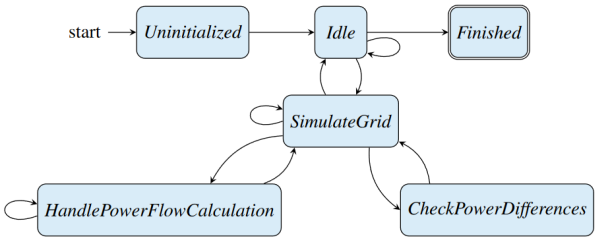

Figure 3.6: The FSM Model of the GA

The interaction protocol between the scheduler, GA, and the SPAs follows the steps of Algorithm 3.1 iteratively until convergence:

Algorithm 3.1: Agent Interaction Protocol to Solve the Power Flow

1. The scheduler triggers the GA to execute a power flow routine
2. the GA starts from the root of the graph and travels to the leaves, requesting the power feed-in or consumption from every SPA connected to the grid
3. After receiving the requested information, the GA performs the local power flow calculation using the NR method
4. If converged, the algorithm terminates; otherwise, the GA restarts the operation from the root

Unlike general SIMONA simulations, in this proposed framework, the GA reports the updated grid state back to the primary EMA after it has completed the power flow calculations to support the optimization routine. Mathematical details for the distributed power flow routine in a multi-voltage level grid simulation are given in [self.1].

This section furnishes a detailed overview of SIMONA by describing its environment, primary agent entities, and communication protocols that facilitate power flow computation.

3.4 Agent-Based Hierarchical Energy Management Architecture

This thesis proposes a hierarchical agent-based EM architecture to execute an optimization routine involving several participants in the electricity market and the connected distribution grid. The central component of the architecture is the primary EMA which is capable of offering DERMS services related to *aggregation*, *simplification*, *optimization*, and *translation* as described in Chapter 1. The primary EMA represents a DER aggregator in a real-world scenario. The GA in SIMONA represents the DSO, which is also the supplier. Numerous parameters must be defined to construct the EM architecture successfully to mimic a real-world scenario and its regulatory conditions. What are the different participants included in the environment? What type of data does the agent have access to from all involved participants? What kind of interactions does the EMA need to establish with other agents in the system? What extent of system control and observability is allowed to the EMA? What should the objectives and solution algorithm be for the optimization? What type of constraints restrict the problem? Figure 3.7 represents a conceptual view of the primary EMA positioned in the electricity market, identifying the other agent-based models and their interaction according to Assumption 3.1.

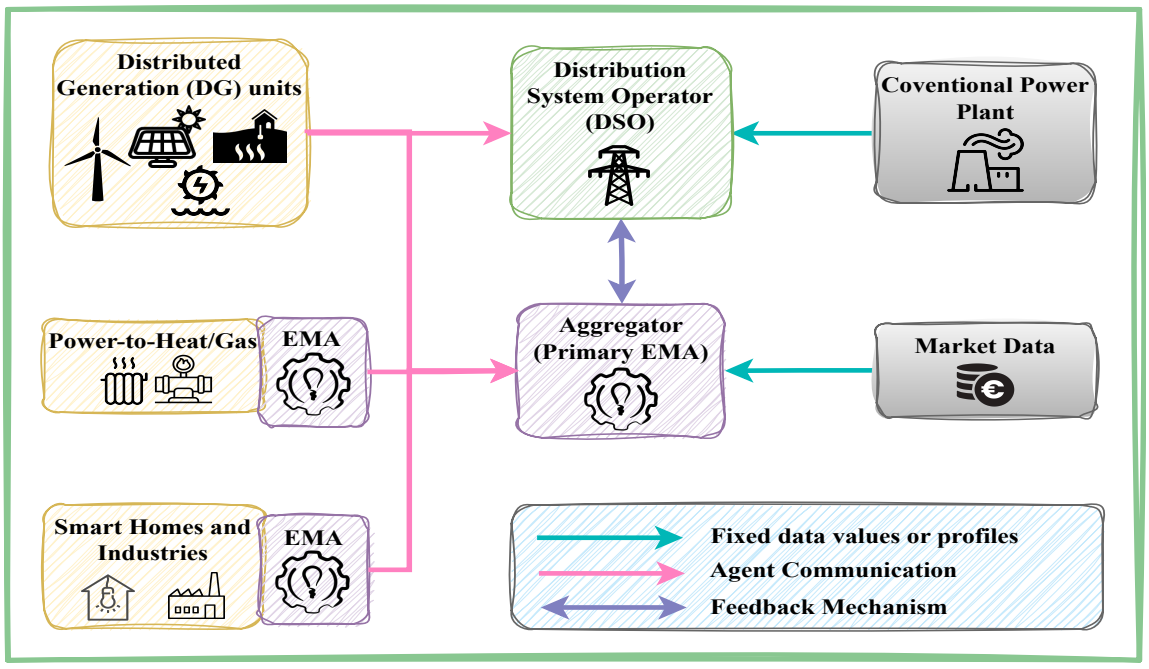

Figure 3.7: Conceptual Overview for Energy Management in the Distribution Grid

3.4.1 Model Specifications

This thesis is dedicated to the crucial area of distribution grid control, assuming the existence of a local flexibility market at this level. Therefore, the TSO and the balancing market are outside the scope of this work. However, future extensions could lead to a comprehensive energy management architecture from transmission to distribution networks. The model specifications are as follows:

Involved Participants

The proposed architecture engages with diverse participants, including DG units and residential and industrial consumers. These participants, such as the distribution grid operator, DG units with PV and wind generation capacities, and DR or flexible load consumers in residential and industrial sectors, can be individual MAS or agent models, all part of the co-simulation environment. It is important to note that these are distinct from the existing SPAs in SIMONA. During the power flow computation, the data received from the dispersed participants are fed in as the *primary data* of the respective SPA in SIMONA. Hence, these are externally connected MAS or agents represented by SPAs in SIMONA. The DSO is also the electricity supplier, as per the assumptions.

Data Flows between the Agents and the Primary EMA

The different kinds of data provided by the involved participants are as follows:

- Smaller DG units share their power generation values with the primary EMA to bid an aggregated value in the market. Standalone DG units with sufficient capacity can bid their energy directly into the market.
- The flexible residential and industrial prosumers provide their demand profiles, i.e., power consumption values after the individual home EMA or industrial EMA calculates the optimal demand following goals of self-optimization, profit-seeking behavior, etc.
- The DSO shares vital *key performance indicators* (KPIs) that signal changes in the grid state under the impact of the current supply and demand.
- The market provides the historical spot market profiles. Therefore, this interaction cannot be regarded as agent communication but as environment variables.

Control Flow

The primary EMA can request permitted data from the participants required for the optimization process and trigger a computation in the individual EMAs or the GA when the calculation needs to be updated to reach optimal goals.

Objectives

With so many influencing factors at the distribution grid level, more than a simple economic objective is needed as it might conflict with the environmental objective. Moreover, supporting renewable growth might lead to technical degradations in the system, increasing the electricity bills for end users. Therefore, the EM problem in a power system is multi-objective and should consider the system's economic, environmental, and technical aspects.

System Constraints

Several constraints govern the system intricately, including the generation capacities of the DG units, reserve capacity in the distribution grid, and operational constraints dictated by the physical laws of the electricity grid. These constraints present significant challenges to the system and add to the complexity of the optimization process.

Functionalities of the EMA

Following the communication protocols and with the help of the available data, the primary EMA performs the DERMS functionalities in the following way:

- *aggregates* the volume for smaller DG units and DR participants to form a sizable capacity for market trading or provision of grid-oriented services,
- *simplifies* the grid-oriented output, i.e., grid-serving load considering granular details of the involved participants through coordination with the individual EMAs,
- *optimizes* for system goals in economic, environmental, and technical terms while respecting the network constraints. Additionally, the individual home EMA or an industrial EMA runs a desired algorithm to achieve optimal and flexible load profiles and

- *translates* and maintains a cohesive data flow between the participants, i.e., the demand or generation profiles from the participating agents should be intelligible by the distribution grid, or market signals should be easily understandable to the participant agents. Aggregating data over time may arise as different MASs have different operation time resolutions.

Figure 3.8 shows the agent-based hierarchical EMA architecture [self.2], the design of which imitates the real-world distribution grid ecosystem. The pink arrows represent the data flow between the participants, and the green arrows show the control flow and direction stemming from the primary EMA to the respective agents. The individual EMAs at the DER units and the primary EMA form a hierarchical architecture. The optimization is solved in a distributed feedback mechanism with the GA. Therefore, the proposed architecture uses a combination of hierarchical and distributed structures. Additionally, the feedback loop facilitates an integrated DER aggregator and utility DERMS deployment.

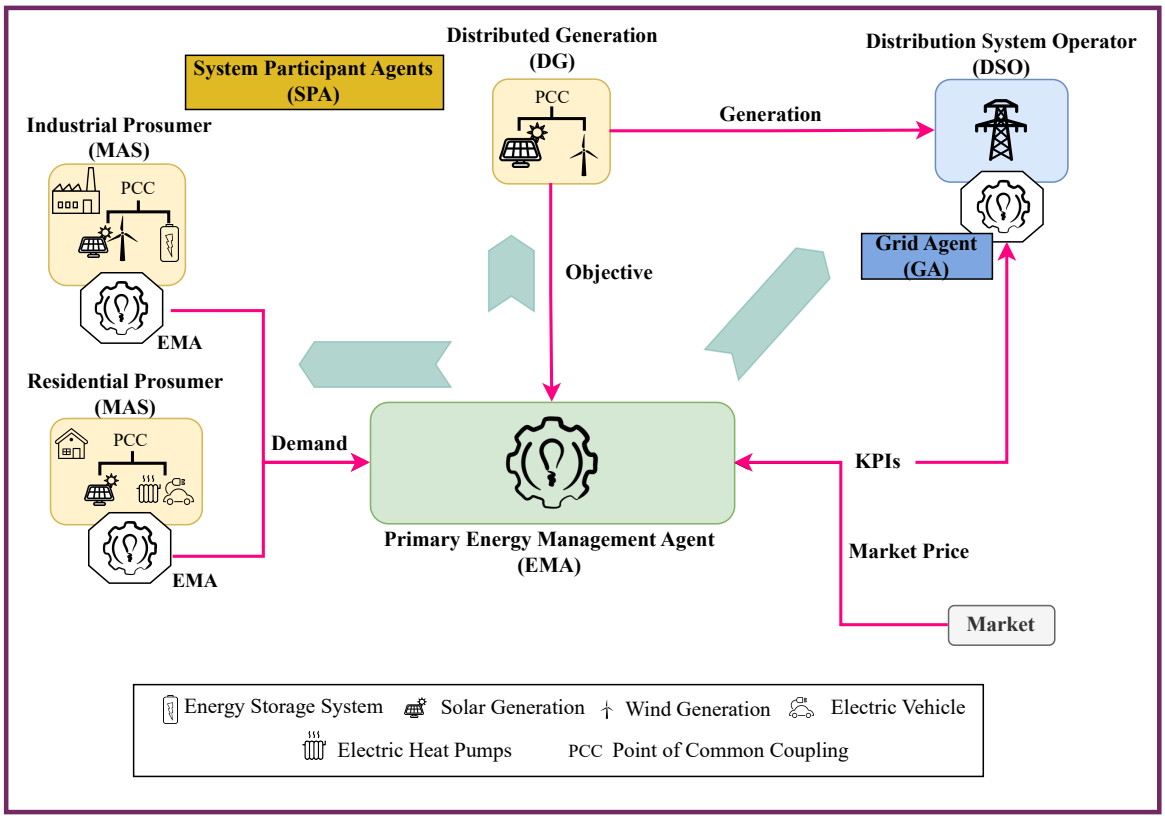

Figure 3.8: Agent-Based Hierarchical Energy Management Architecture

3.4.2 Agent Interaction between GA, SPAs, and the Primary EMA

The primary EMA uses an *online*, distributed optimization routine to solve for its multiple objectives. This section outlines the agent interaction protocols between the primary EMA, GA, and the SPAs present in the simulation environment. Figure 3.9 illustrates the communication protocol between the several agents and the EMAs, where green boxes represent all agents that are either built within SIMONA or receive their primary data from external agents, yellow boxes are the EM agents that can be developed within SIMONA or connected as external agents, and the brown boxes represent the industrial and residential prosumers which are external MAS. Solid arrows denote communication lines with the involvement of SIMONA, and dashed arrows represent communication with externally connected MAS. The message-driven toolkit, AKKA, facilitates communication between agents in SIMONA and uses software messages. Software APIs facilitate the interaction between external agents and SIMONA.

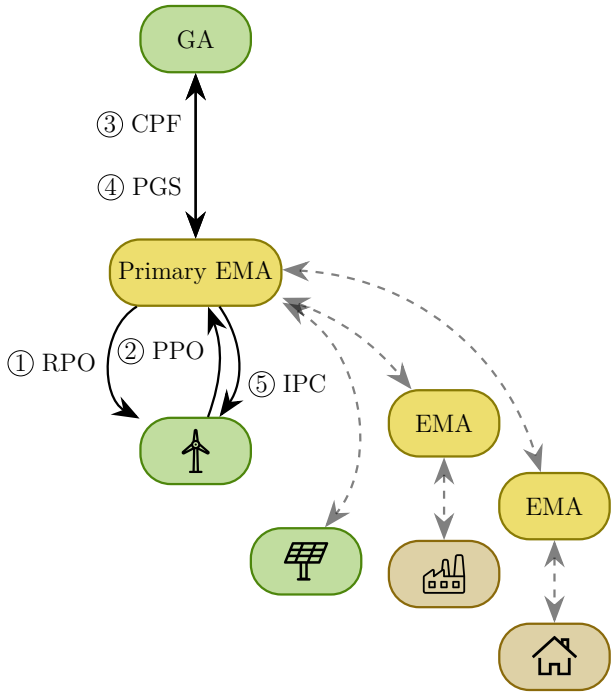

Figure 3.9: Interaction Protocol between the Primary EMA, GA, and SPAs

Algorithm 3.2 provides the step-by-step interaction protocol. However, the granular details of the optimization routine and related agent communication protocols are presented in Chapter 4.

Algorithm 3.2: Agent Interaction Protocol with the Primary EMA

① The primary EMA requests current power generation or consumption from all available parties using the *RequestPowerOptions* (RPO) message,

② The individual EMA instances relay the request to their underlying devices,

③ The connected devices provide their available power and objective function values to their individual EMAs,

④ Individual EMAs send self-optimized demand, and the DG units send their available power to the primary EMA via the *ProvidePowerOptions* (PPO) message,

⑤ The primary EMA shares the power generation and demand with the GA and triggers a power flow computation via the *Compute Power Flow* (CPF) message,

⑥ The GA computes the power flow and reports the updated grid state back to the primary EMA with predesigned KPIs indicating constraint violations via the *ProvideGridState* (PGS) message,

⑦ The primary EMA checks for convergence in terms of the objectives and constraint violations in the system,

⑧ In case of convergence without constraint violations, the primary EMA sends *IssuePowerControl* (IPF) message to everyone and sets the optimal solution for the current time step; otherwise, it restarts the process by requesting updated powers ①

This section details the agent-based hierarchical EM architecture, including model specifications and interaction protocols with other system participants. It also provides the communication protocol between the GA from SIMONA and the newly developed primary EMA.

3.5 Implementation in a Co-Simulation Framework

As already discussed, the new-age energy systems are a complex socio-technical system whose transition to a sustainable entity demands changes in various domains and dimensions spanning the demand side (consumer practices), supply-side (advanced technologies and infrastructure), intermediate layers (transmission, distribution, and market), and institutional dimensions (policies and regulations). Evaluating future transition pathways of such complex systems in terms of predefined sustainability targets (e.g., economic, environmental, technical, and social) is helpful to policy making that boosts an ecological expansion of the electricity infrastructure while being cost-efficient [114]. *Co-simulation* approaches aim to couple diverse models in an integrated simulation scenario, where the particular elements of each model are incorporated into the model without inaccurate simplifications [115]. The mitigating technique of co-simulation is the appropriate orchestration of all involved simulators regarding time, control, and data flows [116]. Using co-simulation for modeling socio-technical transitions brings the following benefits:

- inherently supports holistic simulation that integrates multiple domains with sub-system interaction,
- allows reusing established, well-suited, and well-developed tools from specific domains,
- simplifies the data and control flows between simulators via suitable scenario definitions,
- permits simulators to remain black boxes, i.e., modelers from different disciplines do not need to know the specifics of the other simulators

However, co-simulation does have its share of challenges listed in [117]:

- Coupling interdependent and diverse models is a complex and challenging task, i.e., involved simulators should be able to understand each other in a co-simulation environment.
- The complexity of multiple coupled models complicates validating scenarios, might decrease the simulation robustness, and reduce the performance.
- Usually, transition processes are long-term scenarios where the models have diverging time scales that need specific handling.

In the context of this thesis's current problem, there are many interdependencies between the different participants in the distribution grid simulation scenario [self.3].

For example, consumer demand and power generation from DG units considerably impact the grid state and the players' economic objectives. Similarly, grid stability should influence the controllable loads and generation for a seamless electricity supply. Therefore, the data flows between the interacting models and the expected simulation output should be well defined. An information model approach [118] that provides an ontological structure to define data flows between models was adopted to assist in the process. This meticulous planning handles the first challenge associated with co-simulation approaches. The second challenge is responsible for the need for micro-level validation of individual simulators and macro-level validations of the coupled co-simulation framework. Macro-level validations are considerably challenging [119], and therefore, intermediate 'meso-level' validations were selected by modularizing the framework and connecting two or more simulators simultaneously to solve a sub-problem. The co-simulation platform *mosaik* handles the third challenge related to time synchronization. Figure 3.10 represents the co-simulation framework denoting the different models or simulators that act as the software equivalent of their respective real-world counterparts.

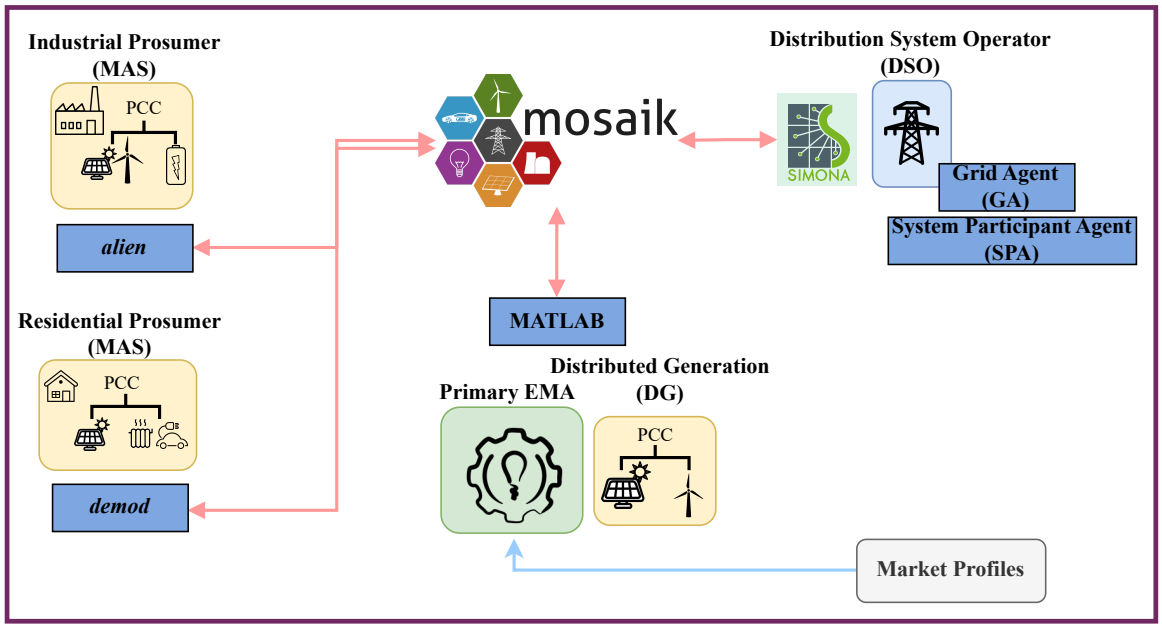

Figure 3.10: Co-Simulation Framework with Individual ABS for Involved Participants

The following sections give a brief insight into the operating fundamentals of the

different simulators — *mosaik*, *demod*, and *alien* to better understand the connection between different simulators and the formulation of residential and industrial demand profiles used in the application case.

3.5.1 *mosaik* - a Co-Simulation Platform

For co-simulation, many frameworks exist, as compared in [120]. The framework *mosaik*[3] was selected here because of its focus on usability and flexibility, as described in [121], and its availability as open-source software. The core of *mosaik* is Python-based and provides a Component-API to connect models from diverse programming languages and integrate them into scenarios with a Scenario-API.

The coupling of diverse models in a co-simulation increases complexity, hampers the validation and robustness of simulation, and raises performance issues. For a robust simulation, the observer/controller architecture described in [122] is proposed, which observes parts of the simulation for critical states and reacts under specific conditions or takes control. Performance, albeit not the primary focus of *mosaik*, can be addressed by distributing computation to multiple computers and optimizing the temporal aspects of a scenario, e.g., by calculating a set of representative days instead of doing a full-year simulation.

Co-simulation frameworks generally address time synchronization issues, as orchestrating the different simulators by organizing their data flows and execution times is one of their primary tasks. A new *mosaik-aggregator* component has been developed for substantial differences in time scale. It can be placed between two simulators, aggregate the outputs of one simulator over time, and provide the aggregated results as input to the other simulator. Thus, simulators do not need to adapt to different time scales and reduce their universality.

SIMONA uses a top-level agent to connect to the *mosaik* APIs. This top-level agent translates control signals from *mosaik* to messages comprehensible by the underlying agents such as GA and the SPAs. Within this framework, the primary EMA triggers the computation of every simulator, i.e., the primary EMA orchestrates the control with the help of *mosaik*. In a real-world scenario, the aggregator should combine the operations of the primary EMA and *mosaik* to facilitate integrated energy management schemes.

[3] `https://mosaik.offis.de`

3.5.2 *demod* - a Residential Demand Simulator

Household load profiles are generated using *demod*[4], a Python library that allows energy demand models to be assembled in a modular and customizable manner [123]. *Demod* adopts a *Time Use Data* (TUD) -based approach, i.e., explicitly models the activity sequences of household members and then associates each activity with the use of one or more devices through a time-dependent probability factor. Thus, load profiles can be obtained with high spatio-temporal resolution, i.e., 1 minute at the level of individual appliances. To better characterize the diversity of space heating across households, self-reported data about the thermostat settings of heat pump users was collected and analyzed. Data collection was conducted in November and December 2022 and included 831 families from Germany and German-speaking cantons of Switzerland that owned or rented homes heated by electric heat pumps. Daily set-point temperature profiles with a time resolution of 30 minutes were derived using self-reported data on space heating practices. The selected PV and EV penetration levels are arbitrary. The following *demod* modules are employed to simulate daily residential demand:

1. **Transit occupancy simulator**: This simulator employs a Markov-chain Monte Carlo simulation approach to generate household occupancy profiles. It considers the number of active or asleep residents and their location, i.e., the number of people at home or outside, to generate state profiles independently for each household.
2. **Appliance and lighting simulators** The **appliance simulator** aggregates activity profiles at the household level depending on the use of electrical appliances in the home. The approach is either deterministic or stochastic depending on the type of appliance, i.e., whether the device is level of usage or activity-dependent and has a constant or stochastic duration. Depending on the appliance switch-on/off profiles and technical characteristics, such as power rating, the simulation generates the daily electrical load profiles at the appliance level with a time resolution of 1 minute. It applies a similar approach to model domestic hot water demand independent of space heating. The **lighting** simulator generates profiles with the help of switch-on and -off events, where irradiance and occupancy are inputs.
3. **Space heating simulators** The energy demand for space heating derives from a

[4]https://pypi.org/project/demod/

complex interaction between user behavior, weather parameters, such as outdoor temperature, irradiance, etc., and technical systems, such as heating supply and control systems, building thermal properties, etc. This simulator consists of three *demod*-modules: (i) building thermal dynamics, (ii) heating control system, and (iii) heat pump system.

The **building thermal dynamics** simulation employs a lumped-capacitance model (4R3C). It solves the heat balance between the different elements of the house by utilizing a discrete time interval approach. The distinct components are namely indoor, emitters, outdoor, and walls. The simulation takes the thermal gains and losses into account. The building type considered for the model parameters is that of a large single-family renovated house (*Improved detached*).

The **heating controller** uses a simple control strategy to match heat supply and demand. Taking the set-point temperature required by the occupants as input, it calculates the difference with the current indoor temperature. After that, the control signal delivers the heat demand from the buffer tank and the heat supply to the emitter system. The controller ensures that temperature limits are restricted for space heating demand. Concerning the heating supply side, the controller calculates the required heat by the heat pump to maintain the hot water buffer tank at its target temperature.

Finally, the **heat pump** simulator is developed using *hplib* [124]. This python library uses the public Heatpump Keymark datasets [125] to parameterize a dynamic model of heat pump operation where the *coefficient of performance* (COP) of heat pumps and electrical and thermal output are interdependent and dependent on the temperature of the heat source and heat sink. Figure 3.11 represents the different types of generated heating control patterns.

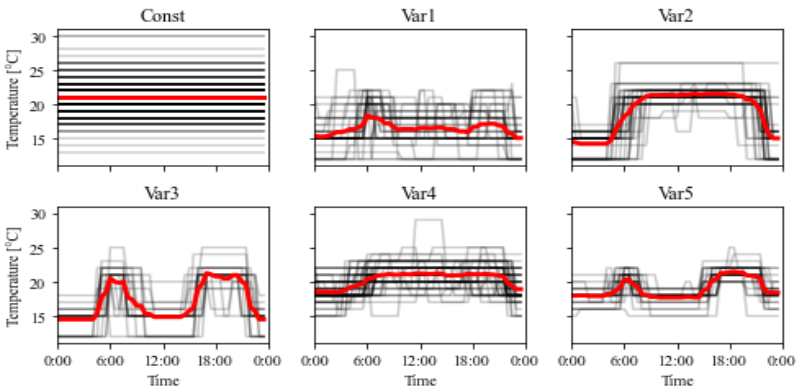

Figure 3.11: Different Types of Heating Control Patterns in the Residential Sector

3.5.3 *alien* - an Industrial Demand Simulator

Alien aims to represent industrial companies, their energy usage, and their energy management agents (EMA). They actively cost-optimize their energy consumption and production by managing their self-load, solar power production, and flexibility from storage. One of the most popular uses of *battery energy storage systems* (BESS) in industrial networks is in peak shaving applications to help reduce electricity bills without affecting production [126, 127]. Due to machinery start-ups, industries produce frequent high power peaks in their demand during operation, impairing power quality and grid stability of electrical power systems. Moreover, grid infrastructure design must take these power peaks into account, which amount to the highest load of the system, making the power systems underutilized for most periods. The network operator imposes a *power price* on industrial consumers on their maximum power demand as compensation. Thus, industrial consumers pay an additional fixed peak power price with the regular energy consumption price [128]. Using a BESS to discharge stored power during high-demand periods can avoid power peaks. However, appropriate dimensioning of the BESS that considers self-aging, charge/discharge efficiency, investment, electricity costs, etc., is essential to achieve optimal benefits [129, 130]. *Alien* extends the use of BESS following [131] and [132] to calculate the optimal battery size depending on various cost factors and technical specifications. Moreover, it uses a stochastic optimization routine to generate optimal day-ahead battery scheduling that considers PV generation uncertainty [133]. Figure 3.12 gives the architecture of an industrial grid with flexible components such as PV and BESS.

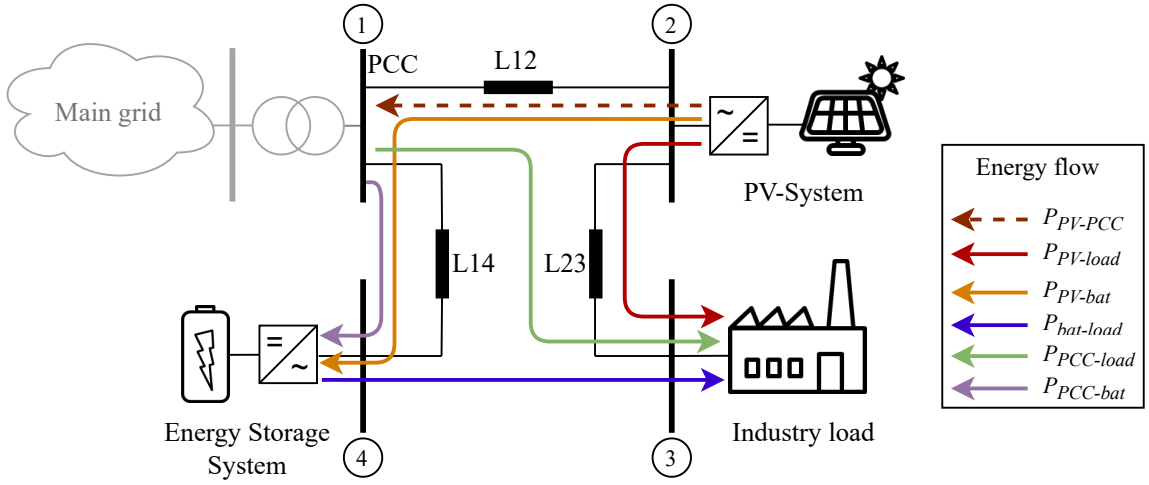

Figure 3.12: Structure of an Industrial Prosumer

Besides using *alien*, this thesis incorporates another industrial demand simulator that optimizes production processes and models the industrial demand considering voltage sensitivity. The static ZIP load model is a well-known model in the power industry that represents the relationship between electrical consumption (active and reactive power) as a function of the applied voltage. As is widely known, the acronym ZIP refers to the three characteristics that an electric device possesses, i.e., constant impedance, *"Z"*, constant current, *"I"*, and constant power, *"P"* [134]. In this paper, we use the ZIP model to represent the industrial load, which is optimized using an AC-OPF algorithm to determine the resulting load at PCC with the distribution power system. The optimization goal is to achieve atypical grid usage, i.e., maximize self-consumption via an installed PV unit and reduce energy exchange with the grid. As industrial electrical consumption changes with time, the ZIP parameters must change, too. For example, a set of electric devices active at time t might not remain active at time $t + n$ [135]. Besides, industrial processes generally consider predefined operating conditions (i.e., loads can be switched on/off depending on production status) according to the type of process [136]. Therefore, a time-variant ZIP load model [137] is as follows:

$$P_t = P_{0,t}(\alpha_{1,t}\tilde{V}_t^2 + \alpha_{2,t}\tilde{V}_t + \alpha_{3,t}) \tag{3.4}$$

$$\tilde{V}_t = V_t/V_0 \tag{3.5}$$

$$\alpha_{1,t} + \alpha_{2,t} + \alpha_{3,t} = 1 \tag{3.6}$$

where P_t denotes the active power consumption at time step t, $P_{0,t}$ represents the nominal active power at nominal voltage V_0, the latter is generally assumed to be 1.0 p.u., $\alpha_{1,t}$, $\alpha_{2,t}$, and $\alpha_{3,t}$ are the time-dependent parameters representing the constant impedance, constant current and constant power features, respectively.

The parameter identification procedure for ZIP coefficients is based on a least-squares optimization problem. Let $\hat{P}_t$ be the estimated active power at time step t, $\vec{P}_d$ denotes the vector of measurements for each time step k ($d \epsilon D$), and D stands for the set of measurements. Therefore, the resulting minimization problem is formulated as follows:

$$\min \quad P_{0,t},\alpha_{i,t} \sum_{(d \epsilon D)} (\overrightarrow{P_d} - \hat{P}_t)^2 \tag{3.7}$$

subject to the non-convex constraints (3.4) and (3.6). Detailed mathematical descriptions of the models are available in [self.4].

In this distinctive co-simulation framework, various simulators, each developed in different software paradigms and operating on different time resolutions, interact with each other and the primary EMA. This interaction, facilitated by the co-simulation platform *mosaik*, is instrumental in solving a distributed optimization routine with multiple objectives.

Chapter 3 Summary and Chapter 4 Preview

Key takeaways from this chapter:

3.1) Assumption related to the regulatory market structure

3.2) Agent-based simulation concepts with a special focus on SIMONA

3.3) Proposed hierarchical and agent-based energy management architecture for the distribution grid ecosystem

3.4) Integration of the proposed architecture within a co-simulation framework

Highlights for the next chapter:

a) Description of the multi-objective distributed optimal power flow algorithm, which is the primary function of the EMA

b) Interaction protocols between various agents that assist in the distributed solution of the multi-objective optimization routine

4 Multi-Objective Distributed Optimal Power Flow

This chapter describes the proposed multi-objective distributed OPF (MO-DOPF) algorithm in detail, which is the leading service offered by the primary EMA introduced in the previous chapter. The optimization routine solves for operation costs, CO_2 emissions, power losses, and voltage deviation subject to physical and operational network constraints. The simplicity, ease, and intuitiveness of gradient-descent methods guide the selection of an online or real-time Gradient projection algorithm to solve a singular optimization problem [78]. This work extends the existing algorithm to apply to multi-objective problems by combining Tchebycheff's decomposition method [138], which converts the multi-objective optimization into a set of scalar subproblems. An alternative gradient computation method broadens the algorithm's scope to meshed networks. An *online* algorithm iterates only on variables related to controllable devices (e.g., distributed generation, intelligent loads) in a closed-loop feedback interaction with the grid, which allows even intermediate iterates to satisfy power balance equations by design [139]. In the EM architecture presented in this work, the primary EMA and the GA participate in this closed-loop feedback mechanism to solve the optimization problem. Moreover, unlike available literature, the Gradient projection algorithm is formulated hierarchically, where the primary EMA executes the optimization without access to sensitive information from the participating distribution grid or prosumers.

The chapter begins with the model description, which includes the formulation of objectives and network constraints in Section 4.1. This section details the underlying physical laws driving the network and discusses the constraint-handling techniques. Section 4.2 delves deep into the methods of gradient computation used in this thesis for radial and meshed networks. Section 4.3 discusses the Gradient projection algorithm step-by-step to solve the OPF problem for a single objective. Finally, Tchebycheff's decomposition method to convert the multi-objective problem into a set of singular subproblems is discussed in Section 4.4. This section also gives insight into multi-objective optimization fundamentals such as *Pareto optimality* and its associated processing. Finally, a flowchart describing the solution algorithm working within the EMA architecture describes the task flow between the participant agents.

4.1 Model Formulation

This section assumes the distribution grid's default topology to be radial, following the general convention. However, it provides the differences in notations and assumptions for meshed networks for the alternative gradient computation method.

4.1.1 Distribution Grid Topology and Parameters

A connected and directed tree graph (N^+,E), models the distribution grid network, where $N^+ := 0 \cup N$, $N := \{1,2,...,n\}$, and $E \subseteq N^+ \times N^+$. For meshed networks, the graph is undirected, keeping everything else similar. Each i in $i \in N^+$ represents a "node", and each $(i,\ j) \in E$ represents a "line" connecting the nodes. The slack bus or the *Point of Contact* (POC) with the upper voltage network is denoted by 0 and acts as the root of the tree (in the case of radial networks).

For each bus $i \in N^+$, let V_i be the complex voltage at node i and $v_i = |Vi|^2$ the square of its magnitude, e.g., if the voltage is $V_i = 1.05\angle 120°$, then $v_i = 1.05^2$. For each line, $(i,\ j) \in E$, let $z_{ij} := r_{ij} + ix_{ij}$ where $r_{ij} > 0$ and $x_{ij} > 0$ are the line resistance and reactance respectively. I_{ij} is the complex current and $l_{ij} = |I_{ij}|^2$ its squared magnitude, e.g., if the current is $I_{ij} = 0.5\angle 10°$, then $l_{ij} = 0.5^2$.

> ***Assumption 4.1:*** *Customarily, the nodal voltage at the slack or reference bus* 0 *is such that* $V_0 = 1\angle 0°$. *However, with the advent and increasing use of tap changing transformers, the voltage at bus* 0 *can also be set at* 110% *or* 90% *of the nominal value, i.e.,* $V_0 = 1.1\angle 0°$ *p. u. or* $V_0 = 0.9\angle 0°$ *p.u.*

Let $s_i = p_i + iq_i$ be the net complex power injection at bus i with p_i and q_i as the real and reactive power injections, respectively.

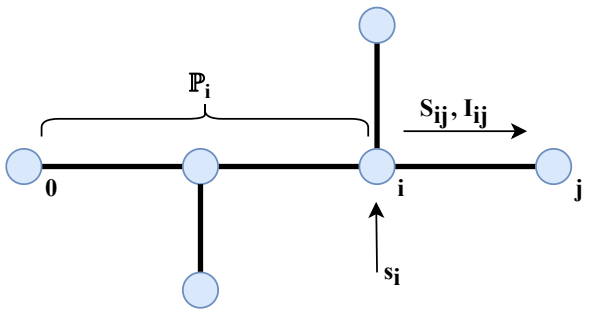

Figure 4.1: Grid Parameters

Let $S_{ij} = P_{ij} + iQ_{ij}$ be the sending end complex power from buses i to j with P_{ij} and Q_{ij} as the real and reactive power respectively. This thesis mainly uses branch flow models in the real domain, so notations such as s_i can either denote the complex number $p_i + iq_i$ or the real pair (p_i, q_i) depending on the context; similarly, for other variables z_{ij}, V_i, S_{ij}, I_{ij}. Let $\mathbb{P}_i$ denote the unique path from bus 0 to bus i. The path $\mathbb{P}_i$ is well-defined for radial networks with a tree topology. Figure 4.1 summarizes some notations.

Let $m := |E| = n$ be the number of lines in E. The bus injections, $x := (p_i,q_i,i \in N) \in \mathbb{R}^{2n}$, and other dependent variables, $y := (p_0,q_0,v_i,i \in N; P_{ij},Q_{ij},l_{ij},(i,j) \in E) \in \mathbb{R}^{3m+n+2}$, together with v_0, satisfy the physical laws that govern the power flow:

$$\sum_{k:j\to k} P_{jk} = P_{ij} - r_{ij}l_{ij} + p_j, \quad \text{for} \quad j \in N^+ \tag{4.1a}$$

$$\sum_{k:j\to k} Q_{jk} = Q_{ij} - x_{ij}l_{ij} + q_j, \quad \text{for} \quad j \in N^+ \tag{4.1b}$$

$$v_i - v_j = 2(r_{ij}P_{ij} + x_{ij}Q_{ij}) - |z_{ij}|^2 l_{ij}, \quad \text{for} \quad i \to j \tag{4.1c}$$

$$v_i l_{ij} = P_{ij}^2 + Q_{ij}^2, \quad \text{for} \quad i \to j \tag{4.1d}$$

where i in (4.1a) and (4.1b) is the unique bus between bus 0 and bus j. Using algebraic power balance equations to model the grid is sufficient for studying slow timescale behavior or steady state operation, which is the scope of this work. The group of equations in (4.1) are called the *DistFlow* equations and were introduced in [68, 140]. M. Farivar *et al.* generalized these equations for meshed networks in [141]. The use of DistFlow equations over conventional AC power flow equations is in its unique structure, which allows the development of computationally efficient and numerically robust solution algorithms.

4.1.2 Control and Dependent Variables

The optimization variables are classified into two categories based on Assumption 4.2 justified in [142], commonly acknowledged by the industry.

> ***Assumption 4.2:*** *There exists a unique power flow solution* $([v_i]_{i\in N^+},[l_{ij}]_{i\to j},[S_{ij}]_{i\to j},s_0)$ *given the substation voltage* v_0 *and the branch bus power injections* s_i *for* $i \in N^+$.

The assumption suggests that the voltages v_i are close to their nominal values.

Control Variables

These include the real and reactive power injections on controllable nodes:

$$x = (p_i, q_i) \quad \text{for} \quad i \in N^+ \tag{4.2}$$

Dependent Variables

These include the variables calculated by the power flow equations (4.1):

$$u = \Big(p_0, q_0, \{v_i \quad \text{for} \quad i \in N^+\}, \{P_{ij}, Q_{ij}, l_{ij} \quad \text{for} \quad i \to j\}\Big) \tag{4.3}$$

where p_0 and q_0 are slack node power injections, v_i are node voltages, and P_{ij}, Q_{ij}, l_{ij} are line power and current flows.

For simulation studies, this thesis considers time-varying loads and generations for the network. The set of time instants is assumed to be discrete and denoted by τ. Let $t \in \tau$ be an arbitrary time instant. Therefore, the parameters defined in (4.2) and (4.3) can also be denoted as a function of t, i.e., $x(t) = (p_i(t), q_i(t)) \;\text{ for }\; i \in N^+$ and $u(t) = (p_0(t), q_0(t), \{v_i(t) \;\text{ for }\; i \in N^+\}, \{P_{ij}(t), Q_{ij}(t), l_{ij}(t) \;\text{ for }\; i \to j\})$. With the help of *Implicit Function Theorem* (IFT), one can map the control variables to the dependent variables as $u(t) = F(x(t))$ [143]. The theorem requires $F(x(t))$ to be continuous and differentiable. The *online* algorithm computes a control signal $x(t)$ in each iteration and applies it to the grid, which then implicitly computes the network state $u(t)$ by exploiting the laws of physics as a power flow solver. The OPF algorithm calculates $x(t)$ by using objectives written as a function of x. Therefore, the OPF problem is given by:

$$\min \quad L = F(x(t)) \quad \text{over} \quad x(t) \tag{4.4}$$

where every dependent variable present in the formulation of L will be written as a function of x:

$$p_0 = p_0(x), q_0 = q_0(x), \quad v_i = v_i(x) \quad \text{for} \quad i \in N^+ \tag{4.5a}$$

$$P_{ij} = P_{ij}(x), Q_{ij} = P_{ij}(x), l_{ij} = l_{ij}(x) \quad \text{for} \quad i \to j \tag{4.5b}$$

In the proposed EM architecture, the EMA computes the control variables $x(t)$ and triggers the GA to execute a power flow routine to update the dependent variables $u(t)$ accordingly.

4.1.3 Objective Function

The objective function is separable, quadratic, and purely a function of p_i. From (4.2), there are two vectors of control variables in real and reactive power injections, p_i and q_i. Thus, one can formulate the objective function as a function of q_i to extend the proposed algorithm for reactive power control. In the presence of controllable tap-changing transformers, the reference node voltage, v_0, can also be a control variable [144]. Four categories of objectives were selected for the optimization problem to address a distribution grid's economic, environmental, and technical aspects.

System Costs

- **Costs of Power Generation**: At each generator node ($i \in N_g$), a cost is incurred proportional to the generated power (p_i). These costs may be fuel and operation costs for fuel-operated generators, the market price for buying energy from the connected renewable DG units, or the flexibility provided by active prosumers. The objective cost function takes the following quadratic form:

$$L_{Costs}(x) = a_0 p_0(x)^2 + b_0 p_0(x) + c_0 + \sum_{i \in N_{DG}} b_m p_i \tag{4.6}$$

  Where a_0, b_0, and c_0 are respective variable and fixed cost coefficients for the fossil fuel generation unit, and b_m is the unit of market price for each unit of power bought from a renewable DG unit. Notably, when the grid buys energy from a connected DG, the corresponding cost function is linear because the price increases linearly with each power generation unit. However, this linearization does not affect the quadratic cost term related to the fuel generator placed on the reference node. We consider the fuel costs required to produce per unit of energy to be the operational cost for the fuel generator.
- **Curtailment Costs**: For each connected renewable DG unit, a curtailment penalty is imposed on the distribution grid operator in case of renewable energy curtailment to futher boost the use of renewables. The cost term is quadratic, following the general norm.

$$L_{Curtailment}(x) = \sum_{i \in N_{DG}} b_m(\bar{p_i} - p_i)^2 + b_m(\bar{p_i} - p_i) \tag{4.7a}$$

$$L_{Curtailment}(x) = \sum_{i \in N_{DG}} a_c(\bar{p_i} - p_i)^2 + b_c(\bar{p_i} - p_i) \tag{4.7b}$$

One option is to make the curtailment cost per power unit equal to the market price b_m, i.e., the distribution grid operator pays the market price equivalent for each unit of curtailed power. Another method is to choose suitable coefficients for a_c and b_c to impose a cost term for curtailment, as seen in (4.7b). This work uses historical spot market profiles to deal with the interaction of the grid with renewable DG units and uses (4.7a).

Carbon Emissions

At each fossil fuel powered generation unit ($i \in N_{ffg}$), harmful *Greenhouse Gas* (GHG) emissions in the form of CO_2, NO_x, etc. are considered and formulated in a quadratic form to the unit of power generation [145] as:

$$L_{GHG}(x) = \alpha_0 p_0(x)^2 + \beta_0 p_0(x) + \gamma_0 + \omega_0 e^{\mu_0 p_0(x)} \tag{4.8}$$

Where $\alpha_0, \beta_0, \gamma_0, \omega_0$, and μ_0 are respective emission coefficients regarding the different GHG gases for the generator. In the present simulation, emissions are encountered only in the case of a conventional generator and, therefore, only computed for p_0.

Technical Parameters

- **Active Power Losses**: Power losses over transmission lines in distribution networks are important in deciding the ultimate system operational costs that affect end users' electricity bills. The total active power losses over the distribution grid are given by:

$$L_{p_{loss}}(x) = \sum_{i \in E} g_{ij} \left[v_i(x)^2 + v_j(x)^2 - 2 v_i(x) v_j(x) \cos\theta_{ij}(x) \right] \tag{4.9}$$

Where g_{ij} is the branch conductance, v_i,v_j are the nodal voltages at each end of the respective branch, and $cos(\theta_{ij})$ is the voltage angle difference between the

two ends of the branch.

- **Voltage Deviation**: Voltage deviation indicates the voltage quality of the network and is an important factor in determining system security. The objective function is the cumulative sum of voltage deviations at all load nodes in the network from their nominal values (generally 1.0 p.u.):

$$L_{V_{dev}}(x) = \sum_{i=1}^{N} |v_i(x) - v_{nom}(x)| \tag{4.10}$$

  where V_{nom} is the nominal nodal voltage, generally equal to 1.0 p.u.

The combined objective function for the multi-objective optimization problem is a vector:

$$L(x) = \{L_{Costs}(x) + L_{Curtailment}(x), L_{GHG}(x), L_{p_{loss}}(x), L_{V_{dev}}(x)\} \tag{4.11}$$

The fuel and energy costs combined with the curtailment cost form a singular economic objective with equal priority in the multi-objective scenario.

4.1.4 Constraint Handling

There are two types of network constraints for the distribution grid and its connected participants.

Network Constraints

- ***Equality Constraints***: The equality constraints are the physical laws governing the network's power balance given in (4.1). It is essential to maintain a supply-demand balance in the distribution grid network. The intermediate iterates of *online* algorithms always satisfy the power balance constraints by design owing to the closed-loop feedback mechanism. The algorithm computes the control variables (4.2) and applies it to the grid, which then implicitly solves the power flow and updates the dependent variables (4.3).
- ***Inequality Constraints***: These operational constraints directly impact the power system's functioning, influencing its efficiency and reliability. There are inequality constraints on both control and dependent variables such as nodal voltages (v_i for $i \in N^+$), including the slack node voltage, real and reactive

power generation limits on generator nodes (p_i, q_i for $i \in N^+$).

$$\underline{v_i} \leq v_i \leq \bar{v}_i \qquad \text{for} \quad i \in N^+ \tag{4.12a}$$

$$\underline{p_i} \leq p_i \leq \bar{p}_i \qquad \text{for} \quad i \in N^+ \tag{4.12b}$$

$$\underline{q_i} \leq q_i \leq \bar{q}_i \qquad \text{for} \quad i \in N^+ \tag{4.12c}$$

Penalty Functions

As previously discussed, the algorithm handles the equality or power balance constraints by design. For a distributed algorithm, i.e., each control node updates its own (p_i, q_i for $i \in N$), the inequality constraints are easier to handle when decoupled. The operational constraints on the control node generation (p_i, q_i) are easy to deal with locally. However, to avoid the coupled constraints on all nodal voltages (v_i) and the slack node real and reactive power generation (p_0, q_0), one can add a log-barrier function to the objective function as:

$$\begin{aligned} P_{log}(x) = &-\underline{\mu} \sum_{i=1}^{n} ln(v_i(x) - \underline{v_i}) - \bar{\mu} \sum_{i=1}^{n} ln(\bar{v_i} - v_i(x)) \\ &-\underline{\mu} \sum_{i=1}^{n} ln(p_0(x) - \underline{p_0}) - \bar{\mu} \sum_{i=1}^{n} ln(\bar{p_0} - p_0(x)) \\ &-\underline{\mu} \sum_{i=1}^{n} ln(q_0(x) - \underline{q_0}) - \bar{\mu} \sum_{i=1}^{n} ln(\bar{q_0} - q_0(x)) \end{aligned} \tag{4.13}$$

Adding the slack node generation limits to decoupled constraints is owed to a power flow failure assumption when the reference node operational limits are not considered.

Log-barrier functions are a class of penalty functions that convert a constrained problem into an unconstrained one by introducing an artificial penalty for violating the constraint [146]. Since this is a minimization problem, one must add some value in case of a constraint violation. The variables (v_0, p_0, q_0) are to be maintained within their limits as shown in (4.12), which is enforced by the log-barrier method since:

$$\lim_{v_i(x) \to \underline{v_i}} -\underline{\mu} ln(v_i(x) - \underline{v_i}) = \infty, \quad \lim_{v_i(x) \to \bar{v_i}} -\bar{\mu} ln(\bar{v_i} - v_i(x)) = \infty \quad \text{for } i \in N^+ \tag{4.14}$$

The same idea applies to the slack generation limits.

$$\begin{aligned} \lim_{p_0(x)\to\underline{p_0}} -\underline{\mu} ln(p_0(x)-\underline{p_0}) = \infty, \quad \lim_{p_0(x)\to\bar{p_0}} -\bar{\mu} ln(\bar{p_0}-p_0(x)) = \infty \\ \lim_{q_0(x)\to\underline{q_0}} -\underline{\mu} ln(q_0(x)-\underline{q_0}) = \infty, \quad \lim_{q_0(x)\to\bar{q_0}} -\bar{\mu} ln(\bar{q_0}-q_0(x)) = \infty \end{aligned} \tag{4.15}$$

Whenever the computed values are close to their limits, the log-barrier method adds a penalty term to the objective function, which discards the solution as a minima [147]. Another available and suitable penalty function is the *max* function used to add the maximum value between 0 and the difference between the variable's actual value and its nearest limit, i.e., $max(0,(\underline{v_i} - v_i(x)))$. However, adding penalty functions can create several slope changes in the graph, which is problematic for typical minimization problems. Therefore, multiplying the penalty factor with a small enough $\mu = (\underline{\mu},\bar{\mu}) > 0$ alleviates this problem.

The remaining unhandled constraints limit the real and reactive power generation of controllable generator nodes seen in (4.12b) and (4.12c). The agents at the control nodes deal with these limits locally, i.e., the EMA sends the computed control signal to each control node. They verify whether the optimal value is within their prescribed limits; if not, the values are rounded off to match their nearest limits as:

$$\begin{aligned} \text{if } \; p_i > \bar{p_i} \; \text{ then } \; p_i = \bar{p_i} \; \text{ else if } \; p_i < \underline{p_i} \; \text{ then } \; p_i = \underline{p_i} \\ \text{if } \; q_i > \bar{q_i} \; \text{ then } \; q_i = \bar{q_i} \; \text{ else if } \; q_i < \underline{q_i} \; \text{ then } \; q_i = \underline{q_i} \end{aligned} \tag{4.16}$$

To summarize the distributed OPF problem this thesis seeks to solve is:

$$\min \quad L(x,\mu) = L(x) - P_{log}(x) \tag{4.17a}$$

$$\text{over} \quad p_i,...,p_n, \; q_i,...,q_n \tag{4.17b}$$

$$\text{s.t.} \quad \underline{p_i} \leq p_i \leq \bar{p_i}, \underline{q_i} \leq q_i \leq \bar{q_i} \quad i = 1,2,...,n \tag{4.17c}$$

over a decreasing sequence of μ.

This section formulated the proposed architecture's multi-objective constrained and distributed OPF problem. Essential elements for modeling are the *DistFlow* power balance equations and the use of Penalty functions to handle inequality constraints.

4.2 Estimation of System Gradients

In each iteration of the algorithm, first-order derivatives of the modified objective function, $L(x,\mu)$ *with respect to* (w.r.t.) the control variables are estimated and then used as the negative direction of updating the control variables, (p_i,q_i). Therefore, each objective function will have two sets of gradients, one w.r.t. p_i and the other w.r.t. q_i. This section first computes the required gradients concerning the OPF problem and then provides two methods to estimate the system gradients for radial and meshed networks.

4.2.1 Required System Gradients

Derivatives of Objective Function $L(x)$

- ***System Costs***: For convenience, equations (4.6) and (4.7a) are taken together.
  - w.r.t. real power injections, p_i

$$\frac{\partial L_{Costs}(x)}{\partial p_i} = (2a_0p_0 + b_0)\frac{\partial p_0}{\partial p_i} + b_m\frac{\partial p_i}{\partial p_i} + b_m\left(2p_i^{max}\frac{\partial p_i^{max}}{\partial p_i} + 2p_i\frac{\partial p_i}{\partial p_i} - 2p_i^{max}\frac{\partial p_i}{\partial p_i} - 2p_i\frac{\partial p_i^{max}}{\partial p_i} + \frac{\partial p_i^{max}}{\partial p_i} - \frac{\partial p_i}{\partial p_i}\right) \tag{4.18a}$$

  - w.r.t. reactive power injections, q_i

$$\frac{\partial L_{Costs}(x)}{\partial q_i} = (2a_0p_0 + b_0)\frac{\partial p_0}{\partial q_i} + b_m\frac{\partial p_i}{\partial q_i} + b_m\left(2p_i^{max}\frac{\partial p_i^{max}}{\partial q_i} + 2p_i\frac{\partial p_i}{\partial q_i} - 2p_i^{max}\frac{\partial p_i}{\partial q_i} - 2p_i\frac{\partial p_i^{max}}{\partial q_i} + \frac{\partial p_i^{max}}{\partial q_i} - \frac{\partial p_i}{\partial q_i}\right) \tag{4.18b}$$

> ***Assumption 4.3:*** The self derivatives of the control variables, i.e., $\frac{\partial p_i}{\partial p_i}$, $\frac{\partial q_i}{\partial q_i}$ equals 1. p_i^{max} is the capacity of the generator that does not depend on the power injections; therefore, $\frac{\partial p_i^{max}}{\partial p_i}$, $\frac{\partial p_i^{max}}{\partial q_i}$ equals 0. Similarly, $\frac{\partial p_i}{\partial q_i} = 0$.

Following this assumption, the equations in (4.18) can be written as:

– w.r.t. real power injections, p_i

$$\frac{\partial L_{Costs}(x)}{\partial p_i} = (2a_0 p_0 + b_0)\,\frac{\partial p_0}{\partial p_i} + 2b_m(p_i - p_i^{max}) \tag{4.19a}$$

– w.r.t. reactive power injections, q_i

$$\frac{\partial L_{Costs}(x)}{\partial q_i} = (2a_0 p_0 + b_0)\,\frac{\partial p_0}{\partial q_i} \tag{4.19b}$$

- ***Carbon Emissions***: The gradients for (4.8) are:

  – w.r.t. real power injections, p_i

$$\frac{\partial L_{GHG}(x)}{\partial p_i} = (2\alpha_0 p_0 + \beta_0 + \omega_0 e^{\mu_0 p_0})\,\frac{\partial p_0}{\partial p_i} \tag{4.20a}$$

  – w.r.t. reactive power injections, q_i

$$\frac{\partial L_{GHG}(x)}{\partial q_i} = (2\alpha_0 p_0 + \beta_0 + \omega_0 e^{\mu_0 p_0})\,\frac{\partial p_0}{\partial q_i} \tag{4.20b}$$

- ***Active Power Losses***: In (4.9), $\cos\theta_{ij} = \cos(\theta_i - \theta_j)$. Therefore, to calculate the derivative, let's expand the expression into $(\cos\theta_i \cos\theta_j - \sin\theta_i \sin\theta_j)$. For the sake of brevity, $\omega = (\cos\theta_i \cos\theta_j - \sin\theta_i \sin\theta_j)$ will be used in the following equation. The gradients for (4.9) are:

  – w.r.t. real power injections, p_i

$$\frac{\partial L_{p_{loss}}(x)}{\partial p_i} = g_{ij}\left(2v_i\frac{\partial v_i}{\partial p_i} + 2v_j\frac{\partial v_j}{\partial p_i} - 2v_j\omega\frac{\partial v_i}{\partial p_i} - 2v_i\omega\frac{\partial v_j}{\partial p_i} - 2v_i v_j\frac{\partial \omega}{\partial p_i}\right) \tag{4.21a}$$

  – w.r.t. reactive power injections, q_i

$$\frac{\partial L_{p_{loss}}(x)}{\partial q_i} = g_{ij}\left(2v_i\frac{\partial v_i}{\partial q_i} + 2v_j\frac{\partial v_j}{\partial q_i} - 2v_j\omega\frac{\partial v_i}{\partial q_i} - 2v_i\omega\frac{\partial v_j}{\partial q_i} - 2v_i v_j\frac{\partial \omega}{\partial q_i}\right) \tag{4.21b}$$

  where,

$$\frac{\partial \omega}{\partial x_i} = \sin\theta_{ij}\left(\frac{\partial \theta_j}{\partial x_i} - \frac{\partial \theta_i}{\partial x_i}\right)$$

- ***Voltage Deviation***: In this case $\frac{\partial V_{nom}}{\partial p_i}$ equals 0. The required gradients for (4.10) are:
  - w.r.t. real power injections, p_i

$$\frac{\partial L_{V_{dev}}(x)}{\partial p_i} = \frac{\partial v_i}{\partial p_i} \tag{4.22a}$$

  - w.r.t. reactive power injections, q_i

$$\frac{\partial L_{V_{dev}}(x)}{\partial q_i} = \frac{\partial v_i}{\partial q_i} \tag{4.22b}$$

Derivatives of Penalty Function $P(x)$

The derivatives for the penalty functions are as follows:

- w.r.t. real power injections, p_i

$$\begin{aligned}\frac{\partial P(x)}{\partial p_i} = &\left(\frac{\underline{\mu}}{v_i - \underline{v_i}} + \frac{\bar{\mu}}{\bar{v_i} - v_i}\right)\frac{\partial v_i}{\partial p_i} \\ &+ \left(\frac{\underline{\mu}}{p_0 - \underline{p_0}} + \frac{\bar{\mu}}{\bar{p_0} - p_0}\right)\frac{\partial p_0}{\partial p_i} \\ &+ \left(\frac{\underline{\mu}}{q_0 - \underline{q_0}} + \frac{\bar{\mu}}{\bar{q_0} - q_0}\right)\frac{\partial q_0}{\partial p_i}\end{aligned} \tag{4.23a}$$

- w.r.t. reactive power injections, q_i

$$\begin{aligned}\frac{\partial P(x)}{\partial q_i} = &\left(\frac{\underline{\mu}}{v_i - \underline{v_i}} + \frac{\bar{\mu}}{\bar{v_i} - v_i}\right)\frac{\partial v_i}{\partial q_i} \\ &+ \left(\frac{\underline{\mu}}{p_0 - \underline{p_0}} + \frac{\bar{\mu}}{\bar{p_0} - p_0}\right)\frac{\partial p_0}{\partial q_i} \\ &+ \left(\frac{\underline{\mu}}{q_0 - \underline{q_0}} + \frac{\bar{\mu}}{\bar{q_0} - q_0}\right)\frac{\partial q_0}{\partial q_i}\end{aligned} \tag{4.23b}$$

Note: For detailed gradient calculation, see Appendix.

The required system gradients are: $\frac{\partial p_0}{\partial p_i}$, $\frac{\partial p_0}{\partial q_i}$, $\frac{\partial q_0}{\partial p_i}$, $\frac{\partial q_0}{\partial q_i}$, $\frac{\partial v_i}{\partial p_i}$, $\frac{\partial v_i}{\partial q_i}$, $\frac{\partial \theta_i}{\partial p_i}$, and $\frac{\partial \theta_i}{\partial q_i}$.

4.2.2 Gradient Computation Methods

This section presents two alternative methods of gradient computation for radial and meshed networks. The first method estimates the gradients using a *Backward Forward Sweep* (BFS) algorithm in a distributed fashion. The second method utilizes the Jacobian and Sensitivity matrices of the system to compute the required gradients. Both methods offer specific advantages. For example, the distributed implementation of the BFS algorithm removes the iterative procedure and thus significantly reduces computational effort. However, the distributed BFS method relies on assumptions to compute the gradients. On the other hand, using the exact derivatives of the system from the Jacobian and Sensitivity matrices has a higher accuracy, which results in superior optimality properties. Moreover, the BFS method is restricted to radial networks as the assumptions exploit the features of radial topology, whereas the Jacobian method is universal and applies to arbitrary grid topologies.

Backward-Forward Sweep Method

The IFT is applied to the power flow equations (4.1) to compute the exact derivatives, with the mild assumption that the gradients $\partial_x(P,Q,v,l)$ exist, where $x = (p_i,q_i)$:

$$\partial_x P_{ij} = r_{ij}\partial_x l_{ij} - \partial_x p_j + \sum_{k:j\to k} \partial_x P_{jk}, \tag{4.24a}$$

$$\partial_x Q_{ij} = x_{ij}\partial_x l_{ij} - \partial_x q_j + \sum_{k:j\to k} \partial_x Q_{jk}, \tag{4.24b}$$

$$\partial_x v_j = \partial_x v_i - 2\left(r_{ij}\partial_x P_{ij} + x_{ij}\partial_x Q_{ij}\right) + |z_{ij}|^2 \partial_x l_{ij}, \tag{4.24c}$$

$$\partial_x l_{ij} = \frac{2P_{ij}}{v_i}\partial_x P_{ij} + \frac{2Q_{ij}}{v_i}\partial_x Q_{ij} - \frac{l_{ij}}{v_i}\partial_x v_i \tag{4.24d}$$

for $i \to j$. Let I denote a 2×2 identity matrix and remove $\partial_x l_{ij}$ to obtain:

$$\left[I - \frac{2}{v_i}\begin{pmatrix} r_{ij} \\ x_{ij} \end{pmatrix}\begin{pmatrix} P_{ij} & Q_{ij} \end{pmatrix}\right]\begin{pmatrix} \partial_x P_{ij} \\ \partial_x Q_{ij} \end{pmatrix} = \sum_{k:k\to j}\begin{pmatrix} \partial_x P_{jk} \\ \partial_x Q_{jk} \end{pmatrix} - \begin{pmatrix} \partial_x p_j \\ \partial_x q_j \end{pmatrix} - \begin{pmatrix} r_{ij} \\ x_{ij} \end{pmatrix}\frac{l_{ij}}{v_i}\partial_x v_i,$$

$$\partial_x v_j = \left(1 - |z_{ij}|^2\frac{l_{ij}}{v_i}\right)\partial_x v_i - 2\left(r_{ij} - |z_{ij}|^2\frac{P_{ij}}{v_i}\right)\partial_x P_{ij} - 2\left(x_{ij} - |z_{ij}|^2\frac{Q_{ij}}{v_i}\right)\partial_x Q_{ij}$$

$$\text{for} \quad i \to j \tag{4.25}$$

Hence, the gradients $\partial_x(P, Q, v, p_0, q_0)$ can be computed by Algorithm 4.1:

Algorithm 4.1: Compute Gradients using BFS Iterative Method

Input: network graph (N,E), power flow solution (p,q,P,Q,v,l), tolerance criteria ϵ

Output: gradient $\partial_x(P,Q,v,p_0,q_0)$ where $x = (p_1,...,p_n,q_1,...,q_n)$

① **Initialization** $\partial_x v_i \leftarrow 0 \quad \text{for} \quad i = 0,1,...,n$

② **Backward Sweep** From the leafs $j \to k$ to the roots $i \to j$, compute

$$\begin{pmatrix} \partial_x P_{ij} \\ \partial_x Q_{ij} \end{pmatrix} \leftarrow \left[I - \frac{2}{v_i} \begin{pmatrix} r_{ij} \\ x_{ij} \end{pmatrix} \begin{pmatrix} P_{ij} & Q_{ij} \end{pmatrix} \right]^{-1} \cdot \left[\sum_{k:k\to j} \begin{pmatrix} \partial_x P_{jk} \\ \partial_x Q_{jk} \end{pmatrix} - \begin{pmatrix} \partial_x p_j \\ \partial_x q_j \end{pmatrix} - \begin{pmatrix} r_{ij} \\ x_{ij} \end{pmatrix} \frac{l_{ij}}{v_i} \partial_x v_i \right]$$

③ **Forward Sweep** From the roots i to the leafs j, compute

$$\partial_x v_j \leftarrow \left(1 - |z_{ij}|^2 \frac{l_{ij}}{v_i}\right) \partial_x v_i - 2 \left(r_{ij} - |z_{ij}|^2 \frac{P_{ij}}{v_i}\right) \partial_x P_{ij} - 2 \left(x_{ij} - |z_{ij}|^2 \frac{Q_{ij}}{v_i}\right) \partial_x Q_{ij}$$

④ **if** update in $\partial_x(P,Q,v) > \epsilon$ go to ②

⑤ **Return**

$$\begin{pmatrix} \partial_x p_0 \\ \partial_x q_0 \end{pmatrix} \leftarrow \sum_{k:0\to k} \left[I - \frac{2}{v_0} \begin{pmatrix} r_{0k} \\ x_{0k} \end{pmatrix} \begin{pmatrix} P_{0k} & Q_{0k} \end{pmatrix} \right]^{-1} \cdot \left[\sum_{l:k\to l} \begin{pmatrix} \partial_x P_{kl} \\ \partial_x Q_{kl} \end{pmatrix} - \begin{pmatrix} \partial_x p_k \\ \partial_x q_k \end{pmatrix} - \begin{pmatrix} r_{0k} \\ x_{0k} \end{pmatrix} \frac{l_{0k}}{v_0} \partial_x v_0 \right]$$

The gradient calculation $\partial_x(P,Q,v,p_0,q_0)$ depends on the power flow solution (P, Q, v, p_0, q_0) at which the gradients are evaluated. Since, the practical power flow solution (P, Q, v, p_0, q_0) is assumed to be unique, given (p, q), the gradients $\partial_x(P, Q, v, p_0, q_0)$ are also unique. The gradient approximation method helps avoid the iterative procedure in Algorithm

4.1 and improves computational efficiency. The current terms in (4.1a) - (4.1c) are much smaller than the other terms in practice, estimating (P, Q, v) by $(\hat{P}, \hat{Q}, \hat{v})$ defined as:

$$\sum_{i:i\to j} \hat{P_{ij}} + p_j = \sum_{k:j\to k} \hat{P_{jk}}, \quad \text{for} \quad j \in N; \tag{4.26a}$$

$$\sum_{i:i\to j} \hat{Q_{ij}} + q_j = \sum_{k:j\to k} \hat{Q_{jk}}, \quad \text{for} \quad j \in N; \tag{4.26b}$$

$$\hat{v_i} - \hat{v_j} = 2\left(r_{ij}\hat{P_{ij}} + x_{ij}\hat{Q_{ij}}\right), \quad \text{for} \quad i \to j \tag{4.26c}$$

The equations are linear and the network is radial. Therefore, it is straightforward to obtain:

$$\partial_x \hat{P_{ij}} = \sum_{k:j\to k} \partial_x \hat{P_{jk}} - \partial_x p_j, \quad \text{for} \quad i \to j \tag{4.27a}$$

$$\partial_x \hat{Q_{ij}} = \sum_{k:j\to k} \partial_x \hat{Q_{jk}} - \partial_x q_j, \quad \text{for} \quad i \to j \tag{4.27b}$$

$$\partial_x \hat{v_j} = \partial_x \hat{v_i} - 2r_{ij}\partial_x \hat{P_{ij}} - 2x_{ij}\hat{Q_{ij}}, \quad \text{for} \quad i \to j \tag{4.27c}$$

Let $i \wedge j$ denote the joint of node i and j for $i, j, \in N$ and let R_i denote the total resistance from the slack node 0 to node i for $i \in N$ as seen in Figure 4.2. Then the estimated gradients $\partial_x(\hat{P}, \hat{Q}, \hat{v})$ has the following closed-form expression:

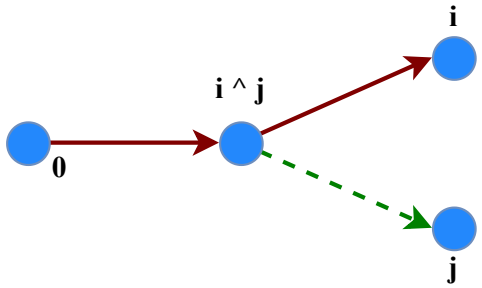

Figure 4.2: Nodes and Lines

$$\partial_{p_k} \hat{P_{ij}} = -1_{j\in P_k}, \quad \partial_{q_k} \hat{P_{ij}} = 0, \quad k = 1,2,...,n, \text{ for } \quad i \to j \tag{4.28a}$$

$$\partial_{p_k} \hat{Q_{ij}} = 0, \quad \partial_{q_k} \hat{Q_{ij}} = -1_{j\in P_k}, \quad k = 1,2,...,n, \text{ for } \quad i \to j \tag{4.28b}$$

$$\partial_{p_k} \hat{v_i} = 2R_{i\wedge k}, \quad \partial_{q_k} \hat{v_i} = 2X_{i\wedge k}, \quad k = 1,2,...,n, \text{ for } \quad i \in N^+ \tag{4.28c}$$

A few essential points are noted from (4.28). The derivatives of the nodal voltages $\partial_x v_i$ are symmetric in (i,k), i.e., the impact of an injection on voltage is symmetric in their respective locations. Furthermore, the effect on voltages of injections close to the substation is minor; similarly, the voltages close to the substation are less sensitive to injections, which agrees with intuition. Therefore, one can say $\partial_x(P,Q,v) \approx \partial_x(\hat{P},\hat{Q},\hat{v})$. Most importantly, $\partial_x(\hat{P},\hat{Q},\hat{v})$ is a constant and does not depend on $\partial_x(P,Q,v)$. Therefore, it has to be computed only once ahead of time. Sum up (4.1b) for $j \in N$ to obtain:

$$\sum_{i=0}^{n} p_i = \sum_{i \to j} r_{ij} l_{ij} = \sum_{i \to j} r_{ij} \frac{P_{ij}^2 + Q_{ij}^2}{v_i} \tag{4.29}$$

Finally, the approximate values for $\partial_x(p_0, q_0)$ are:

$$\partial_{p_i} p_0 \approx -1 + \sum_{k \to l} r_{kl} \left(\frac{2P_{kl}}{v_k} \partial_{p_i} \hat{P}_{kl} + \frac{2Q_{kl}}{v_k} \partial_{p_i} \hat{Q}_{kl} - \frac{l_{kl}}{v_k} \partial_{p_i} v_k \right) \tag{4.30a}$$

$$\partial_{q_i} p_0 \approx \sum_{k \to l} r_{kl} \left(\frac{2P_{kl}}{v_k} \partial_{q_i} \hat{P}_{kl} + \frac{2Q_{kl}}{v_k} \partial_{q_i} \hat{Q}_{kl} - \frac{l_{kl}}{v_k} \partial_{q_i} v_k \right) \tag{4.30b}$$

for $i = 1,2,...,n$. The derivatives for $\partial_x q_0$ are symmetric with x_{ij} replacing r_{ij}.

Putting (4.28), the gradients can be further approximated to:

$$\partial_{p_i} p_0 \approx -\left[1 + \sum_{k \to l} r_{kl} \left(\frac{2P_{kl}}{v_k} 1_{l \in P_i} + \frac{l_{kl}}{v_k} R_{i \wedge k} \right) \right] \tag{4.31a}$$

$$\partial_{q_i} p_0 \approx \sum_{k \to l} r_{kl} \left(\frac{2Q_{kl}}{v_k} 1_{l \in P_i} - \frac{l_{kl}}{v_k} X_{i \wedge k} \right) \tag{4.31b}$$

$$\partial_{p_i} q_0 \approx -\left[1 + \sum_{k \to l} x_{kl} \left(\frac{2Q_{kl}}{v_k} 1_{l \in P_i} + \frac{l_{kl}}{v_k} X_{i \wedge k} \right) \right] \tag{4.31c}$$

$$\partial_{q_i} q_0 \approx \sum_{k \to l} x_{kl} \left(\frac{2Q_{kl}}{v_k} 1_{l \in P_i} - \frac{l_{kl}}{v_k} X_{i \wedge k} \right) \tag{4.31d}$$

Therefore, all required gradients have been approximated, and they can be calculated using a distributed BFS method, as described ahead.

Let $down(i) := \{j \in N | i \in \mathbb{P}_{\rfloor}\}$ denote the downstream nodes of node $i \in N$. Then, the approximate gradients can be represented as:

$$c_i = \sum_{k=1}^{n} 2R_{i\wedge k}\left(\frac{\underline{\mu}}{v_k - \underline{v_k}} + \frac{\bar{\mu}}{v_k - \bar{v_k}}\right) \tag{4.32a}$$

$$d_i = \sum_{k=1}^{n} 2X_{i\wedge k}\left(\frac{\underline{\mu}}{v_k - \underline{v_k}} + \frac{\bar{\mu}}{v_k - \bar{v_k}}\right) \tag{4.32b}$$

$$e_i = \sum_{k\to 1} r_{kl}\left(\frac{2P_{kl}}{v_k}1_{l\in\mathbb{P}_\sqsupset} + \frac{l_{kl}}{v_k}R_{i\wedge k}\right) \tag{4.32c}$$

$$f_i = \sum_{k\to 1} r_{kl}\left(\frac{2Q_{kl}}{v_k}1_{l\in\mathbb{P}_\sqsupset} + \frac{l_{kl}}{v_k}X_{i\wedge k}\right) \tag{4.32d}$$

$$e_i^q = \sum_{k\to 1} x_{kl}\left(\frac{2P_{kl}}{v_k}1_{l\in\mathbb{P}_\sqsupset} + \frac{l_{kl}}{v_k}R_{i\wedge k}\right) \tag{4.32e}$$

$$f_i^q = \sum_{k\to 1} x_{kl}\left(\frac{2Q_{kl}}{v_k}1_{l\in\mathbb{P}_\sqsupset} + \frac{l_{kl}}{v_k}X_{i\wedge k}\right) \tag{4.32f}$$

The coefficient c_i will have equivalent terms corresponding to the log-barrier functions for the slack node generation limits. These can be calculated with the help of e_i, f_i, e_i^q, and f_i^q. These coefficients are computed recursively, exploiting the network's radial topology. Note that for each $i \to j$, one has $R_{i\wedge k} - R_{j\wedge k} = -r_{ij}1_{k\in down(J)}$, and therefore:

$$c_i - c_j = -2r_{ij}\sum_{k\in down(j)}\left(\frac{\underline{\mu}}{v_k - \underline{v_k}} + \frac{\bar{\mu}}{v_k - \bar{v_k}}\right) \tag{4.33a}$$

$$d_i - d_j = -2x_{ij}\sum_{k\in down(j)}\left(\frac{\underline{\mu}}{v_k - \underline{v_k}} + \frac{\bar{\mu}}{v_k - \bar{v_k}}\right) \tag{4.33b}$$

$$e_i - e_j = -\frac{2r_{ij}P_{ij}}{v_i} - r_{ij}\sum_{k\in down(j)}\frac{r_{kl}P_{kl}}{v_k} \tag{4.33c}$$

$$f_i - f_j = -\frac{2r_{ij}Q_{ij}}{v_i} - x_{ij}\sum_{k\in down(j)}\frac{r_{kl}P_{kl}}{v_k} \tag{4.33d}$$

Therefore, with

$$g_i = \sum_{k\in down(j)}\left(\frac{\underline{\mu}}{v_k - \underline{v_k}} + \frac{\bar{\mu}}{v_k - \bar{v_k}}\right) \tag{4.34a}$$

$$h_i = \sum_{k\in down(j)}\frac{r_{kl}P_{kl}}{v_k} \tag{4.34b}$$

one can recursively compute:

$$c_j = c_i + 2r_{ij}g_j \tag{4.35a}$$

$$d_j = d_i + 2x_{ij}g_j \tag{4.35b}$$

$$e_j = e_i + \frac{2r_{ij}P_{ij}}{v_i} + r_{ij}h_j \tag{4.35c}$$

$$f_j = f_i + \frac{2r_{ij}Q_{ij}}{v_i} + x_{ij}h_j \tag{4.35d}$$

Jacobian and Sensitivity Matrices

This method of gradient computation applies IFT to the AC power flow equations to obtain the system gradients. However, this leads to the inversion of the Jacobian matrix, which is a computationally heavy operation with an increasing number of grid nodes. Y. Tang *et al.* in [144] suggests that in practical situations, there will be a small number of nodes or lines with a voltage or current constraint violation in a single instant. Therefore, one needs to compute only the derivatives of voltages and line loadings corresponding to the nodes and lines with violations, which will be only a fraction of the Jacobian matrix, speeding up the computation process. Notably, this method helps to extend the algorithm to meshed networks. For this method, the bus injection model represents the AC power flow model and uses the exponential form $V_i = |V_i|e^{j\theta_i}$ to represent the complex voltages. The power flow equations for the meshed network are:

$$p_0 = F_0^p(V_0, |V_{1:n}|, \theta_{1:n}), \quad q_0 = F_0^q(V_0, |V_{1:n}|, \theta_{1:n}) \tag{4.36a}$$

$$p_i = F_i^p(V_0, |V_{1:n}|, \theta_{1:n}), \quad q_i = F_i^q(V_0, |V_{1:n}|, \theta_{1:n}) \tag{4.36b}$$

Referring back to IFT and viewing $(v_i,\ p_0,\ q_0)$ as functions of $(p_i,\ q_i)$, the derivatives of (4.36) are computed as:

$$\begin{bmatrix} \dfrac{\partial F_i^p}{\partial v_i} & \dfrac{\partial F_i^p}{\partial \theta_i} \\ \dfrac{\partial F_i^q}{\partial v_i} & \dfrac{\partial F_i^q}{\partial \theta_i} \end{bmatrix} \begin{bmatrix} \dfrac{\partial V_i}{\partial p_i} & \dfrac{\partial V_i}{\partial q_i} \\ \dfrac{\partial \theta_i}{\partial p_i} & \dfrac{\partial \theta_i}{\partial q_i} \end{bmatrix} = I_{2n} \tag{4.37}$$

and

$$\begin{bmatrix} \frac{\partial p_0}{\partial p_i} & \frac{\partial p_0}{\partial q_i} \\ \frac{\partial q_0}{\partial p_i} & \frac{\partial q_0}{\partial q_i} \end{bmatrix} = \begin{bmatrix} \frac{\partial F_0^p}{\partial v_i} & \frac{\partial F_0^p}{\partial \theta_i} \\ \frac{\partial F_0^q}{\partial v_i} & \frac{\partial F_0^q}{\partial \theta_i} \end{bmatrix} \begin{bmatrix} \frac{\partial V_i}{\partial p_i} & \frac{\partial V_i}{\partial q_i} \\ \frac{\partial \theta_i}{\partial p_i} & \frac{\partial \theta_i}{\partial q_i} \end{bmatrix} \tag{4.38}$$

and I_{2n} is a $2_n \times 2_n$ identity matrix.

From (4.37), it is noted:

$$\begin{bmatrix} \frac{\partial V_i}{\partial p_i} & \frac{\partial V_i}{\partial q_i} \\ \frac{\partial \theta_i}{\partial p_i} & \frac{\partial \theta_i}{\partial q_i} \end{bmatrix} \begin{bmatrix} \frac{\partial F_i^p}{\partial v_i} & \frac{\partial F_i^p}{\partial \theta_i} \\ \frac{\partial F_i^q}{\partial v_i} & \frac{\partial F_i^q}{\partial \theta_i} \end{bmatrix} = I_{2n} \tag{4.39}$$

Now let:

$$\begin{aligned} \mathbb{J} = \left\{ i \in N : |I_{ij}|^2 \geq \bar{l_{ij}} \quad \text{for} \quad \text{some} \quad j \in N^+ \right\} \\ \cup\, i \in N : \text{is a neighbour of the slack bus} \end{aligned} \tag{4.40a}$$

$$\mathbb{I} = \mathbb{J} \cup \left\{ i \in N : |V_i|^2 \geq \bar{v_i} \quad \text{or} \quad |V_i|^2 \leq \underline{v_i} \right\} \tag{4.40b}$$

Then:

$$\begin{bmatrix} \frac{\partial V_{\mathbb{I}}}{\partial p_i} & \frac{\partial V_{\mathbb{I}}}{\partial q_i} \\ \frac{\partial \theta_{\mathbb{J}}}{\partial p_i} & \frac{\partial \theta_{\mathbb{J}}}{\partial q_i} \end{bmatrix} \begin{bmatrix} \frac{\partial F_i^p}{\partial v_i} & \frac{\partial F_i^p}{\partial \theta_i} \\ \frac{\partial F_i^q}{\partial v_i} & \frac{\partial F_i^q}{\partial \theta_i} \end{bmatrix} = \begin{bmatrix} I_{\mathbb{I}} & 0 \\ 0 & I_{\mathbb{J}} \end{bmatrix} \tag{4.41}$$

where $I_{\mathbb{I}}$ and $I_{\mathbb{J}}$ are the submatrices formed by the rows of I_n corresponding to $\mathbb{I}$ and $\mathbb{J}$. This can be solved efficiently when $|\mathbb{I}| + |\mathbb{J}| \ll n$, i.e., the number of nodes or lines with constraint violations is significantly lesser than the number of nodes in the grid. The matrices on the left-hand side of (4.37) are the Jacobian and the Sensitivity matrices, respectively. The Sensitivity matrix already provides us with the class of gradients $\frac{\partial v_i}{\partial x_i}$ and $\frac{\partial \theta_i}{\partial x_i}$. The remaining gradients of the slack node generation w.r.t. the control variables are derived by:

$$\begin{bmatrix} \frac{\partial p_0}{\partial p_i} & \frac{\partial p_0}{\partial q_i} \\ \frac{\partial q_0}{\partial p_i} & \frac{\partial q_0}{\partial q_i} \end{bmatrix} = \begin{bmatrix} \frac{\partial F_0^p}{\partial |V_{\mathbb{I}}|} & \frac{\partial F_0^p}{\partial \theta_{\mathbb{J}}} \\ \frac{\partial F_0^q}{\partial |V_{\mathbb{I}}|} & \frac{\partial F_0^q}{\partial \theta_{\mathbb{J}}} \end{bmatrix} \begin{bmatrix} \frac{\partial |V_{\mathbb{I}}|}{\partial p_i} & \frac{\partial |V_{\mathbb{I}}|}{\partial q_i} \\ \frac{\partial \theta_{\mathbb{J}}}{\partial p_i} & \frac{\partial \theta_{\mathbb{J}}}{\partial q_i} \end{bmatrix} \tag{4.42}$$

Note: $\frac{\partial F_0^p}{\partial |V_i|} = \frac{\partial F_0^p}{\partial \theta_i} = \frac{\partial F_0^q}{\partial |V_i|} = \frac{\partial F_0^q}{\partial \theta_i} = 0$ if i is not a neighbour of the reference node 0.

This method of gradient computation improves the accuracy of the solution as compared to the BFS method described in the previous section. Moreover, it also allows the algorithm to apply to meshed networks. Distribution grids, especially in urban areas, have radial topology. However, under specific scenarios, especially in rural areas, integration of a DG unit might lead to a switch closing and forming loops in the system, making the grid a weakly meshed network.

4.2.3 Distributed Gradient Computation in an Agent-Based System

For the distributed BFS algorithm method of gradient computation, we consider an individual EMA at each DG unit or controllable node i. These agents are aware of the parameters $(\underline{\mu}, \bar{\mu})$ and impedance values (r_{ij}, x_{ij}) and can measure the voltage and line flows connected to i. With the help of the substation GA, these agents compute the required gradient coefficients given in (4.35) traversing through the leaves to the root of the network (*backward sweep)* for (g_i, h_i) and again from the root to the leaves (*forward sweep*) for (c_i, d_i, e_i, f_i). With the computed gradients and power injection values p_i and q_i, the agents can update their injections, compute their share of the objective function $L(x,\mu)$, and share this information with the primary EMA. After that, the primary EMA will execute a line search algorithm to find the optimal point in the negative direction of the gradients.

When using the Jacobian and Sensitivity matrix, the GA is assumed to have information regarding grid topology parameters such as μ, nodal voltages, and line flows. Such information can calculate the admittance and Jacobian matrices and invert them to obtain the Sensitivity matrix (4.37). With all required gradients computed, the GA can form the objective function to send through to the primary EMA for the reference node. The other control nodes receive their gradients from the GA, update their injections, and share the new objective function with the primary EMA. With the help of this information, the primary EMA can formulate the multi-objective OPF problem.

There is a slight difference between the two methods: in the BFS method, the GA or the grid operator does not need all measurements collected at the coordinator node for gradient computation, like in the Jacobian method. Therefore, the BFS method can primarily assist in situations where the network measurements are unknown.

4.3 Gradient Projection Algorithm

The Gradient projection algorithm has two essential steps for every time instant t: 1) compute (or approximate) gradients, and 2) choose a step size to update the optimization variables. The step size is determined with the help of a line search method along the direction of $-\partial_x L(x,\mu)$, i.e., back-off the step size until the approximation of the modified objective function by its linearization around the current solution point is pretty accurate. Three parameters help in the line search algorithm, namely:

- α determines the back-off speed,
- β decides whether the linearization of the objective is accurate enough,
- ϵ stops the iterations when progress is too slow, i.e., no significant update in (p, q).

For a single time instant, t, the algorithm iterates over a decreasing sequence of μ until it reaches a suitable suboptimal solution. The algorithm starts with initial values for the objective $L(x;\mu)$ and the control variables (p_i,q_i). It updates them using the system gradients that steer the search utilizing a descent path through the solution space. The algorithm uses the value from the previous time instant $x(t-1)$, a predefined step size η, and the system gradients $\partial_x L(x;\mu)$ in the following manner:

$$x(t) = \left[x(t-1) - \eta \frac{\partial L(x)(t-1)}{\partial x(t-1)}; \mu\right] \tag{4.43}$$

Note: The line search algorithm (Algorithm 4.2) is executed by the primary EMA with only the updates to the control variables being done by their respective agents.

To state the algorithm, let:

$$\prod_C x := argmin_{y \in C} ||y - x||_2 \tag{4.44}$$

denote the (unique) projection of a point x onto a non-empty compact convex set C.

> ***Theorem 4.1:*** *(well defined). Given specified input, Algorithm 4.2 always produces (p^{new},q^{new},stopFlag). For proof, please see [148].*

Algorithm 4.2: Line Search

Input: back-off parameter $\alpha \in (0,1)$, linearization parameter $\beta \in (0,1)$, progress parameter $\epsilon \ll 1$, current solution (p,q), constraints $(\underline{p},\bar{p},\underline{q},\bar{q},\underline{v},\bar{v})$, system gradient $\partial_x L(x;\mu)$

Output: update value (p^{new},q^{new}), stopping Flag *stopFlag*

① $\eta = 1$, $stopFlag = 0$

② $(p^{new},q^{new}) \leftarrow (p,q) - \eta \partial_x L(x;\mu)$

③ $p^{new} \leftarrow \prod_{[\underline{p},\bar{p}]} p^{new}$, $q^{new} \leftarrow \prod_{[\underline{q},\bar{q}]} q^{new}$

④ execute the BFS algorithm to obtain the power flow solution $(v^{new},p_0^{new},q_0^{new})$ w.r.t. (v_0,p,q)

⑤ **if** $v^{new} \notin [\underline{v},\bar{v}]$
then $\eta \leftarrow \alpha\eta$
go to ②
end

⑥ $\Delta p \leftarrow p^{new} - p$, $\Delta q \leftarrow q^{new} - q$

⑦ **if** $||\Delta p|| + ||\Delta q|| \leq \epsilon$
then $stopFlag = 1$
else if $L(x)^{new} > L(x) + \beta(\partial_p L \cdot \Delta p + \partial_q L \cdot \Delta q)$
then $\eta \leftarrow \alpha\eta$
go to ②
end

⑧ **if** $L(x)^{new} > L(x)$
then $p^{new} \leftarrow p$, $q^{new} \leftarrow q$
end

The introduction of ϵ in the *"if"* branch in Step 7. is to stop the iteration when progress gets too slow, i.e., $||\Delta p|| + ||\Delta q|| \leq \epsilon$. When this happens, *stopFlag* is set to 1, which stops the iterative procedure. Otherwise, a large number of iterations will run without a significant update to (p, q). With the *"if"* branch in Step 7., it is possible that $L(x)^{new} > L(x)$. In this case, the older values (p, q) are considered

the solution for this time instant to ensure that the new point does not have a larger objective. However, the assumption holds true if $\epsilon > 0$, and the algorithm produces an updated solution.

A point (p, q) is a local optimum for minimizing $L(x)$ if:

$$\langle \partial_{p_i} L, \tilde{p_i} - p_i \rangle \geq 0 \quad \forall \tilde{p_i} \in (\underline{p_i}, \bar{p_i}), \quad \forall i \in N^+ \tag{4.45a}$$

$$\langle \partial_{q_i} L, \tilde{q_i} - q_i \rangle \geq 0 \quad \forall \tilde{q_i} \in (\underline{q_i}, \bar{q_i}), \quad \forall i \in N^+ \tag{4.45b}$$

In the line search algorithm, if $\epsilon = 0$, then

$$(p, q) = (p^{new}, q^{new}) \leftrightarrow (p, q) \text{ is a local optimum.} \tag{4.46}$$

which implies that the values from the previous iteration are considered as a solution if and only if (p, q) is a local optimum of minimizing $L(x)$.

To summarize the gradient descent algorithm, Algorithm 4.3 solves the OPF problem for a decreasing sequence of μ that approaches 0:

Algorithm 4.3: A Gradient Descent Algorithm

Input: A feasible point (p, q)

Output: A numerical solution (p^*, q^*) of (4.17)

① $p^* = p$, $q^* = q$

② **for** $\mu = \mu_1, \mu_2, ..., \mu_K$
do

③ execute the BFS algorithm to obtain the power flow solution (v^*, p_0^*, q_0^*) w.r.t. (v_0, p^*, q^*)

④ compute gradient $\partial_x L(x; \mu)$

⑤ run a line search method (Algorithm 4.2) to get an updated $(p^*, q^*, stopFlag)$

⑥ **while** $stopFlag \neq 1$
end

There are two key components in the distributed implementation of Algorithm 4.3: 1) compute the gradients in a distributed way, and 2) run line search (Algorithm 4.2) in a distributed way. Section 4.2.2 explains the distributed implementation of the gradient computation method. Three main requirements suit the agent-based EMA architecture:

- There is an agent i at each node whose power injections are controllable (p_i, q_i).
- Agent i knows the impedances and can measure the nodal voltage v_i and line flows (P_{ij}, Q_{ij}, l_{ij}). It can also control the injections (p_i, q_i) and communicate with the substation agent at the reference node 0. This substation agent will be the GA.
- The coordinator agent can compute the similar substation parameters required in calculations.

The distributed implementation of the line search method in Algorithm 4.2 gives rise to a distributed implementation of the inner loop of Algorithm 4.3, presented in Algorithm 4.4.

In Algorithm 4.4, each agent at a control node stores its last approved power injections (p_i^{old}, q_i^{old}) and proposes tentative power injections (p_i^{new}, q_i^{new}) while computing some other quantities $(\Delta s_i, \Delta L_i, x_i^{new})$. These help the coordinator decide whether to accept or reject the solution, i.e., the network and operational constraints are handled, and the power flow is solved to update the dependent variables. The tentative injections are computed with the help of the system gradients where η is controlled by the coordinator agent, in this case, the primary EMA. The EMA initializes $\eta = 1$ and reduces η by a fraction $1 - \alpha$ until the inequality constraints are satisfied and the modified objective function $L(x,\mu)$ is well approximated by its linearization, i.e., $L^{new} < L^{thres}$. The primary EMA decides whether to accept or reject the tentative injections and terminate the algorithm. The decision is based on $(\Delta s_i, \Delta L_i)$ computed by the agents i. The quantity Δs_i gives the update size of (p_i, q_i), and ΔL_i is the product of the gradient and the power injection. The convergence criteria for the algorithm is given by:

- if $\Delta s_i \leq \epsilon$ then stop the inner loop in Algorithm 4.3
- else if $L^{new} \leq L^{old} + \beta \sum_{i \in N+} \Delta L_i$ then approve the tentative injections
- else reduce the step size η by a fraction of $(1 - \alpha)$

Algorithm 4.4: Distributed Gradient Projection Algorithm

Input: Each agent i at a controllable node knows its original power injection (p_i, q_i), voltage v_i, impedance (r_{ij}, x_{ij}) for neighboring lines and power flow for downstream lines. The primary EMA knows algorithm parameters α, β, μ, and ϵ

Output: Updated (p^*, q^*) for each agent i

(1) The EMA broadcasts μ to all agents i

(2) Each agent i sets $(p_i^{old}, q_i^{old} \leftarrow (p_i, q_i))$ and computes $value^{old}(x)$ and reports to the EMA. The GA solves an initial power flow to obtain (p_0, q_0) and reports $L_0(x)$ to the EMA

(3) The EMA computes the objective function of the system $L^{old}(x)$

(4) The agents i (BFS method) or the GA (Jacobian method) computes the system gradients and therefore $\partial_x L(x,\mu)$

(5) The primary EMA initializes $\eta \leftarrow 1$ and broadcasts the same to all agents

(6) Each agent computes $(p_i^{new}, q_i^{new}, \Delta s_i, \Delta L_i, value^{new}(x))$ and reports back to the EMA

(7) The GA applies the tentative injections to the grid and executes a power flow to obtain a steady state (P, Q, v, p_0, q_0)

(8) In case of constraint violations for inequality constraints, the GA and the agent i send out a signal to the coordinator to reduce η

(9) The primary EMA computes $\sum_{i \in N^+} \Delta s_i$, $L^{new}(x)$, and $L^{thres}(x) \leftarrow L^{old}(x) + \beta \sum_{i \in N^+} \Delta L_i$
if $\sum_{i \in N^+} \Delta s_i \leq \epsilon$; go to Step (11)
else if $L^{new}(x) > L^{thres}(x)$; reduce $\eta \leftarrow \alpha\eta$ and go to Step (5)
else Update (p_i^{old}, q_i^{old}); i.e., go to Step (10)

(10) Each agent i sets $(p_i^{old}, q_i^{old} \leftarrow (p_i^{new}, q_i^{new}))$ and returns to Step (2)

(11) The primary EMA sets $resetFlag \leftarrow 1$ if $L^{new}(x) > L^{old}(x)$ or $resetFlag \leftarrow 0$ otherwise

(12) Each agent i sets $(p_i^*, q_i^* \leftarrow (p_i^{old}, q_i^{old}))$ if $resetFlag = 1$ or $(p_i^*, q_i^* \leftarrow (p_i^{new}, q_i^{new}))$ otherwise

4.4 Tchebycheff's Decomposition

The Gradient projection algorithm solves a single-objective constrained optimization problem and delivers a single optimal point for each time instant t. This thesis's optimization problem is multi-objective, with conflicting objectives often paired together. The multi-objective optimization problem (MOP) has a vector form:

$$\min \qquad F(x) = \{f_1(x), f_2(x), ..., f_M(x)\} \tag{4.47}$$

Where M is the number of objectives. Please note that (4.47) is the general representation of (4.11).

The solution of a MOP is popularly discerned by *Pareto Optimality*. Let us consider a decision space, which is the graph of the constrained feasible region for solutions to the problem [149]. Let R^M be the objective space for M objectives. The decision vector space is Ω where for every $x \in \Omega$, there exists a $F(x) \in R^M$ (criterion space bound by the number of objectives). To understand *Pareto Optimality*, let us consider two M-objective vectors, v,$w \in R^M$. v dominates w if and only if [145]:

$$v_i \leq w_i \quad \text{for every} \quad i \in \{1,2,...,M\} \tag{4.48a}$$

$$v_j < w_j \quad \text{for at least one index} \quad j \in \{1,2,...,M\} \tag{4.48b}$$

The space enclosed by the lowest points (minima) of the objective functions in the criterion space is called the *Pareto Front* (PF) [150]. For the example of a 2-objective problem, a line joining v_{min} and w_{min} will represent the PF. Any point on the PF is *pareto optimal*. Along this line, one objective improves at the cost of another. However, neither objective can improve simultaneously.

On the contrary, any point in the feasible space but not on the PF is a "bad" solution, as either objective can improve without harming the other. There is no mathematical "best" solution on the PF. Selecting a suitable optimal point from the available PF requires negotiations between system participants.

Pareto Optimality

A point x^* is *Pareto optimal* if there is no point x such that $F(x)$ dominates $F(x^*)$. Therefore, x^* is termed a non-dominated solution and forms the *Pareto Set* (PS). The *pareto optimal* objective vector is $F(x^*)$.

Decomposition of an optimization problem into smaller subproblems was first introduced in [151], where the subproblems are solved separately. The decomposition could be at different levels: decision variables, functions, and objectives. In this work, the multi-objective objective function $L(x;\mu)$ is decomposed into singular subproblems for the Gradient projection algorithm to solve separately. Decomposition is a widely used scalarization technique to deal with an MOP. The weighted sum (WS) approach [152] is preferred popularly in traditional methods due to its ease of use and search efficiency. In this approach, a multiplicative predefined weight factor linearly aggregates the multiple objectives into a single objective problem. However, for non-convex problems, such as the OPF problem, the WS approach cannot guarantee a well-spread PF [152]. Moreover, as the value is predefined, the solutions obtained are not flexible enough to showcase different scenarios with varying benefits to each involved participant with a conflict of interest.

Tchebycheff's decomposition approach [138] resolves previously stated issues of the WS method by generating an equally spaced weight vector, λ, for an arbitrarily chosen population size, which successfully provides a well-spread PF, even for non-convex problems. Afterward, selecting the best solution depends on negotiation between all participants. To start the decomposition process, let us consider a population size N calculated as:

$$N = C_{M-1}^{H+M-1} \tag{4.49}$$

where H is the resolution of weight vector λ and M is the number of objectives. Let's define N evenly spaced weight vectors λ^1,λ^2,...,λ^N. Each weight vector will be of M dimensions i.e., $\lambda^m = (\lambda_1^m,\lambda_2^m,...,\lambda_M^m)^T$ for $m = 1,2,...,N$. The summation of all elements in the weight vector equals 1, i.e.,

$$\lambda_1^m + \lambda_2^m + ... + \lambda_M^m = 1 \tag{4.50}$$

Each element in a weight vector can take values such as:

$$\lambda_i^m \in \left\{0,\frac{1}{H},\frac{2}{H},...,\frac{H}{H}\right\} \quad \text{for} \quad i = 1,2,...,M \tag{4.51}$$

Let $z^* = \{z_1^*,z_2^*,...,z_M^*\}$ be the vector of minimum objective values for each objective and act as a reference point in the optimization algorithm. The elements of this

vector are computed by $z_i^* = \min\{f_i(x)_{x \in \Omega}\}$, which means the weight vector for a single objective is at the highest priority to solve for the point where the objective reaches its lowest point. z^* is usually not known beforehand, and during the iterative process, the algorithm finds the lowest values of $f_i(x)$ and substitutes them for z_i^* in the objective. The scalarized objective function after decomposition looks like this:

$$g^{te}(x|\lambda,z^*) = \min \ \{\lambda_i^m | f_i(x) - z_i^*\} \tag{4.52}$$

Traditionally, when solving MOP with evolutionary algorithms, there is a requirement to normalize the objectives as the absolute values can be highly disparate. For example, the total system operational costs for a single time instant t maybe $60€/MWh$, and the voltage deviation is 2.37 p.u. Normalization brings all objective values within the [0,1] range. However, there is no such requirement for the numerical Gradient projection algorithm because each objective is associated with its corresponding gradient that steers the search through the decision space.

The steps of Tchebycheff's decomposition approach can be summarized in Algorithm 4.5.

Algorithm 4.5: Tchebycheff's Decomposition

Input: The primary EMA knows the resolution for weight vectors H and the number of objectives M

Output: Decomposed vector of objective function $L(x;\mu)$

(1) The EMA calculates N and constructs an evenly spaced weight vector λ

(2) The EMA triggers the agents to optimize for the initial minima z_i^*

(3) The GA and the agents i incorporate z_i^* into their corresponding $L(x,\mu)$ and report back to the EMA

(4) The EMA multiplies each objective with its corresponding weight vector and returns N single-objective subproblems for the Gradient projection algorithm to solve

Note: The solution from the Gradient projection algorithm is not the desired non-dominated PF. Using the criteria stated in (4.48), the obtained vector is sorted to find the non-dominated *Pareto Optimal* solution.

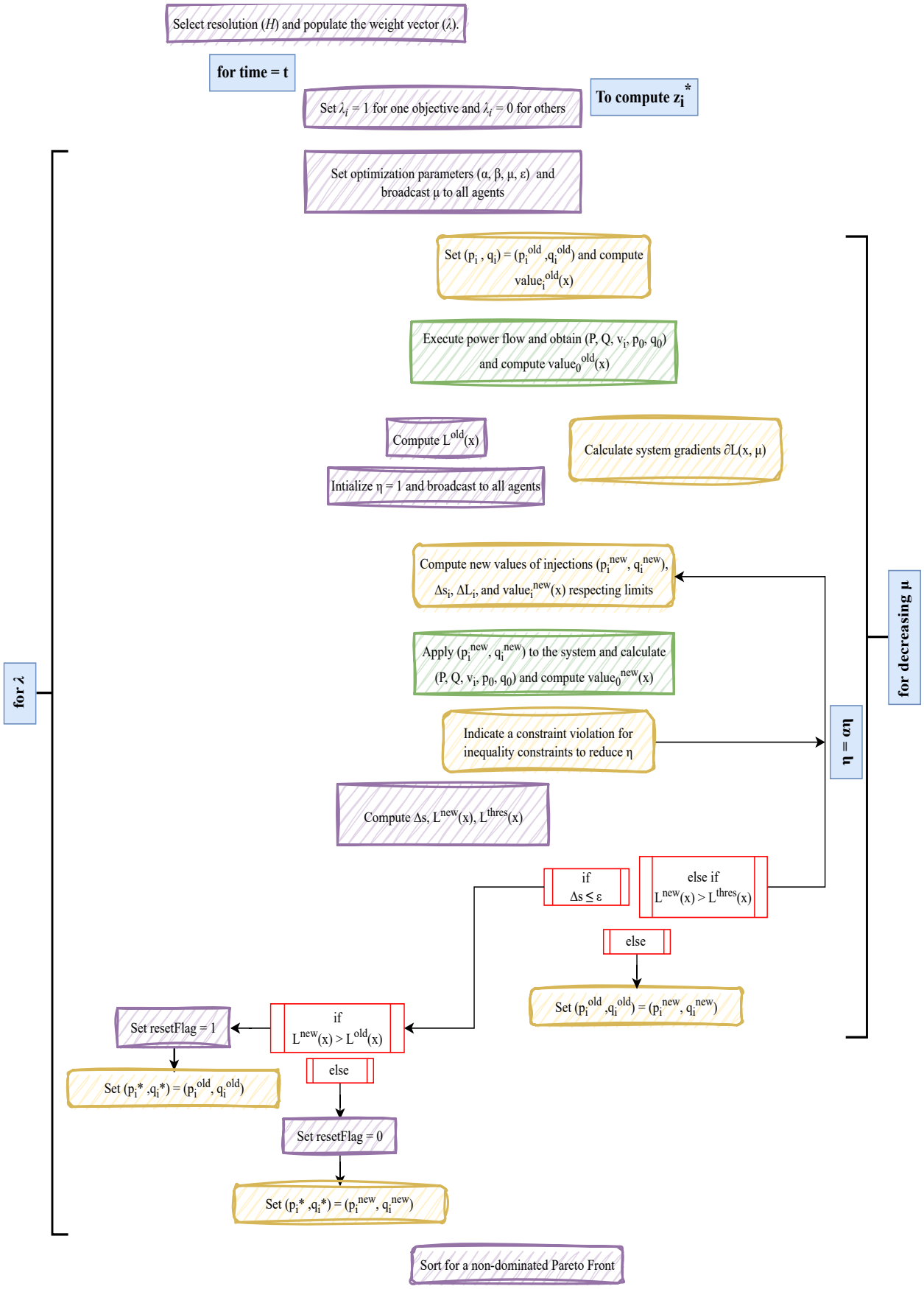

Figure 4.3: Multi-Objective Distributed Optimal Power Flow

Figure 4.3 describes the two-fold approach of solving the multi-objective distributed OPF problem using a combination of Tchebycheff's decomposition method and the Gradient projection algorithm. The purple boxes in the figure represent the tasks performed by the primary EMA, the yellow boxes are the DG units or the prosumer agents, and the green boxes are for the GA in SIMONA.

Chapter 4 Summary and Chapter 5 Preview

Key takeaways from this chapter:

4.1) Formulation of grid topology and parameters

4.2) Definition of network constraints and their handling using Penalty functions

4.3) Two alternative methods to compute system gradients for radial and meshed topologies

4.4) The proposed two-fold approach to solving the multi-objective distributed OPF problem

Highlights for the next chapter:

a) Performance evaluation of the solution algorithm w.r.t. a state-of-the-art centralized approach

b) Application to the system architecture with industrial and residential prosumers

5 Performance Evaluation and Application

The previous chapters developed the agent-based EM architecture and the multi-objective OPF problem. Detailed algorithms describe the distributed computation of system gradients and the interaction protocols between several agents to solve the OPF problem in a distributed fashion. Additionally, a brief insight was provided into the operations of external MAS, which furnishes the industrial and residential demand for simulations. This chapter verifies the performance of the optimization algorithm and validates the proposed hierarchical architecture. To verify the *online* distributed algorithm, this thesis compares the optimality gap between the distributed solution and a state-of-the-art centralized solution in Section 5.1. This section also highlights the differences in performance between the BFS method and the Jacobian method of gradient computation. Section 5.2 and Section 5.3 validate the proposed architecture by implementing it in a co-simulation framework and present two application cases regarding:

- **Industrial Prosumer**
  In this thesis, two types of industrial prosumers are considered for simulation studies:
  - *Prosumer Type A*: *alien*, the industrial demand simulator, models an industrial grid with a PV and BESS unit. The industry follows a self-optimization strategy with the goal of peak shaving to optimally coordinate the available flexible units. Peak shaving reduces the penalty the connected utility grid assigns to demand peaks. It also provides flexible services, such as power injected back into the grid or storage charging and discharging based on grid-oriented objectives.
  - *Prosumer Type B*: This industrial prosumer uses the ZIP modeling technique to optimize its production processes following voltage sensitivity principles. It also owns a BESS unit that assists in providing flexibility.

  The application case helps study the impact of industrial flexibility actions on the distribution grid's economic, technical, and environmental factors. The choice of an industrial prosumer is owed to the following reasons: 1) deterministic modeling efforts following purely economic interests of an industrial prosumer

with available investment capacity to adopt flexible technologies, 2) the theoretical potential in the collaborative operation of the utility grid with one of the highest energy consumers in the market, and 3) novelty of scope in industrial consumer modeling due to the lack of research in the same direction.

- **Residential Prosumer**
  The residential demand profiles are generated by the residential demand simulator *demod* with a time resolution of 15 minutes. The profiles account for daily household activities and capture the changes according to different building types, heating control patterns, and penetration percentages of rooftop PV. The electricity consumption considers the end-user's socio-behavioral aspects, such as their willingness to adopt advanced technologies and partake in the flexibility market. In this application case, the impact of residential adoption of advanced technologies is thoroughly studied on different aspects of the distribution grid, including the excess active power injected back into the connected medium-voltage (MV) grid. The choice of residential prosumers in the second application case stems from the need to investigate the potential impact of many dispersed units capable of energy generation and demand by manipulating granular details of human electricity consumption patterns following socio-behavioral aspects.

It is worth mentioning that the demand modeling from *alien* and *demod* reflect the impact of governance policies and regulations on technology adoption by the end-users in the energy transition scenario. However, as the thesis author did not develop the governance simulator [153], which neither connects to SIMONA nor the primary EMA, there is no need to describe the concept and functionality behind the interaction of the prosumer MAS and the governance model.

5.1 Performance Evaluation

This section provides a brief insight into the optimality properties of the distributed OPF algorithm. The results are compared with that of a state-of-the-art centralized OPF solver [154] to gauge the optimality properties of the algorithm. Both methods of gradient computation are tested on radial and weakly meshed grid configurations and compared in terms of time efficiency. The objective of the optimization problem is cost minimization w.r.t. physical and operational constraints, represented by a

condensed version of the MOP (4.17).

$$L(x;\mu) = a_0 p_0^2(x) + b_0 p_0(x) + b_i p_i(x) - \underline{\mu} \sum_{i=1}^{n} ln(v_i(x) - \underline{v_i}) - \bar{\mu} \sum_{i=1}^{n} ln(\bar{v_i} - v_i(x)) \quad (5.1)$$

where p_0 is the active power generation of the reference node, p_i is the active power output from the connected DG units, v_i are the nodal voltages, and a_0, b_0, b_i are respective cost coefficients. A weekly simulation time horizon is considered, i.e., τ equals 7 days, and the time resolution, i.e., t, is 1-minute. The optimization parameters related to the Gradient projection algorithm are as follows:

- back-off and linearization parameters, $(\alpha, \beta) = 0.5$
- convergence criteria, $\epsilon = 0.01$
- decreasing sequence of $\mu = [10^{-1}, ..., 10^{-8}]$

Distribution Grid Topology and Parameters

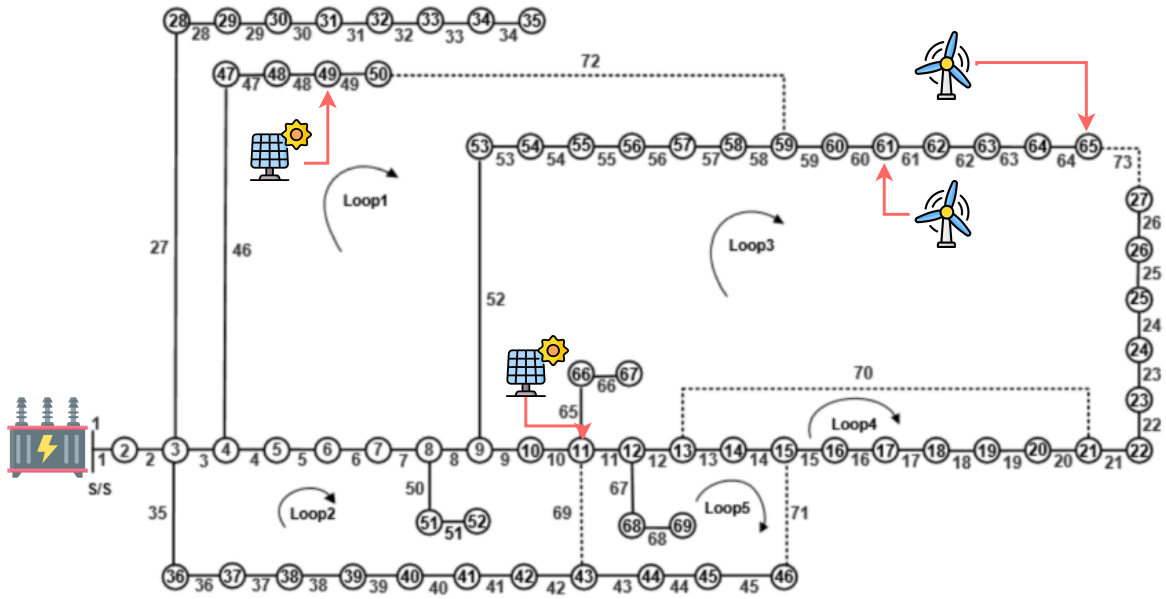

Figure 5.1: Modified Configuration of IEEE 69-node Distribution Grid with DG Units

Figure 5.1 represents the modified configuration for the IEEE benchmark test grid with 69 nodes [155]. The default grid topology is radial with 68 lines, but when the dashed lines in the figures are connected, i.e., the respective switches are closed, the

grid can be transformed into a weakly meshed topology with 5 loops and 73 lines. The grid is operated with active tie lines for simulation tests, i.e., the network is weakly meshed. However, for the BFS gradient computation, the meshed network is transformed into a radial network with the help of virtual nodes. The allocation of DG units follows a network reconfiguration strategy for loss reduction and load balancing [156]. Two additional PV units are placed at nodes (11) and (49), and two other *Wind Energy Converter* (WEC) units are connected to nodes (61) and (65). The slack node (1) acts as the POC to the superordinate grid. A weekly aggregated load normalized to fit the test grid is applied to all grid nodes. Weekly generation and demand profiles are collected from [157].

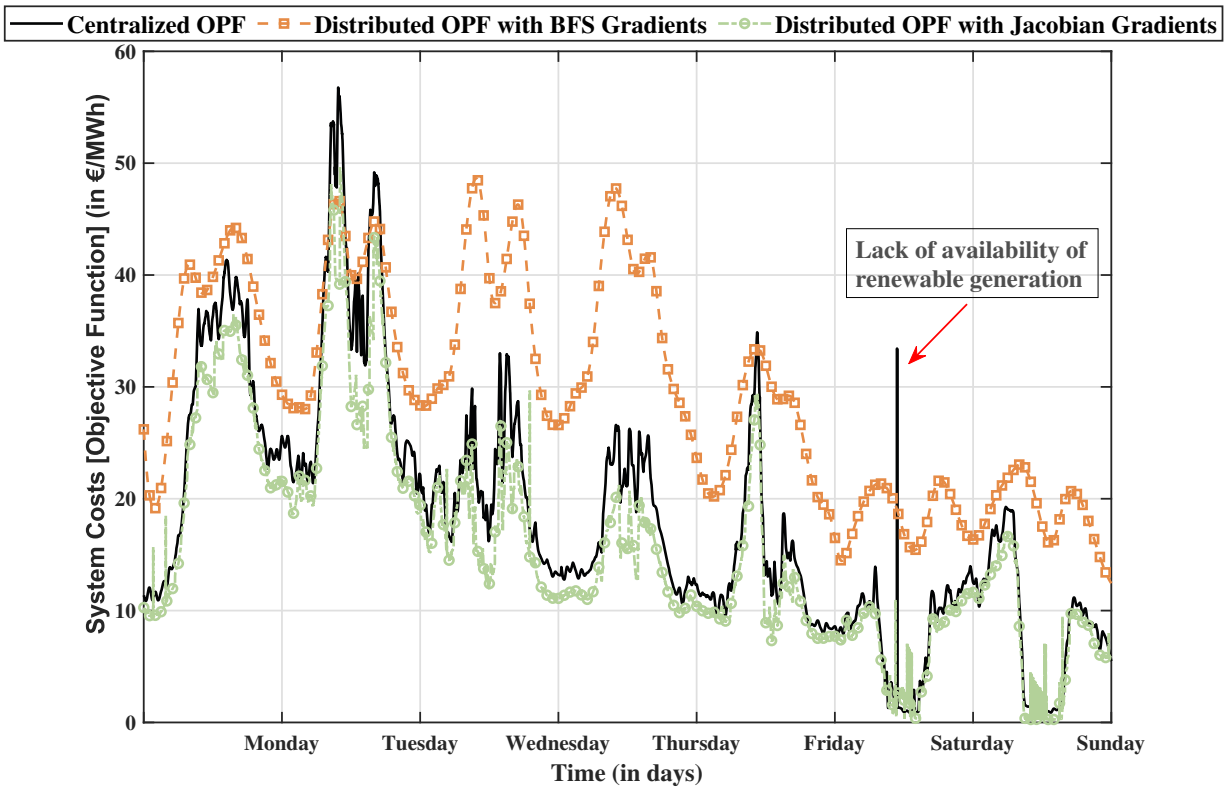

Figure 5.2: Optimal Costs from Centralized and Distributed OPF Algorithms

The optimization results are compared between a centralized OPF solver with exact non-linear computation abilities and the distributed OPF problem with two alternative methods of gradient computation: BFS and Jacobian. The optimal value of the objective function, i.e., generation costs in the system for three algorithms, are presented in Figure 5.2. As the plot shows, the Jacobian computing of the sensitivities or system gradients delivers superior optimality compared to the BFS method

of approximate gradient estimation. The optimality gap with the centralized OPF results is 1.72% and 0.2% for the BFS and the Jacobian method, respectively. The distributed OPF algorithm with both gradient computation methods shows an acceptable optimality gap compared to the results of a centralized OPF. Although the Jacobian method performs better when discussing optimality, the outcomes reverse in terms of time efficiency.

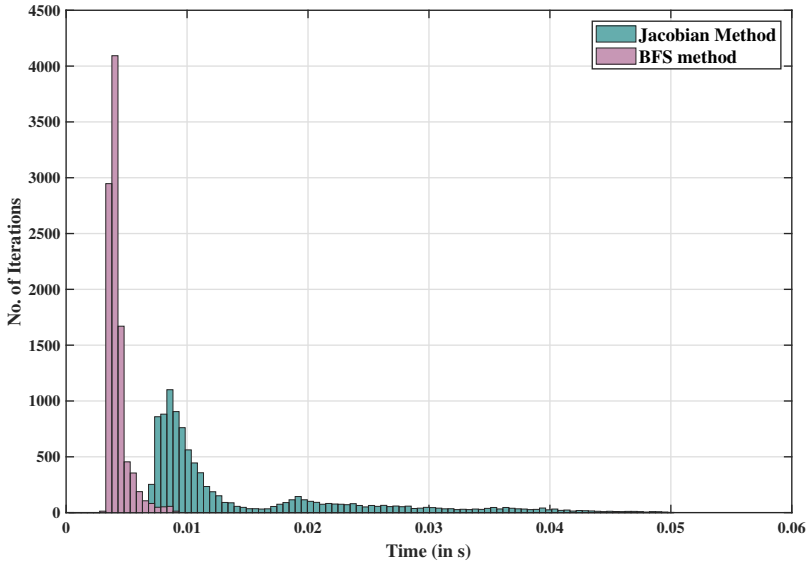

Figure 5.3: Time Taken per Iteration by the Distributed OPF Algorithm

Figure 5.3 represents a histogram showing the time per iteration for the distributed OPF algorithm using the two alternative gradient computation methods. The average time the BFS method takes for a single time step is 4.3ms, and the Jacobian method takes an average time of 15.2ms to converge. Therefore, the BFS method is computationally faster owing to the avoidance of matrix inversion. However, if the test grid has a sparse Jacobian matrix, which is valid for radial distribution networks, the Jacobian method shows considerable speed up. The gradient computation methods provide a trade-off between optimality and time efficiency. Nevertheless, both methods offer significantly higher computational efficiency than the centralized non-linear programming method, which requires 3.32s to converge for a single-time step. These computational efficiency and optimality performances make the selected *online* algorithm suited to real-time implementation, where there is a necessity to solve the optimization problem in a distributed fashion, preserving the data privacy of involved participants.

5.2 Application Case with Industrial Prosumers

In this application case, the two industrial consumers, types A and B, are connected to a weakly-meshed MV distribution grid to study the impact of their self-optimized demand on several grid parameters. The change in their electricity consumption following peak shaving and voltage sensitivity principles provides energy savings to the industrial consumer. The effect of using a BESS unit in the industrial grid with optimal scheduling is primarily studied.

5.2.1 Distribution Grid Topology and Parameters

Figure 5.4 represents the modified configuration for the IEEE benchmark test grid with 33 nodes [155]. The default grid topology is radial with 32 lines, but when the dashed lines in the figures are connected, i.e., the respective switches are closed, the grid can be transformed into a weakly meshed topology with 5 loops and 37 lines. The allocation of DG units follows a network reconfiguration strategy for loss reduction and load balancing [158]. Two additional PV units are placed at nodes (13) and (24), and an extra WEC unit is connected to node (30). The slack node (1) acts as the POC to the superordinate grid. The industrial prosumer load is connected to node (26). The prosumers are connected one at a time to form two simulation scenarios.

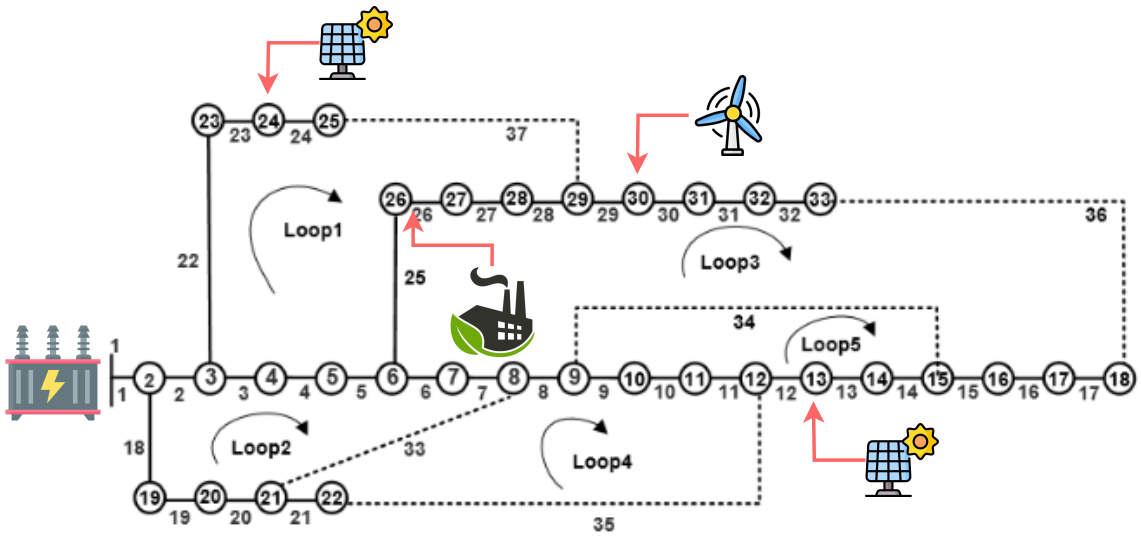

Figure 5.4: Modified Configuration of IEEE 33-node Distribution Grid with DG Units

Cost Coefficients	Values
a_0	0.005
b_0	2.3
c_0	36

Emission Coefficients	Values
α_0	0.04091
β_0	-0.05554
γ_0	0.0649
ω_0	0.000002
μ_0	0.06667

Table 5.1: Costs and Carbon Emission Coefficients for the Slack Generator

The test grid has a nominal voltage of 12.66 kV and a 10 MVA rating. The generation capacities of the PV and WEC-powered DG units are weather-dependent. The data for generation profiles are obtained from the ENTSO-E Transparency Platform that provides daily generation profiles for several technologies in Germany [157]. The balancing reserve or conventional generation source at the slack node is restricted to a maximum of 5 MW. Following the general convention, the slack node voltage is set to 1.0 p.u. The renewable generation cost per unit follows the historical spot market prices in the German wholesale market chosen for the same day as the selected PV and WEC generation profiles, taken from [157]. The fuel cost coefficients for the conventional generator at the reference node follow the *Levelized Cost of Electricity* (LCOE) values [159]. The conventional generator's cost and carbon emission coefficients are summarized in Table 5.1. Carbon emissions for renewable generation are assumed to be negligible; thus, there is no corresponding equation accounting for the carbon emissions for the dispersed DG units.

Optimization parameters

The multi-objective OPF is executed with 2 objectives simultaneously, i.e., $M = 2$. The chosen value for weight resolution, i.e., H, is 199 for 2-objective problems following [145]. Consequently, the calculated population size N using (4.49) equals 200. The population size signifies that the distributed algorithm solves 200 singular subproblems for every time instant, t. The time horizon τ is 24 hours for each simulation with a resolution of 15 minutes. The Jacobian method of gradient computation is used. The relevant optimization parameters for the algorithm are as follows:

- back-off and linearization parameters, $(\alpha, \beta) = 0.5$
- convergence criteria, $\epsilon = 0.1$
- decreasing sequence of $\mu = [10^{-3}, ..., 10^{-10}]$

5.2.2 Industrial Prosumer Type A

This prosumer uses an optimal BESS unit, whose size is determined with the help of a power flow optimization to achieve peak shaving. For this case study, the solar generation unit is assumed to be installed on the industry roof on 1^{st} March 2015, which has a revenue cap for solar panels on non-residential buildings with a maximum capacity of 10 MWp [160]. Therefore, a company feed-in remuneration of 9.05 cts/kWh is assumed for the following 20 years. The investment costs for the solar generation unit are not considered because the benefits of an additional storage unit are accounted for. The first step is to compute the BESS size and the peak shaving limit. The industrial load and PV generation profiles are taken from 2018. Ten days are randomly selected, and solar energy production is set to zero to account for PV failures and maintenance. Table 5.2 gives the optimization parameters and the relevant results obtained from the optimization, such as the optimum BESS capacity, E_{bat}^{nom} and the peak shaving limit, P_{peak_shave}. The simulation takes 147.7s for a year.

Variable	**Value**	**Unit**	**Description**
$T_{sim,total}$	365	[day]	Total simulation time
d	96	[-]	Time steps per day
Δt_{res}	1	[h]	Time resolution
S	1	[-]	Number of samples

Variable	**Value**
P_{inv}^{nom}	0.126 MW
E_{bat}^{nom}	0.173 MWh
P_{peak}	1.732 MW
$P_{peak-shave}$	1.520 MW

Table 5.2: Optimization Parameters and Results for the Industrial Prosumer

The industrial MAS executes a stochastic optimization to obtain a day-ahead BESS dispatch schedule. The computation time per time step is 3.8s. PV generation uncertainty is represented in three ways: using stochastic *Probability Density Function* (PDF) (50 samples), *point percent function* (PPF) 30%, and 1%. It is observed that the scheduling results look comparable at first glance, averaging at the same value with negligible differences during active PV hours. However, with a closer look, it is seen that the result obtained by using a PPF of 1% potentially estimates the smoothest load at *Point of Common Contact* (PCC), i.e., lesser peaks. However, it is advised that all three scheduling results be considered during actual operation to get the best optimum load at the PCC. Finally, the industrial EMA executes an OPF routine for the industrial grid in real-time with actual PV generation to obtain the optimal load at the PCC, which follows BESS scheduling and the peak shaving limits. The primary EMA can also execute this optimization routine in a distributed

fashion without the explicit knowledge of peak shaving and BESS constraints using the Gradient projection algorithm. The flexible load profiles for weekdays and weekends are generated to focus on the load differences owing to whether the industry operations are active. As seen in Figure 5.5a, using an optimal BESS unit for peak shaving saves the industrial prosumer on their electricity bill and the peak power price during operational days. In Figure 5.5b, the combined effort of the PV unit and the BESS keeps the PCC load at a minimum during non-operational days (weekends), thus promoting self-consumption in the industry. The subscripts 1, 2, and 3 stand for the results obtained from stochastic PDF, PPF-30%, and PPF-1%, respectively. Depending on the amount of PV generation, the surplus energy could also be sold directly to the market during weekends after meeting self-demand, generating greater profits for the industrial prosumer [self.5].

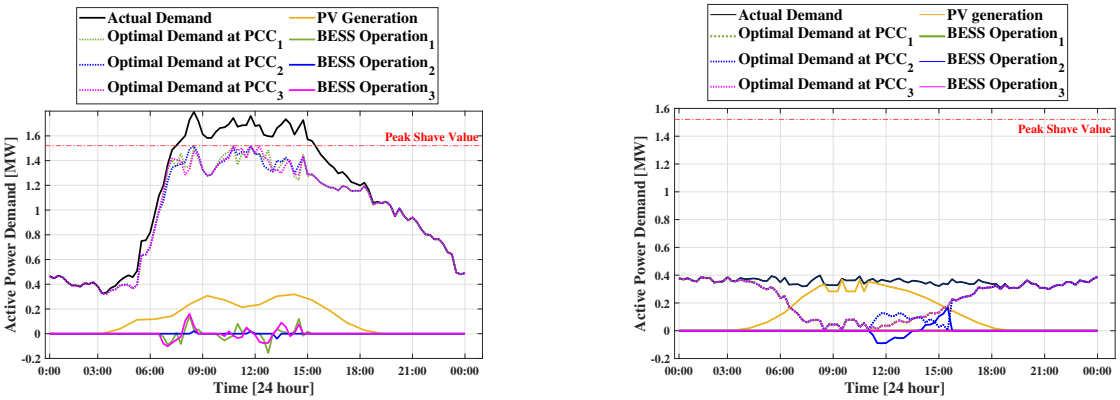

(a) Optimal Industrial Demand at PCC - Weekday

(b) Optimal Industrial Demand at PCC - Weekend

Figure 5.5: Demand Profiles for Industrial Prosumer Type A (*alien*)

Industrial benefits are quantified in Table 5.3. The industrial prosumer type A achieves a daily average savings of 4.85% in energy costs.

Variable	Scheduling			Operation		
	PDF	PPF 30%	PPF 1%	PDF	PPF 30%	PPF 1%
C_{buy} [€]	3611	3264	3617	3428	3407	3430
C_{sell} [€]	248	—	—	—	—	—
$C_{buy}^{nopeakshave}$ [€]	3823			3823		
$C_{sell}^{nopeakshave}$ [€]	455	360	137	262		

Table 5.3: Summary of Expenses for Day-Ahead Scheduling and Operation

Distribution Grid Results

In this scenario, the distribution grid has available generation sources from PV and WEC-powered DG units. There are two types of demand: 1) the industrial prosumer load and 2) the aggregated load on all grid nodes. The generation and demand profiles are selected and modeled for summer days in July. Moreover, all profiles are normalized for the simulation to ensure accurate weightage and representation of available models. A daily simulation is executed for the grid on weekdays and weekends. The objectives are different combinations of operational costs, carbon emissions, and active power losses. The primary EMA executes the proposed two-fold approach to solve the MO-DOPF problem.

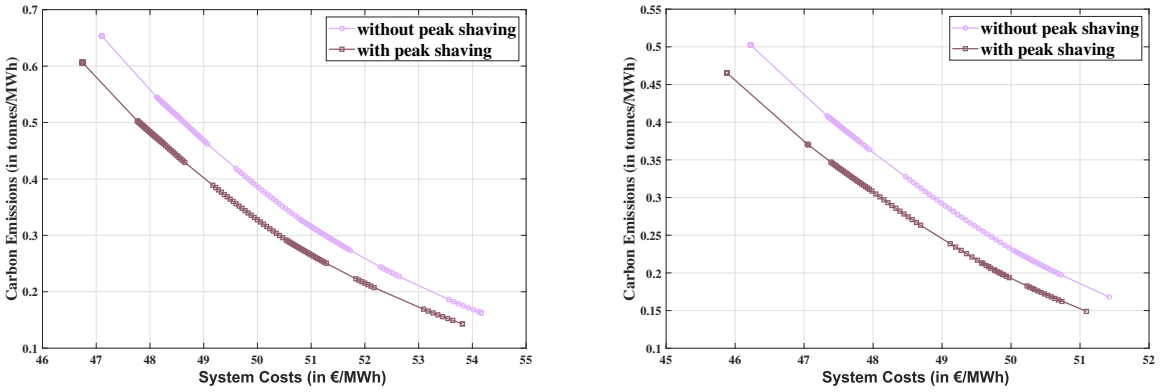

(a) Pareto Front at 9 : 00 a.m. - Weekday (b) Pareto Front at 10 : 00 a.m. - Weekend

Figure 5.6: Pareto Front with Costs and Carbon Emissions in the Distribution Grid

Figure 5.6a and Figure 5.6b showcase the obtained PF for a weekday and weekend operation. The time step of the selected PF is 9 : 00 a.m. for the weekday when industrial processes and PV and wind generation are active. For the weekend, the time step for 10 : 00 a.m. is chosen for an active PV and wind generation hour. As can be seen, when the industry adopts peak shaving strategies, there is a reduction in overall costs and emissions on the distribution grid side because the optimal demand at PCC is reduced for both days. The number of non-dominated *pareto optimal* points are 150 for weekday operations and 140 for weekend operations. Therefore, the algorithm successfully calculates a well-spread PF under industrial prosumer activity. The reductions in costs and emissions on the distribution grid side w.r.t. the use of peak shaving strategy by the industrial prosumer is summarized in Table 5.4. $t_{average}$ and $\tau_{average}$ are the average savings for the selected time step and time horizon, respectively, whereas t_{max} and τ_{max} are the maximum savings, i.e., the optimal

values obtained when the priority or weight for the corresponding objective is highest. Although the reduction in operational costs is minimal compared to the decrease in emissions, the distribution grid benefits from connecting to the industrial prosumer in terms of costs and emissions throughout the obtained PF.

Weekday	**Costs ↓**	**Emissions ↓**
$t_{average}$	1.1%	5.2%
$\tau_{average}$	0.36%	3.28%
t_{max}	0.76%	12.1%
τ_{max}	0.3%	4.15%

Weekend	**Costs ↓**	**Emissions ↓**
$t_{average}$	0.68%	7.9%
$\tau_{average}$	0.37%	3.35%
t_{max}	0.75%	11.42%
τ_{max}	0.32%	3.8%

Table 5.4: MO-DOPF Results for the Distribution Grid in terms of Costs and Emissions

When treated as an objective, active power losses in the distribution grid see a daily average 1.75% reduction on weekdays and an increase of 0.15% on weekends, i.e., during industrial inactivity. Hence, the industrial optimal demand at PCC is minimal, whereas the PV and wind generation are high. The average power losses increase because the supply exceeds the demand, leading to increased power losses. In such a case, the primary EMA can negotiate with the industrial EMA and incentivize the charge of the BESS unit with power from the grid to increase demand and reduce power losses in the system. However, a more exciting result is between the *pareto optimal* points. Figure 5.7a and Figure 5.7b demonstrate the changes in the active power losses in the distribution grid under different priorities, i.e., setting $\lambda = 1$ for the cost or the emissions objective. Power losses steeply decline, up to 35%, on weekdays and weekends while using the renewable-sourced DG units against the balancing reserve, i.e., the reference node generator.

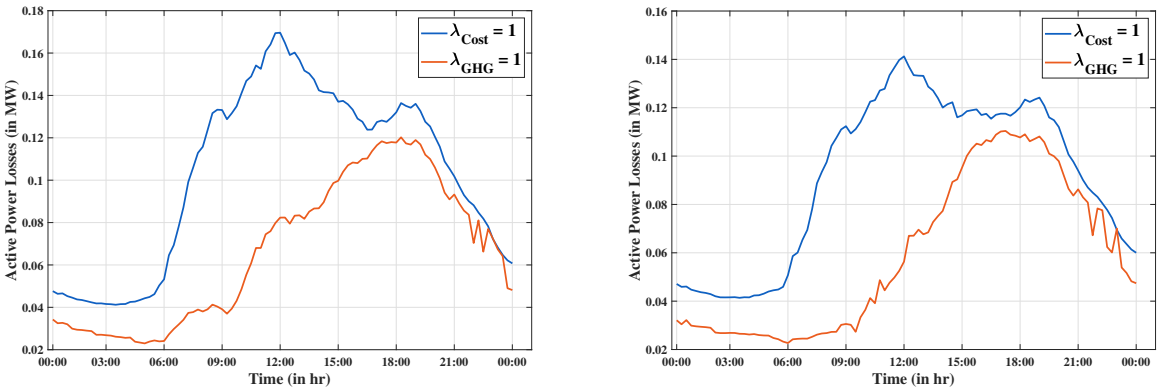

(a) Average Active Power Losses - Weekday (b) Average Active Power Losses - Weekend

Figure 5.7: Average Daily Active Power Losses in the Distribution Grid

The optimal operation of the industrial grid can reduce power losses in the distribution grid by shaving their demand peaks. However, to achieve optimal power losses, the distribution grid has to incur additional operational costs when buying renewable power from the market. Similarly, an overall reduction of 0.4% is observed under optimal industrial demand for voltage deviations, whereas on weekends, peak shaving strategies lead to an increase of 0.26%. Figure 5.8a and Figure 5.8b show the average voltage deviation per node for weekdays and weekends. The value of the voltage deviation suggests the difference between the nodal voltage value and nominal voltage, i.e., V_{nom}. For example, if the voltage deviation is 0.07 p.u., this means that the actual nodal voltage is at 0.93 p.u. which is well within the boundaries of $(\underline{v}, \bar{v}) = [1.0, 0.9]p.u.$

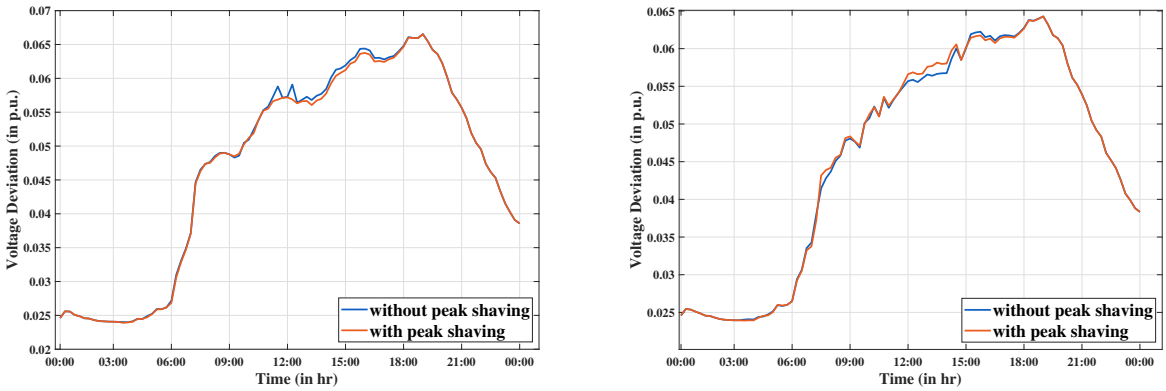

(a) Average Voltage Deviation per Node - Weekday

(b) Average Voltage Deviation per Node - Weekend

Figure 5.8: Average Daily Voltage Deviation in the Distribution Grid Nodes

In conclusion, technological adoption on the industrial prosumer side leads to self-optimization strategies such as peak shaving, which considerably impacts the distribution grid's economic, environmental, and technical parameters. However, there remains a conflict of choice between the cheapest, environment-conscious, and most robust solutions. The proposed MO-DOPF algorithm converges in an average of 2.72s for weekdays and 2.45s for weekends for a single iteration, i.e., the time it takes to solve 200 singular OPF problems. The maximum computation time for the algorithm to solve for a 24-hour simulation with a 15-minute time resolution is 3.5 minutes. Therefore, the proposed algorithm can be employed on comparable grid sizes in real-world scenarios to solve for day-ahead and intraday markets.

5.2.3 Industrial Prosumer Type B

This type of prosumer uses the same industrial network and its components. However, industrial self-load modeling uses the ZIP approach, which considers the effect of applied voltage. Active power measurements from an industrial process help identify the ZIP parameters described in Section 3.5.3 [161]. An AC-OPF algorithm optimizes the industrial production processes and returns an optimal load considering PV generation, BESS unit, and the ZIP load. The BESS unit is charged/discharged depending on the market price [162] to maximize profits for the industrial prosumer. The PV generation profile for industrial prosumers and the DERs is taken from [163]. Three different scenarios are selected for simulation:

- *Without ZIP model and BESS unit*

  The industrial self-load is not modeled according to the ZIP approach, i.e., the effect of applied voltage at PCC on the industrial load is not considered. Furthermore, no BESS unit has been installed. Therefore, the values for the energy consumed and corresponding expenses incurred by the industrial consumer are the base values without any flexibility practices.

- *With ZIP model and without a BESS unit*

  This scenario uses the ZIP approach to model the industrial load. Here, the least energy is purchased from the distribution grid because the ZIP load enables the optimizer to keep voltages at the lower limit and reduce the load. Moreover, the absence of a BESS unit further reduces the load.

- *With ZIP model and a BESS unit*

  In this case, the energy purchased from the grid is higher compared to the second case. However, the total expenses are lower owing to the gained profit by taking advantage of the storage energy arbitrage, i.e., offering BESS charge/discharge on market incentives.

The computational complexity of the optimization algorithms used for the industrial network is mixed: polynomial for continuous variables and exponential for binary variables. Binary variables are used only in the ZIP load modeling approach. However, as the computations are executed on independent agents, the increasing size of the system will not affect the EMA processes. Moreover, as this grid represents a small-scale industrial network, it is doubtful that it can scale up to the size of a power distribution network. The average computational time taken per time step is 0.2s.

Figure 5.9a and Figure 5.9b present the optimal load profiles generated using the ZIP approach and the BESS operation, including the *State of Charge* (SOC).

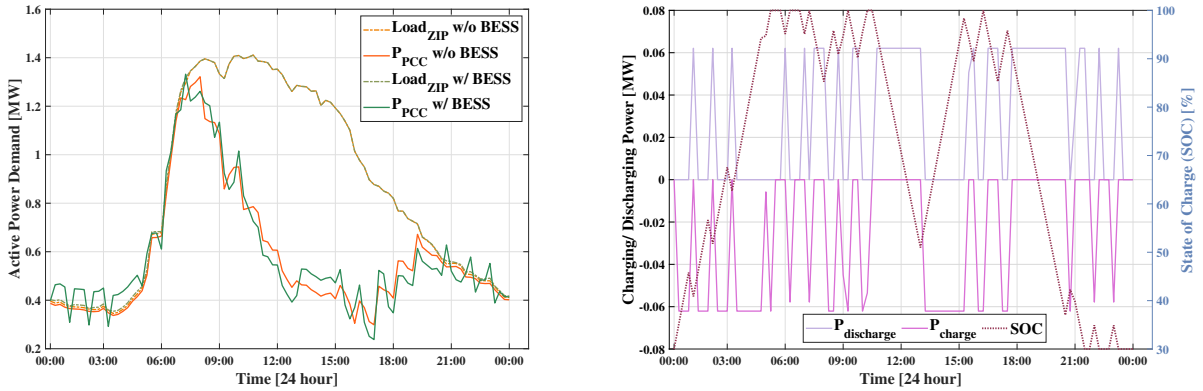

(a) ZIP profiles and Optimal Demand at PCC(b) BESS Charge/Discharge Profiles and SOC

Figure 5.9: Demand Profiles and BESS Operations for Industrial Prosumer Type B

Table 5.5 summarizes the results and gives the achieved percentage reduction in energy exchange with the grid and expenses for the concerned industrial prosumer.

Scenario	$Load_{PCC}$	% ↓	Total Expenses	% ↓
No ZIP + No BESS	17.09	-	1209.12	-
ZIP + No BESS	13.90	18.66	979.49	18.99
ZIP + BESS	14.09	17.55	971.22	19.68

Table 5.5: Summary of Energy Exchange and Expenses

Distribution Grid Results

In this scenario, the distribution grid infrastructure remains the same except for the industrial prosumer load, which is now modeled using the ZIP approach. The generation and demand profiles are selected and modeled for summer days in July. Moreover, all profiles are normalized for the simulation to ensure accurate weightage and representation of available models. A daily simulation is executed for the grid with three different industrial load profiles: 1) without ZIP modeling or BESS (NZNB), 2) with ZIP modeling but not BESS (YZNB), and 3) with ZIP modeling and BESS (YZYB). The objectives are different combinations of operational costs, carbon emissions, and voltage deviation. The primary EMA executes the proposed two-fold approach to solve the MO-DOPF problem. Figure 5.10a illustrates the obtained PF

at 9 : 00 a.m. for industrial prosumer type B. The number of non-dominated *pareto optimal* points is 149. ZIP modeling approach delivers a 0.32% and 2.35% decrease in the grid's operation costs and carbon emissions by curtailing its load. When used for storage arbitrage in the market, the additional BESS unit reduces the grid costs and emissions by 0.48% and 3.7%, respectively. Figure 5.10b highlights the reduction in balancing reserve requirements under flexibility practices by the industrial prosumer. The ZIP modeling approach draws 1.6% less power from the reference node. However, adding a BESS unit does not contribute to further reduced slack usage on average. Moreover, reductions of 1.6% and 0.5% are observed in the distribution grid's total active power losses and total voltage deviation under the ZIP modeling approach.

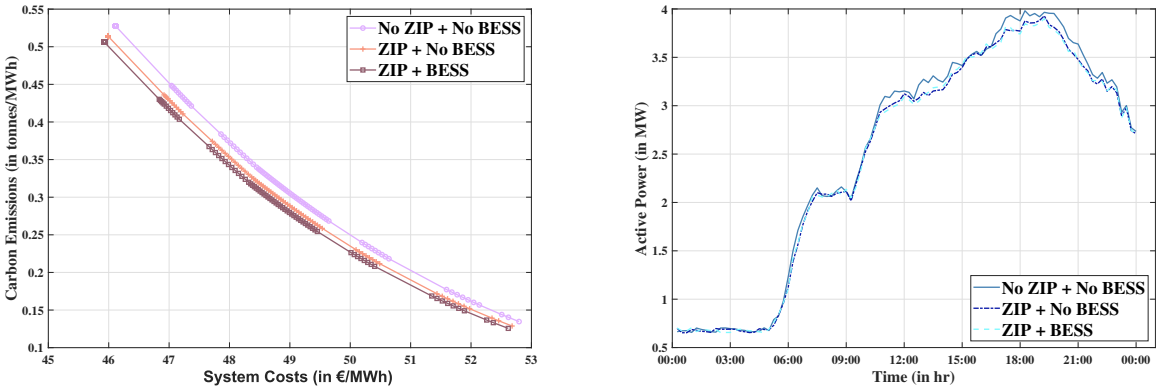

(a) Pareto Front at 9 : 00 a.m.

(b) Usage of Slack Active Power

Figure 5.10: Pareto Front and Slack Active Power Usage in the Distribution Grid

The proposed MO-DOPF algorithm takes an average of 2.5s to converge at every iteration, solving 200 singular OPF problems. The total computation time for a 24-hour simulation with 15-minute time resolution is 2.73 minutes.

The results show that industrial consumers' adoption of advanced technologies and optimal management schemes significantly impacts sustainable and secure distribution grid operation, both positively and negatively. The proposed MO-DOPF algorithm, with its ability to produce well-spread PFs for every scenario and determine a depreciation of the concerned objectives without violating system constraints, such as generation capacities and nodal voltages, is not only computationally efficient but also suitable for real-time 5-min or 15-min intra-day market simulations, particularly for smaller distribution networks.

5.3 Application Case with Residential Prosumers

The residential consumers are studied differently in this thesis. Unlike the profit-seeking industrial prosumer that optimally manages available components of PV and BESS to reduce energy prices, the residential prosumer electricity usage follows socio-behavioral aspects. Diverse social classifications group residential consumers into clusters of similar age, gender, political ideologies (green leaning), economic status, etc., to model their respective electricity demand. The model also includes technology adoption data for these residential groups, providing the penetration levels of rooftop PV, electric heat pumps, etc. The percentage of adoptions gives a population size with dispersed flexible units under control, turning them into active DR participants. Using this population size, *demod* generates residential load profiles for several pre-defined scenarios, imitating the behavioral activities of the social groups. This section presents simulation results for the following scenarios, which can be used to inform energy policies and strategies:

- **Heating Control Patterns** — There are 7 scenarios for changing heating control patterns in homes equipped with electric heat pumps according to the heating temperature being:

  (1) **constant** *(const)*
  Includes those households that keep a constant temperature during the day (average set-point 21°C and standard deviation 2.2°C, data according to conducted survey)

  (2-6) **variable** *(var0, var1, var2, var3, var4)*
  Households associated with the *var0* pattern generally set the thermostat to have a single, short temperature rise during the day, usually in the morning or evening; in contrast, households in pattern *var1* set the temperature higher during all daylight hours, while at night the temperature is considerably lower; the temperature set-point profile of the pattern *var2* is characterized by two temperature rises, one in the morning and the other in the late afternoon/evening; the pattern *var3* follows a similar behavior as *var1*, but with a lower difference between the daytime and nighttime temperature set-points; finally, households with pattern *var4* usually set the thermostat to have two periods of higher temperature in the morning and afternoon/evening. Still, the temperature rise is lower than pattern *var2*.

(7) or a **mix** of control patterns *(mix)*.

- **Types of Dwelling** — Four different kinds of accommodation or building types are examined:
  - *improved detached* which are renovated single apartments
  - *detached* single apartments,
  - *terraced* family homes,
  - *improved terraced* renovated family homes
- **PV Penetration Levels** — Arbitrary levels of rooftop PV penetration are selected to study the impact of increasing PV generation in a *low-voltage* (LV) distribution network, i.e., the effect of decreasing residential load during peak PV generation hours. The maximum installation capacity of a rooftop PV is 5 KW.

5.3.1 Distribution Grid Topology and Parameters

Figure 5.11 represents the modified configuration for the IEEE benchmark test grid with 85 nodes [164]. The default grid topology is radial with 84 lines. The allocation and sizing of DG units follow a two-stage approach to minimize grid operation costs in distribution networks [165]. Two additional PV units are placed at nodes (67) and (71), and an extra WEC unit is connected to node (37). The slack node (1) acts as the POC to the superordinate grid. 84 residential consumers are connected to corresponding nodes in the distribution grid. The residential demand profiles for these 84 households are modeled and classified according to the abovementioned scenarios. Additionally, the scenarios dealing with heating control patterns and building types are modeled using demand and generation data for winter days, and the PV penetration scenarios are tested for both winter and summer.

The test grid has a nominal voltage of 11 kV and a 1 MVA rating. The generation capacities of the PV and WEC-powered DG units are weather-dependent. The data for generation profiles are obtained from the ENTSO-E Transparency Platform that provides daily generation profiles for several technologies in Germany [157]. The balancing reserve or conventional generation source at the slack node is restricted to a maximum of 10 MW. However, unlike the industrial scenario, the lower limits for the reference node are negative, i.e., -10 MW, to signify the potential of reverse power flow to the MV network during high penetration of rooftop PV. The base demand for

the case is 2.5143 MW. The residential load profiles are normalized and multiplied by the base demand at each node. The slack node voltage is set to 1.0 p.u. The renewable generation cost per unit follows the historical spot market prices in the German wholesale market chosen for the same day as the selected PV and WEC generation profiles, taken from [157]. The fuel cost and carbon emissions coefficients for the reference node balancing reserve are equal to the values used in the industrial study, summarized in Table 5.1. Carbon emissions for renewable generation are assumed to be negligible; thus, there is no corresponding equation accounting for the carbon emissions for the dispersed DG units.

Note: There are two distinct PV unit types used in the simulation: 1) a PV-sourced DG connected directly to the grid; 2) rooftop PV installation on a selected portion of the residential population size. The increase in PV penetration signifies the increase in rooftop PV numbers, not the directly connected DG units.

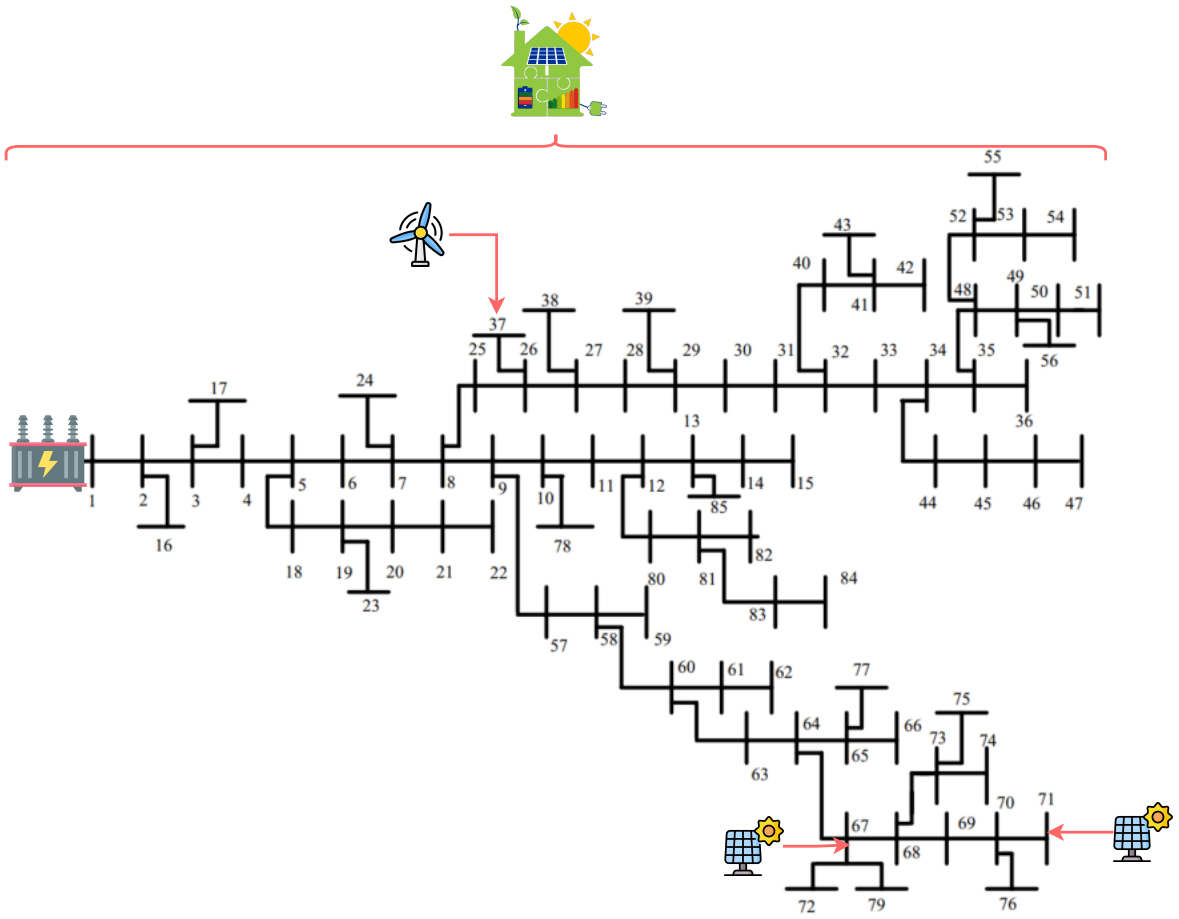

Figure 5.11: Modified Configuration of IEEE 85-node Distribution Grid with DG Units

Optimization parameters

The multi-objective OPF is executed simultaneously with 2 or 3 objectives, i.e., $M = 2$ or $M = 3$. The chosen value for weight resolution, i.e., H, is 23 for 3-objective problems, following [145]. Consequently, the calculated population size N using (4.49) equals 300. Therefore, in a 3-objective problem, the OPF algorithm solves 300 singular sub-problems for every instant, t. The specifics of a 2-objective problem are mentioned in the previous section. The time horizon τ is 24 hours for each simulation with a resolution of 15 minutes. The relevant optimization parameters are equivalent to those used for the industrial prosumer application case. The BFS method of gradient computation is used for this application case.

5.3.2 Heating Control Patterns

As mentioned earlier, there are 7 different heating control patterns depending on the heating temperature variation (*const*, *var0*, *var1*, *var2*, *var3*, *var4*, *mix*). The daily demand profiles of 84 residential households are modeled according to the type of heating control the consumers exercise. The 84 load profiles modeled for each different household, acting as an agent in the *demod* environment, are applied to 84 corresponding grid nodes. Figure 5.12a and Figure 5.12b demonstrate the average daily demand for 84 households under different heating control patterns for weekdays and weekends, respectively. Daily consumption due to other household appliances is also accounted for. The benchmark scenario uses constant temperature (*const*), renovated apartments (*improved detached*), and a 0% penetration of rooftop PV.

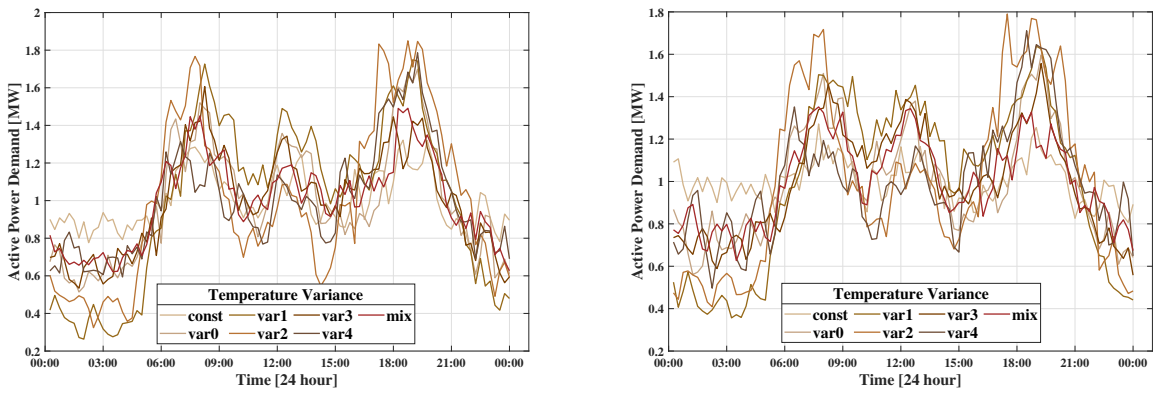

(a) Average Daily Demand - Weekday

(b) Average Daily Demand - Weekend

Figure 5.12: Average Daily Residential Demand Profiles acc. to Heating Control Patterns

Distribution Grid Results

The MOP for the connected radial distribution grid considers operational costs and power losses. The MO-DOPF algorithm delivers well-spread PFs for the time interval of intensive renewable generation averaging at least 120 Pareto optimal points. However, two instances exist where the MOP problem ceases to conflict, i.e., a single optimal point is satisfactory. Firstly, if there is no available renewable generation, the only option to supply the demand is to use the conventional generator at the slack node. Secondly, during negative spot market prices, the generators whose power is bought from the market are cheaper than any other alternatives. However, during some steps, the power losses and the costs of operation conflict even when market prices are negative. The MO-DOPF algorithm successfully produces well-spread PFs for such instances, albeit only in a few cases. The results indicate the importance of analyzing the effect of market prices on the technical parameters of the distribution grid. Figure 5.13 represents the minimum operational costs achieved by the MO-DOPF algorithm for the distribution grid under changing residential heating control patterns.

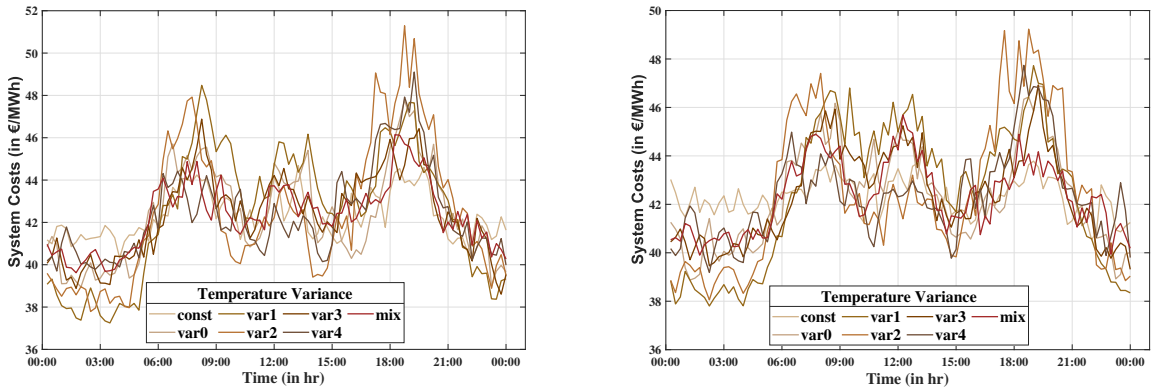

(a) Minimum Operation Costs - Weekday (b) Minimum Operation Costs - Weekend

Figure 5.13: Minimum Operation Costs for the Distribution Grid

Figure 5.14 represents the minimum active power losses achieved by the MO-DOPF algorithm for the distribution grid under changing residential heating control patterns. As the figures show, the algorithm maintains the system's operational costs close to the benchmark operation of a constant heating temperature with minor increases of up to 0.4%. However, the change in the total active power losses is distinct. Table 5.6 summarizes the results for both objectives. *var2* provides the worst combination of increasing costs and power losses, whereas *mix* offers the best trade-off between costs

and power losses of the system. However, minimizing the power losses comes at the expense of incurring high carbon emissions of up to 20% as the network draws from the reference node instead of connected DG units. Therefore, a random operation of heating control patterns in the population promises the potential to support an optimized grid operation regarding its system costs and power losses.

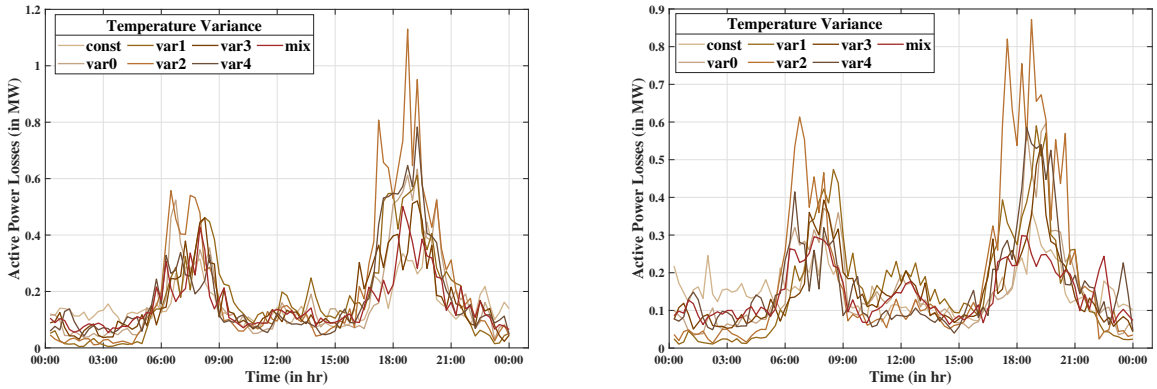

(a) Minimum Active Power Losses - Weekday (b) Minimum Active Power Losses - Weekend

Figure 5.14: Minimum Total Active Power Losses for the Distribution Grid

Control Pattern	**Weekday**		**Weekend**	
	Costs (%)	Power Losses (%)	Costs (%)	Power Losses (%)
const	—	—	—	—
var0	0.19	15.6	0.18	7.46
var1	0.37	17	0.35	11.36
var2	0.44	39.42	0.42	34.09
var3	0.11	8.82	0.14	2
var4	0.15	17.84	0.12	10.77
mix	0.04	1.9	0.06	2.56 ↓

Table 5.6: Summary of Changes in the System Costs and Power Losses in the Distribution Grid

The proposed MO-DOPF algorithm's average time to solve the 2-objective MOP for a 24-hour simulation is 1.36 minutes for all cases. The average time per iteration to solve 200 singular subproblems is 1.52 seconds. In conclusion, heating control patterns considerably impact the grid's economic, environmental, and technical parameters. Extensive simulation studies can help identify suitable incentives and mechanisms to control electric heat pumps in a grid-oriented manner.

5.3.3 Types of Dwelling

This section examines four different types of apartments. It compares the impact of renovated homes with better insulation to previous technology. Figure 5.15 represents the different load profiles depending on the accommodation type for weekdays and weekends, respectively. The data shows only a considerable difference between renovated family homes and all other types of buildings, especially during the daytime. According to the results, renovation of single apartments does not contribute towards energy savings. Figure 5.16 shows the respective PFs for weekdays and weekends at midday. Improvement of costs and carbon emissions by 3% and 40%, respectively, can be seen for *improved terraced* designs. Time efficiency parameters follow the results from the previous section.

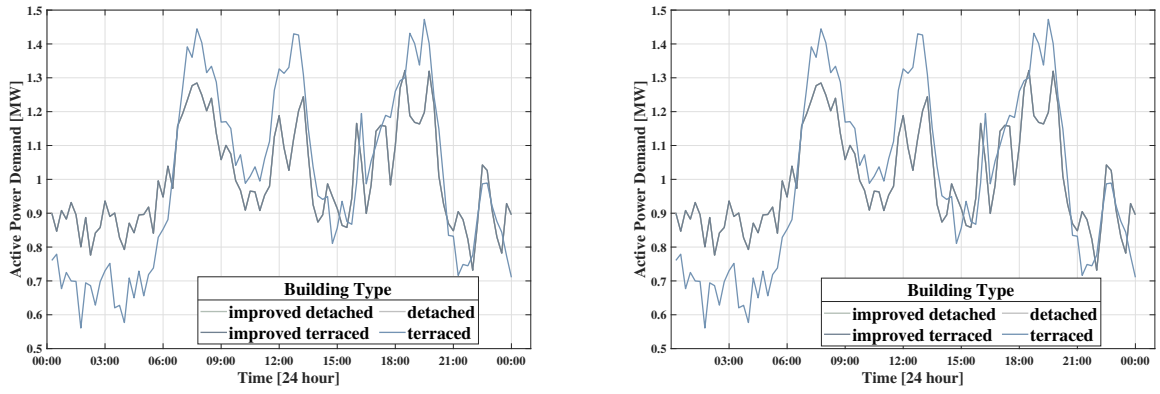

(a) Active Power Demand - Weekday (b) Active Power Demand - Weekend

Figure 5.15: Average Daily Residential Demand Profiles acc. to Types of Dwelling

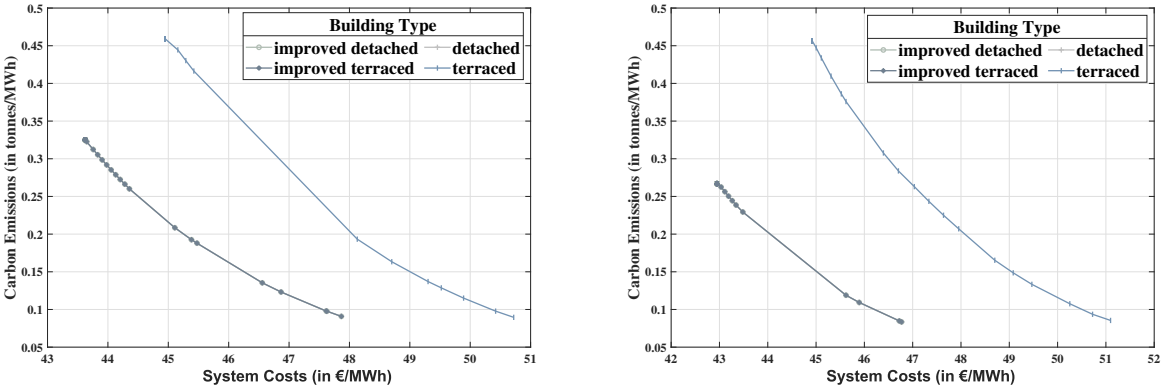

(a) Pareto Front at 12 : 00 p.m. - Weekday (b) Pareto Front at 12 : 00 p.m. - Weekend

Figure 5.16: Mid-day Pareto Front of Costs and Emissions for the Distribution Grid

5.3.4 PV Penetration Levels

In this section, six arbitrary levels of rooftop PV penetration are selected and applied to the population to simulate self-consumption availability on the prosumer side. The benchmark scenario assumes a 0% penetration level, i.e., no households are equipped with a rooftop PV. Subsequently, we increase the presence of rooftop PV as:

- 5%, i.e., 4 households with rooftop PVs,
- 15%, i.e., 12 households with rooftop PVs,
- 35%, i.e., 29 households with rooftop PVs,
- 50%, i.e., 42 households with rooftop PVs, and
- 75%, i.e., 63 households with rooftop PVs

The daily simulations are carried out during the summer and winter days in June and January. Demand for heating control pattern with constant temperature (*const*) is included for the winter simulations. Figure 5.17 demonstrates the average residual demand profiles for 84 households under different levels of rooftop PV penetration. As is evident, the decrease in residential load reaches a maximum of 6.47% in winter and 101.47% in summer. Therefore, during winters, the residential load is still positive. However, in summer, the residential demand for a time step with high PV generation might be negative and treated as a potential generation source. Table 5.7 summarizes the percentage decrease in average daily residential demand under different levels of rooftop PV penetration.

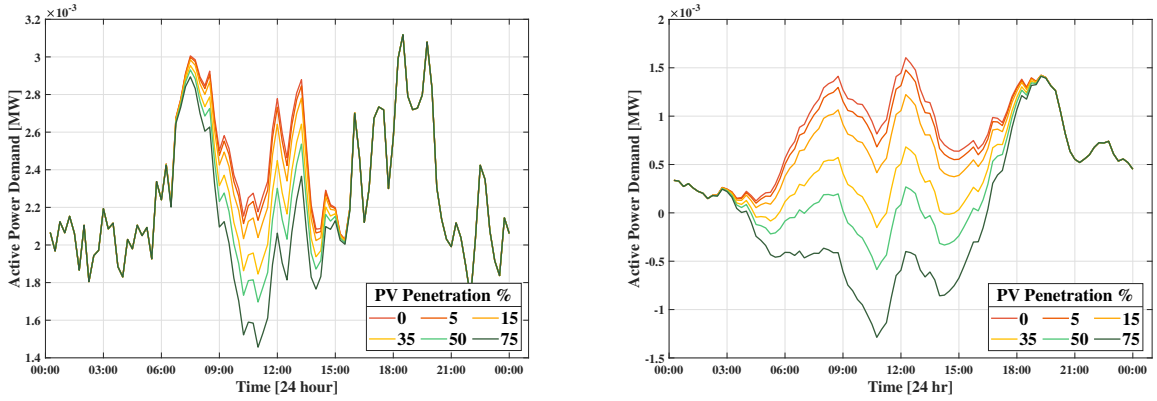

(a) Daily Residential Demand - Winter (b) Daily Residential Demand - Summer

Figure 5.17: Average Daily Residential Demand Profiles acc. to PV Penetration Levels

PV Penetration Level [%]	**Summer Demand** [% ↓]	**Winter Demand** [% ↓]
0	—	—
5	6.44	0.41
15	19.33	1.23
35	46.71	2.98
50	67.65	4.32
74	101.47	6.47

Table 5.7: Summary of Decreasing Residential Demand

Distribution Grid Results

The MOP considers three objectives simultaneously: system costs, power losses, and voltage deviation. The MO-DOPF algorithm successfully produces a well-spread PF for the winter simulation, averaging 190 Pareto optimal points. However, for the summer simulations, the residential load is negligible or even negative during high levels of PV penetration. In such cases, the PF is a straight line corresponding to the weight vector. The impact of the influx of rooftop PV is studied on the technical parameters of the distribution grid, such as the active power losses, see Figure 5.18 and total voltage deviation, see Figure 5.19. As seen from the plots, as the residential load decreases during active PV periods for winter days, the power losses and the voltage deviation decrease. At first glance, the result follows a similar pattern for summer days. However, the issue arises in different areas during high levels of PV penetration in the summer. Besides, the distribution grid saves up to 5% in winter and 1.06% in summer regarding system costs with increasing PV penetration.

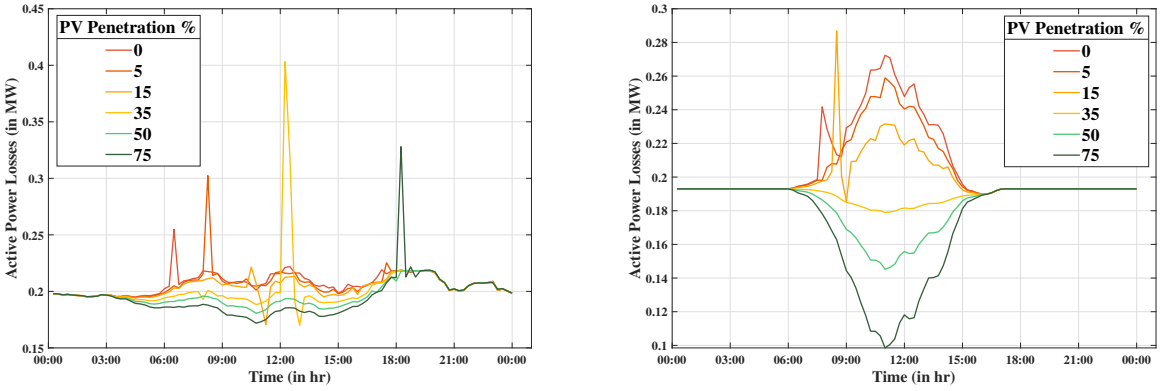

(a) Active Power Losses - Winter

(b) Active Power Losses - Summer

Figure 5.18: Average Active Power Losses in the Distribution Grid

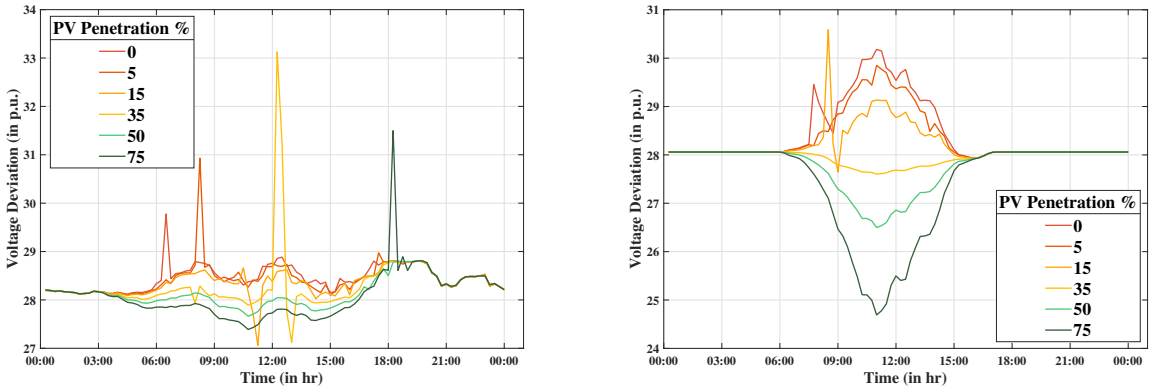

(a) Total Voltage Deviation - Winter (b) Total Voltage Deviation - Summer

Figure 5.19: Average Voltage Deviation in the Distribution Grid

Finally, Figure 5.20 shows the active power injection at the substation node during summers. The negative sign signifies that active power is generated or injected into the MV grid. The quantity of reverse power flow under the influx of rooftop PV on the consumer side is a key performance indicator when determining the PV hosting capacity of a distribution grid. Therefore, these results help in distribution grid planning.

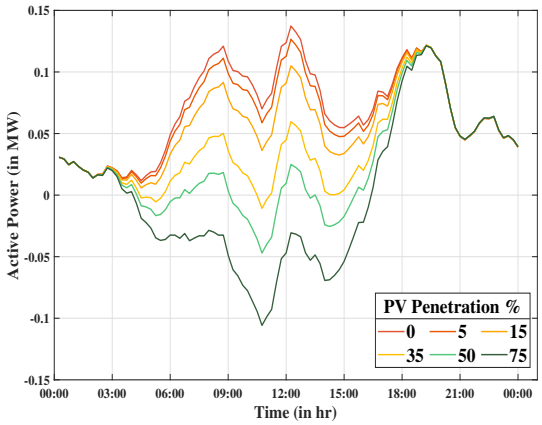

Figure 5.20: Active Power Injection at the Substation Node

The results show that residential consumers' adoption of advanced technologies and varied usage schemes that depend on their socio-behavioral aspects considerably impacts distribution grid operation. The proposed MO-DOPF algorithm can produce well-spread PFs for every scenario and handle negative spot market prices and negative load at the nodes.

Summarizing the application cases, this thesis studies two types of industrial prosumers with profit-seeking goals of self-optimization using a peak shaving strategy or the energy arbitrage of a BESS unit. In the second application case, the impact of residential consumers' daily demand on diverse aspects of distribution grid operation is studied. The demand profiles are modeled using socio-behavioral phenomena of the involved human beings in the residential sector. The proposed EM architecture in a co-simulation framework can communicate with different MAS systems or agents and solve a grid-oriented multi-objective OPF problem with economic, environmental, and technical objectives. The MO-DOPF algorithm successfully produces well-spread PFs for all scenarios, maintains operational constraints, and minimizes concerned objectives. Importantly, the calculation of the optimization problem follows a distributed routine, ensuring the data privacy of all involved participants.

Chapter 5 Summary

Key takeaways from this chapter:

5.1) Optimality and computational efficiency of the distributed OPF algorithm

5.2) Performace of the proposed EMA architecture in a co-simulation framework

5.3) An application case studying industrial prosumers and the impact of their self-optimization practices

5.4) An application case studying the impact of residential consumers' demand depending on heat pump usage, building type, and PV penetration levels considering socio-behavioral aspects

6 Conclusion and Outlook

This thesis develops an agent-based hierarchical energy management architecture that solves a constrained multi-objective optimal power flow problem by considering the distribution grid's economic, environmental, and technical parameters in a distributed fashion to maintain the data privacy of the involved participants. The developed model is applied in a co-simulation framework to interact with other agent-based models, generating the necessary time series for simulation studies. This chapter summarizes the research objective and the proposed solution. It critically discusses the results obtained and clarifies the benefits and limitations of the proposed EM solution. Finally, a future outlook for potential extensions and application cases concludes the chapter.

Summary

To summarize the ongoing energy transition, the large influx of renewable generation in supply and demand sectors and controllable loads such as storage units, EVs, and electric heat pumps is permanently changing the structure of power system operations and electricity markets. With the inclusion of recently developed sectors with electrification, such as power-to-gas and power-to-heat technologies, the scope of distribution systems extends to multi-energy integrated systems. This increase in the number of autonomous participants forming localized energy communities at the distribution grid level beckons the importance of energy management models to optimally operate all involved participants in a distribution grid ecosystem to deliver a sustainable and secure electricity supply. Before such efficient and optimal EMS can be deployed in the real world, simulation studies regarding EM models in their associated environment help identify the essential properties in a satisfactory solution. Moreover, the results from EM models can assist in distribution grid planning and operation by providing KPIs that signify the impact of technology adoption and flexibility practices on the prosumer side in the electricity market. To this end, this thesis posed the following research question:

How do we design and model an energy management architecture for low/medium-voltage distribution grids that can optimally address the grid's economic, environmental, and technical aspects under intensive electrification and flexibility practices by industrial and residential consumers?

Reviewing recent literature on EMS for modern distribution systems helps identify the primary properties in terms of objectives, architecture, types, involved participants, and communication and control protocols to consider while modeling an efficient and optimal EMS. Plenty of work is being conducted on distributed EM systems offering diverse functions for different players in the electricity value chain. However, this thesis identifies a few critical research gaps: a holistic EMS model applicable to the integrated distribution systems that can tackle flexible prosumers with increasing electrification and controllable loads, dispersed volume of renewable generation, evolving business models, and providing grid-aware optimal solutions. EMS models have been applied to optimally manage available resources in microgrids, smart homes, and industries. However, suitable solutions need to be found that can facilitate a closed-loop interaction between the involved participants and the connected distribution grid to ensure system constraints are respected. The optimal set-points should be achieved with limited information to preserve the data privacy of market participants. Regarding the inclusion of consumer demand, expository modeling of active prosumers in industrial and residential sectors following socio-technical principles and their integration within the EMS without over-simplification is a necessary next step.

Therefore, this thesis answers the research question by proposing an agent-based hierarchical EMS architecture. Agent-based modeling inherently supports parallel and distributed computation through pre-defined communication protocols. The hierarchical architecture shields relevant information from being shared with a central coordinator agent to preserve data privacy. The information flow between the EM models and the participants follows the regulatory structure of the German electricity market. The proposed EMA offers an *online* optimization function that solves a multi-objective problem in a distributed fashion, utilizing agent communication infrastructure while adhering to system constraints. An *online* algorithm facilitates the closed-loop feedback mechanism between the participants and the distribution grid, ensuring that the physical laws of the grid are always satisfied. Finally, for the application cases, this thesis implements the proposed architecture in a co-simulation framework, a practical setting that mirrors real-world conditions, to form a holistic model of the distribution grid ecosystem. The co-simulation environment consists of industrial and residential prosumers. Diverse simulation scenarios are designed and executed to study the impact of consumer flexibility on the distribution grid characteristics. The results provide essential KPIs that can help in distribution grid planning and operation.

Critical Review

As is evident from Chapter 5, the agent-based EMA architecture connects to other MAS or agent-based simulators in a co-simulation framework solving a constrained multi-objective problem. It handles industrial and residential prosumers under diverse scenarios and generates manifold *pareto optimal* points that provide essential KPIs for distribution grid planning and operation. For example, the BESS capacity of an industrial prosumer can provide ancillary services to the distribution grid, as the results show the potential of offering BESS scheduling into the electricity market under specific scenarios. Similarly, for residential prosumers, the reverse power flow under high levels of rooftop PV penetration can indicate the hosting capacity of the distribution grid. Furthermore, the algorithm respects system constraints and finds the optimal solution in a distributed manner. The optimality and computational efficiency of the proposed distributed OPF algorithm using two alternative methods of gradient computation support the method's applicability to real-time implementation in real-world scenarios. Although the current version of the algorithm applies to arbitrary grid topologies, the examples consider single-phase networks. Appropriate modifications can extend the algorithm to multi-phase unbalanced networks.

Furthermore, it is crucial to acknowledge that the architecture has its limitations due to model errors, incorrect assumptions, and failed hypotheses. For instance, the assumption of an aggregator acting as an EMA will depend on several regulatory and infrastructure guidelines in the future, which might prompt modification in data and control flows in the proposed architecture. The arbitrary levels of rooftop PV penetration and their capacity sizes can exhibit different behaviors when real-world data is used on both the consumer and grid side without data normalization or aggregation inaccuracies. The consideration of socio-behavioral aspects of residential prosumers and the unavailability of local market data hindered closing the negotiation loop with the distribution grid to establish tangible DR strategies. Similarly, the hypothesis that adding a curtailment penalty will help raise the use of renewable generation in the system does not hold to the current MOP problem. The curtailment penalty is a proxy to minimize emissions within other objectives, introducing unnecessary redundancy. Although this thesis experimented with a vast number of simulation scenarios stemming from several combinations regarding the optimization parameters, day, season, prosumer activity, market price, adoption level, etc., there is still room for developing further scenarios involving aspects beyond the scope of this thesis.

Future Outlook

Several possibilities exist for extending the application of the proposed EMA architecture. Appropriate modifications to the agent-based architecture and the MO-DOPF algorithm can significantly strengthen the solution's functionalities.

Simulation Architecture

The first step could be to extend the application case with residential prosumers to communicate in a feedback loop with the distribution grid via the primary EMA to facilitate direct load control of flexible units such as electric heat pumps, BESS units, or EVs. Variations in heating and EV charging for residential consumers heavily depend on their comfort and willingness to adopt flexibility. Therefore, innovative data analysis tools developed to study the output from the EMA architecture can suggest suitable incentives to motivate consumer willingness. The simulation environment can include more participant models representing gas and heat networks, hydrogen production units, and localized markets. Integrating the EMS with a localized market simulator will help envision the future scenario of neighbor-to-neighbor trading at the distribution grid level. SIMONA can be modified to host the primary EMA and treat the optimization routine as a library, which opens up a variety of further application cases for SIMONA, which are being examined in Redispatch 3.0 [5], Transense [6], and ReCoDe [7].

MO-DOPF Algorithm

As stated before, there is a large number of distributed algorithms available to solve power flow optimization. The *online* Gradient projection algorithm was selected for its suitability to the agent communication protocol presented. Extensive scalability analysis to differentiate the computational efficiency and accuracy of the alternative gradient computation methods in real-world distribution grid scenarios is required to verify the robustness and applicability of the algorithm substantially. Examination of other distributed methods and their integration as alternate agent behavior states or

[5] https://ie3.etit.tu-dortmund.de/research/third-party-projects/distribution-grid-planning-operation/redispatch-30/

[6] https://ie3.etit.tu-dortmund.de/research/third-party-projects/distribution-grid-planning-operation/transense/

[7] https://ie3.etit.tu-dortmund.de/research/third-party-projects/distribution-grid-planning-operation/recode/

software libraries can extend the scope of the simulation framework. SIMONA can calculate the power flow for multiple voltage levels. Therefore, introducing transformer handling in the MO-DOPF algorithm to include multiple voltage levels in a single simulation, i.e., multiple GA agents interacting with the primary EMA, could be another potential improvement. In this way, reverse power flows between grids can be optimally regulated. The objectives of the EMA can offer further parameters such as line loadings and frequency regulation to support congestion management and power system stability. Stricter constraint handling techniques for the generation limit on DG units will numerically improve the algorithm's performance.

Closing Remarks

The energy management solution developed in this thesis represents a significant response to the formulated research question. Modeling emerging technologies and business models is inherently an iterative process, with each iteration refining the model to reflect real-world scenarios more accurately. Despite the progress made, numerous open research questions and critical implementation challenges remain in the transformation of power systems. Consequently, this thesis contributes significant advancements toward realizing a sustainable and secure operation for modern distribution systems in liberalized electricity markets. While much work still needs to be done, these contributions mark crucial steps forward in the ongoing evolution due to energy transition.

References

[1] IRENA. *Energy Transition Outlook*. 2023. URL: https://www.irena.org/Energy-Transition/Outlook.

[2] S and P Global. *What is Energy Transition?* 2020. URL: https://www.spglobal.com/en/research-insights/articles/what-is-energy-transition.

[3] Bundesministerium für Bildung und Forschung (BMBF). *German Energy Transition*. 2020. URL: https://www.bmbf.de/bmbf/en/research/energy-and-economy/german-energy-transition/german-energy-transition_node.html.

[4] A. Zare. "Multistage Expansion Planning of Active Distribution Systems: Towards Network Integration of Distributed Energy Resources". In: 2018. URL: https://api.semanticscholar.org/CorpusID:169303509.

[5] K. Appunn. *Sector coupling - Shaping an integrated renewable energy system*. 2018. URL: https://www.cleanenergywire.org/factsheets/sector-coupling-shaping-integrated-renewable-power-system.

[6] "IEEE Guide for Distributed Energy Resources Management Systems (DERMS) Functional Specification". In: *IEEE Std 2030.11-2021* (2021), pp. 1–61. DOI: 10.1109/IEEESTD.2021.9447316.

[7] L. Strezoski. "Utility DERMS and DER Aggregators: An Ideal Case for Tomorrow's DSO". In: *2022 IEEE PES Innovative Smart Grid Technologies Conference Europe (ISGT-Europe)*. 2022, pp. 1–5. DOI: 10.1109/ISGT-Europe54678.2022.9960384.

[8] P. Joy. *Smart Grid Enables Quantum Improvement in Energy management Efficiency*. 2020. URL: https://www.powerelectronicsnews.com/smart-grid-enables-quantum-improvement-in-energy-management-efficiency/.

[9] *Gesetz über die Elektrizitäts- und Gasversorgung (Energiewirtschaftsgesetz - EnWG)*. URL: https://www.gesetze-im-internet.de/enwg_2005/__14a.html.

[10] gridX. *Paragraph 14a EnWG*. 2024. URL: https://www.gridx.ai/knowledge/paragraph-14a-enwg.

[11] W. A. Menner. “Introduction to Modeling and Simulation”. In: *Johns Hopkins APL Technical Digest* 16.1 (1995), pp. 6–17. URL: https://secwww.jhuapl.edu/techdigest/Content/techdigest/pdf/V16-N01/16-01-Menner.pdf.

[12] F. Maghsoodlou, R. Masiello, and T. Ray. “Energy management systems”. In: *IEEE Power and Energy Magazine* 2.5 (2004), pp. 49–57. DOI: 10.1109/MPAE.2004.1338122.

[13] E. Handschin and A. Petroianu. *Energy management systems: operation and control of electric energy transmission systems*. Springer Science & Business Media, 2012.

[14] M. S. Alam and S. A. Arefifar. “Energy Management in Power Distribution Systems: Review, Classification, Limitations and Challenges”. In: *IEEE Access* 7 (2019), pp. 92979–93001. DOI: 10.1109/ACCESS.2019.2927303.

[15] A. Hussain, V.-H. Bui, and H.-M. Kim. “A resilient and privacy-preserving energy management strategy for networked microgrids”. In: *IEEE Transactions on Smart Grid* 9.3 (2016), pp. 2127–2139.

[16] C. L. Nge, I. U. Ranaweera, O.-M. Midtgård, and L. Norum. “A real-time energy management system for smart grid integrated photovoltaic generation with battery storage”. In: *Renewable energy* 130 (2019), pp. 774–785.

[17] A. Keyhani, M. N. Marwali, and M. Dai. *Integration of green and renewable energy in electric power systems*. John Wiley & Sons, 2009.

[18] S. K. Rathor and D. Saxena. “Energy management system for smart grid: An overview and key issues”. In: *International Journal of Energy Research* 44.6 (2020), pp. 4067–4109. DOI: https://doi.org/10.1002/er.4883. eprint: https://onlinelibrary.wiley.com/doi/pdf/10.1002/er.4883. URL: https://onlinelibrary.wiley.com/doi/abs/10.1002/er.4883.

[19] P. Astero, B. J. Choi, and H. Liang. “Multi-agent transactive energy management system considering high levels of renewable energy source and electric vehicles”. In: *IET Generation, Transmission & Distribution* 11.15 (2017), pp. 3713–3721.

[20] N. Anglani, G. Oriti, and M. Colombini. “Optimized energy management system to reduce fuel consumption in remote military microgrids”. In: *IEEE Transactions on Industry Applications* 53.6 (2017), pp. 5777–5785.

[21] L. Guo, W. Liu, X. Li, Y. Liu, B. Jiao, W. Wang, C. Wang, and F. Li. "Energy management system for stand-alone wind-powered-desalination microgrid". In: *IEEE Transactions on Smart Grid* 7.2 (2014), pp. 1079–1087.

[22] M. Marzband, F. Azarinejadian, M. Savaghebi, and J. M. Guerrero. "An optimal energy management system for islanded microgrids based on multi-period artificial bee colony combined with Markov chain". In: *IEEE systems journal* 11.3 (2015), pp. 1712–1722.

[23] Z. Wang, B. Chen, J. Wang, et al. "Decentralized energy management system for networked microgrids in grid-connected and islanded modes". In: *IEEE Transactions on Smart Grid* 7.2 (2015), pp. 1097–1105.

[24] J. M. Home-Ortiz, M. Pourakbari-Kasmaei, M. Lehtonen, and J. R. Sanches Mantovani. "Optimal location-allocation of storage devices and renewable-based DG in distribution systems". In: *Electric Power Systems Research* 172 (2019), pp. 11–21. ISSN: 0378-7796. DOI: https://doi.org/10.1016/j.epsr.2019.02.013. URL: https://www.sciencedirect.com/science/article/pii/S0378779619300690.

[25] M. R. Dorostkar-Ghamsari, M. Fotuhi-Firuzabad, M. Lehtonen, and A. Safdarian. "Value of Distribution Network Reconfiguration in Presence of Renewable Energy Resources". In: *IEEE Transactions on Power Systems* 31.3 (2016), pp. 1879–1888. DOI: 10.1109/TPWRS.2015.2457954.

[26] S. Bahrami, M. Toulabi, S. Ranjbar, M. Moeini-Aghtaie, and A. M. Ranjbar. "A decentralized energy management framework for energy hubs in dynamic pricing markets". In: *IEEE Transactions on Smart Grid* 9.6 (2017), pp. 6780–6792.

[27] C. D. Rodríguez-Gallegos, O. Gandhi, D. Yang, M. S. Alvarez-Alvarado, W. Zhang, T. Reindl, and S. K. Panda. "A siting and sizing optimization approach for PV–battery–diesel hybrid systems". In: *IEEE Transactions on Industry Applications* 54.3 (2017), pp. 2637–2645.

[28] B. Yuan, A. Chen, C. Du, and C. Zhang. "Hybrid AC/DC microgrid energy management based on renewable energy sources forecasting". In: *2017 36th Chinese Control Conference (CCC)*. IEEE. 2017, pp. 2870–2875.

[29] M. S. Taha, H. H. Abdeltawab, and Y. A.-R. I. Mohamed. “An online energy management system for a grid-connected hybrid energy source”. In: *IEEE Journal of Emerging and Selected Topics in Power Electronics* 6.4 (2018), pp. 2015–2030.

[30] L. S. Guedes, A. C. Lisboa, D. A. Vieira, and R. R. Saldanha. “A multiobjective heuristic for reconfiguration of the electrical radial network”. In: *IEEE Transactions on Power Delivery* 28.1 (2012), pp. 311–319.

[31] J. T. Bialasiewicz. “Renewable energy systems with photovoltaic power generators: Operation and modeling”. In: *IEEE Transactions on industrial Electronics* 55.7 (2008), pp. 2752–2758.

[32] J. M. Sexauer, K. D. McBee, and K. A. Bloch. “Applications of probability model to analyze the effects of electric vehicle chargers on distribution transformers”. In: *IEEE Transactions on Power Systems* 28.2 (2012), pp. 847–854.

[33] B. Lunz, Z. Yan, J. B. Gerschler, and D. U. Sauer. “Influence of plug-in hybrid electric vehicle charging strategies on charging and battery degradation costs”. In: *Energy Policy* 46 (2012), pp. 511–519.

[34] K. M. Muttaqi, A. D. Le, M. Negnevitsky, and G. Ledwich. “An algebraic approach for determination of DG parameters to support voltage profiles in radial distribution networks”. In: *IEEE Transactions on Smart Grid* 5.3 (2014), pp. 1351–1360.

[35] L. S. Guedes, A. C. Lisboa, D. A. Vieira, and R. R. Saldanha. “A multiobjective heuristic for reconfiguration of the electrical radial network”. In: *IEEE Transactions on Power Delivery* 28.1 (2012), pp. 311–319.

[36] V. I. Herrera, A. Milo, H. Gaztanaga, and H. Camblong. “Multi-objective optimization of energy management and sizing for a hybrid bus with dual energy storage system”. In: *2016 IEEE vehicle power and propulsion conference (VPPC)*. IEEE. 2016, pp. 1–6.

[37] B. S. K. Patnam and N. M. Pindoriya. “Centralized stochastic energy management framework of an aggregator in active distribution network”. In: *IEEE Transactions on Industrial Informatics* 15.3 (2018), pp. 1350–1360.

[38] A. Rajaei, S. Fattaheian-Dehkordi, M. Fotuhi-Firuzabad, M. Moeini-Aghtaie, and M. Lehtonen. "Developing a Distributed Robust Energy Management Framework for Active Distribution Systems". In: *IEEE Transactions on Sustainable Energy* 12.4 (2021), pp. 1891–1902. DOI: 10.1109/TSTE.2021.3070316.

[39] F. Ahmad, M. S. Alam, and M. Asaad. "Developments in xEVs charging infrastructure and energy management system for smart microgrids including xEVs". In: *Sustainable cities and society* 35 (2017), pp. 552–564.

[40] N. Bazmohammadi, A. Tahsiri, A. Anvari-Moghaddam, and J. M. Guerrero. "A hierarchical energy management strategy for interconnected microgrids considering uncertainty". In: *International Journal of Electrical Power & Energy Systems* 109 (2019), pp. 597–608.

[41] Y. Han, G. Zhang, Q. Li, Z. You, W. Chen, and H. Liu. "Hierarchical energy management for PV/hydrogen/battery island DC microgrid". In: *International Journal of Hydrogen Energy* 44.11 (2019), pp. 5507–5516.

[42] H. Kikusato, K. Mori, S. Yoshizawa, Y. Fujimoto, H. Asano, Y. Hayashi, A. Kawashima, S. Inagaki, and T. Suzuki. "Electric vehicle charge–discharge management for utilization of photovoltaic by coordination between home and grid energy management systems". In: *IEEE Transactions on Smart Grid* 10.3 (2018), pp. 3186–3197.

[43] Y. Huang, L. Wang, W. Guo, Q. Kang, and Q. Wu. "Chance constrained optimization in a home energy management system". In: *IEEE Transactions on Smart Grid* 9.1 (2016), pp. 252–260.

[44] M. Rastegar, M. Fotuhi-Firuzabad, and M. Lehtonen. "Home load management in a residential energy hub". In: *Electric Power Systems Research* 119 (2015), pp. 322–328. ISSN: 0378-7796. DOI: https://doi.org/10.1016/j.epsr.2014.10.011. URL: https://www.sciencedirect.com/science/article/pii/S0378779614003654.

[45] A. Safdarian, M. Fotuhi-Firuzabad, and M. Lehtonen. "Optimal Residential Load Management in Smart Grids: A Decentralized Framework". In: *IEEE Transactions on Smart Grid* 7.4 (2016), pp. 1836–1845. DOI: 10.1109/TSG.2015.2459753.

[46] A. Ożadowicz and J. Grela. "An event-driven building energy management system enabling active demand side management". In: *2016 second international conference on event-based control, communication, and signal processing (EBCCSP)*. IEEE. 2016, pp. 1–8.

[47] N. T. Mbungu, R. C. Bansal, R. Naidoo, V Miranda, and M Bipath. "An optimal energy management system for a commercial building with renewable energy generation under real-time electricity prices". In: *Sustainable cities and society* 41 (2018), pp. 392–404.

[48] M. Elsisi, M.-Q. Tran, K. Mahmoud, M. Lehtonen, and M. M. F. Darwish. "Deep Learning-Based Industry 4.0 and Internet of Things towards Effective Energy Management for Smart Buildings". In: *Sensors* 21.4 (2021). ISSN: 1424-8220. DOI: 10.3390/s21041038. URL: https://www.mdpi.com/1424-8220/21/4/1038.

[49] Z. Liang, Q. Alsafasfeh, T. Jin, H. Pourbabak, and W. Su. "Risk-constrained optimal energy management for virtual power plants considering correlated demand response". In: *IEEE Transactions on Smart Grid* 10.2 (2017), pp. 1577–1587.

[50] X. Liu, B. Gao, Z. Zhu, and Y. Tang. "Non-cooperative and cooperative optimisation of battery energy storage system for energy management in multi-microgrid". In: *IET Generation, Transmission & Distribution* 12.10 (2018), pp. 2369–2377.

[51] A. Safdarian, M. Fotuhi-Firuzabad, and M. Lehtonen. "A Distributed Algorithm for Managing Residential Demand Response in Smart Grids". In: *IEEE Transactions on Industrial Informatics* 10.4 (2014), pp. 2385–2393. DOI: 10.1109/TII.2014.2316639.

[52] A. Safdarian, M. Fotuhi-Firuzabad, and M. Lehtonen. "Benefits of Demand Response on Operation of Distribution Networks: A Case Study". In: *IEEE Systems Journal* 10.1 (2016), pp. 189–197. DOI: 10.1109/JSYST.2013.2297792.

[53] M. Wei, S. H. Hong, and M. Alam. "An IoT-based energy-management platform for industrial facilities". In: *Applied Energy* 164 (2016), pp. 607–619. ISSN: 0306-2619. DOI: https://doi.org/10.1016/j.apenergy.2015.11.107. URL: https://www.sciencedirect.com/science/article/pii/S0306261915015883.

[54] W. Yu, P. Patros, B. Young, E. Klinac, and T. G. Walmsley. "Energy digital twin technology for industrial energy management: Classification, challenges and future". In: *Renewable and Sustainable Energy Reviews* 161 (2022), p. 112407. ISSN: 1364-0321. DOI: https://doi.org/10.1016/j.rser.2022.112407. URL: https://www.sciencedirect.com/science/article/pii/S136403212200315X.

[55] A. Dini, A. Hassankashi, S. Pirouzi, M. Lehtonen, B. Arandian, and A. A. Baziar. "A flexible-reliable operation optimization model of the networked energy hubs with distributed generations, energy storage systems and demand response". In: *Energy* 239 (2022), p. 121923. ISSN: 0360-5442. DOI: https://doi.org/10.1016/j.energy.2021.121923. URL: https://www.sciencedirect.com/science/article/pii/S036054422102171X.

[56] S. Zhou, Y. Han, A. S. Zalhaf, M. Lehtonen, M. M. Darwish, and K. Mahmoud. "Risk-averse bi-level planning model for maximizing renewable energy hosting capacity via empowering seasonal hydrogen storage". In: *Applied Energy* 361 (2024), p. 122853. ISSN: 0306-2619. DOI: https://doi.org/10.1016/j.apenergy.2024.122853. URL: https://www.sciencedirect.com/science/article/pii/S0306261924002368.

[57] L. Ding, G. Y. Yin, W. X. Zheng, Q.-L. Han, et al. "Distributed energy management for smart grids with an event-triggered communication scheme". In: *IEEE Transactions on Control Systems Technology* 27.5 (2018), pp. 1950–1961.

[58] T. F. Megahed, S. M. Abdelkader, and A. Zakaria. "Energy management in zero-energy building using neural network predictive control". In: *IEEE Internet of Things Journal* 6.3 (2019), pp. 5336–5344.

[59] M. Ruiz-Cortes, E. González-Romera, R. Amaral-Lopes, E. Romero-Cadaval, J. Martins, M. I. Milanes-Montero, and F. Barrero-Gonzalez. "Optimal charge/discharge scheduling of batteries in microgrids of prosumers". In: *IEEE Transactions on Energy Conversion* 34.1 (2018), pp. 468–477.

[60] B. V. Solanki, K. Bhattacharya, and C. A. Canizares. "A sustainable energy management system for isolated microgrids". In: *IEEE Transactions on Sustainable Energy* 8.4 (2017), pp. 1507–1517.

[61] J. Carpentier. “Optimal Power Flows: Uses, Methods and Developments”. In: *IFAC Proceedings Volumes* 18.7 (1985). IFAC Symposium on Planning and Operation of Electric Energy Systems., Rio de Janeiro, Brazil, 22-25 July, pp. 11–21. ISSN: 1474-6670. DOI: https://doi.org/10.1016/S1474-6670(17)60410-5. URL: https://www.sciencedirect.com/science/article/pii/S1474667017604105.

[62] Z. Qiu, G. Deconinck, and R. Belmans. “A literature survey of optimal power flow problems in the electricity market context”. In: *2009 IEEE/PES Power Systems Conference and Exposition*. IEEE. 2009, pp. 1–6.

[63] J. A. Momoh, R. Adapa, and M. El-Hawary. “A review of selected optimal power flow literature to 1993. I. Nonlinear and quadratic programming approaches”. In: *IEEE transactions on power systems* 14.1 (1999), pp. 96–104.

[64] J. A. Momoh, M. El-Hawary, and R. Adapa. “A review of selected optimal power flow literature to 1993. II. Newton, linear programming and interior point methods”. In: *IEEE transactions on power systems* 14.1 (1999), pp. 105–111.

[65] P. Panciatici, M. C. Campi, S. Garatti, S. H. Low, D. K. Molzahn, A. X. Sun, and L. Wehenkel. “Advanced optimization methods for power systems”. In: *2014 power systems computation conference*. IEEE. 2014, pp. 1–18.

[66] J. P. Lopes, N. Hatziargyriou, J. Mutale, P. Djapic, and N. Jenkins. “Integrating distributed generation into electric power systems: A review of drivers, challenges and opportunities”. In: *Electric Power Systems Research* 77.9 (2007). Distributed Generation, pp. 1189–1203. ISSN: 0378-7796. DOI: https://doi.org/10.1016/j.epsr.2006.08.016. URL: https://www.sciencedirect.com/science/article/pii/S0378779606001908.

[67] B. Stott, J. Jardim, and O. Alsaç. “DC power flow revisited”. In: *IEEE Transactions on Power Systems* 24.3 (2009), pp. 1290–1300.

[68] M. E. Baran and F. Wu. “Optimal capacitor placement on radial distribution systems”. In: *IEEE Transactions on Power Delivery* 4.1 (1989), pp. 725–734. DOI: 10.1109/61.19265.

[69] H. Yuan, F. Li, Y. Wei, and J. Zhu. “Novel Linearized Power Flow and Linearized OPF Models for Active Distribution Networks With Application in Distribution LMP”. In: *IEEE Transactions on Smart Grid* 9.1 (2018), pp. 438–448. DOI: 10.1109/TSG.2016.2594814.

[70] S. Bolognani and S. Zampieri. “On the existence and linear approximation of the power flow solution in power distribution networks”. In: *IEEE Transactions on Power Systems* 31.1 (2015), pp. 163–172.

[71] S. V. Dhople, S. S. Guggilam, and Y. C. Chen. “Linear approximations to AC power flow in rectangular coordinates”. In: *2015 53rd Annual Allerton Conference on Communication, Control, and Computing (Allerton)*. IEEE. 2015, pp. 211–217.

[72] X. Bai, H. Wei, K. Fujisawa, and Y. Wang. “Semidefinite programming for optimal power flow problems”. In: *International Journal of Electrical Power & Energy Systems* 30.6-7 (2008), pp. 383–392.

[73] J. Lavaei and S. H. Low. “Zero duality gap in optimal power flow problem”. In: *IEEE Transactions on Power systems* 27.1 (2011), pp. 92–107.

[74] R. A. Jabr. “Radial distribution load flow using conic programming”. In: *IEEE transactions on power systems* 21.3 (2006), pp. 1458–1459.

[75] S. Sojoudi and J. Lavaei. “Physics of power networks makes hard optimization problems easy to solve”. In: *2012 IEEE Power and Energy Society General Meeting*. IEEE. 2012, pp. 1–8.

[76] A. Kargarian, J. Mohammadi, J. Guo, S. Chakrabarti, M. Barati, G. Hug, S. Kar, and R. Baldick. “Toward distributed/decentralized DC optimal power flow implementation in future electric power systems”. In: *IEEE Transactions on Smart Grid* 9.4 (2016), pp. 2574–2594.

[77] J. Nocedal and S. J. Wright. *Numerical optimization*. Springer, 1999.

[78] L. Gan and S. Low. “An Online Gradient Algorithm for Optimal Power Flow on Radial Networks”. In: *IEEE Journal on Selected Areas in Communications* 34.3 (2016), pp. 625–638. DOI: 10.1109/JSAC.2016.2525598.

[79] D. B. Arnold, M. Negrete-Pincetic, M. D. Sankur, D. M. Auslander, and D. S. Callaway. “Model-free optimal control of VAR resources in distribution systems: An extremum seeking approach”. In: *IEEE Transactions on Power Systems* 31.5 (2015), pp. 3583–3593.

[80] E. Dall’Anese, S. V. Dhople, and G. B. Giannakis. “Photovoltaic inverter controllers seeking AC optimal power flow solutions”. In: *IEEE Transactions on power systems* 31.4 (2015), pp. 2809–2823.

[81] E. Dall'Anese and A. Simonetto. "Optimal Power Flow Pursuit". In: *IEEE Transactions on Smart Grid* 9.2 (2018), pp. 942–952. DOI: 10.1109/TSG.2016.2571982.

[82] M. Farivar, L. Chen, and S. Low. "Equilibrium and dynamics of local voltage control in distribution systems". In: *52nd IEEE Conference on Decision and Control*. 2013, pp. 4329–4334. DOI: 10.1109/CDC.2013.6760555.

[83] S. Bolognani and S. Zampieri. "A Distributed Control Strategy for Reactive Power Compensation in Smart Microgrids". In: *IEEE Transactions on Automatic Control* 58.11 (2013), pp. 2818–2833. DOI: 10.1109/TAC.2013.2270317.

[84] L.-N. Liu and G.-H. Yang. "Distributed Optimal Energy Management for Integrated Energy Systems". In: *IEEE Transactions on Industrial Informatics* 18.10 (2022), pp. 6569–6580. DOI: 10.1109/TII.2022.3146165.

[85] S. Kerscher and P. Arboleya. "The key role of aggregators in the energy transition under the latest European regulatory framework". In: *International Journal of Electrical Power Energy Systems* 134 (2022), p. 107361. ISSN: 0142-0615. DOI: https://doi.org/10.1016/j.ijepes.2021.107361. URL: https://www.sciencedirect.com/science/article/pii/S0142061521006001.

[86] *Build, Operate and Secure Low Latency Systems*. URL: https://akka.io/.

[87] Deloitte. *European Energy Market Reform, Country Profile: Germany*. 2015. URL: https://www2.deloitte.com/content/dam/Deloitte/global/Documents/Energy-and-Resources/gx-er-market-reform-germany.pdf.

[88] Muncon. *The German Electricity Market - Simplified*. URL: https://muncon.com/2022/09/20/the-german-electricity-market-simplified/.

[89] EPEX. *Basics of the Power Market*. URL: https://www.epexspot.com/en/basicspowermarket#day-ahead-and-intraday-the-backbone-of-the-european-spot-market.

[90] *dena* German Energy Agency. *Liberalization of the Electricity Market*. URL: https://www.dena.de/en/topics/energy-systems/electricity-market/.

[91] *The value of Aggregators in Electricity Systems, MIT Center for Energy and Environmental Policy Research*. 2016. URL: http://energy.mit.edu/publication/the-value-of-aggregators-in-electricity-systems/.

[92] Z. Ma, J. D. Billanes, and B. N. Jørgensen. "Aggregation Potentials for Buildings—Business Models of Demand Response and Virtual Power Plants". In: *Energies* 10.10 (2017), pp. 1996–1073. DOI: 10.3390/en10101646.

[93] ENERGINET. *What is an Aggregator?* URL: https://en.energinet.dk/Electricity/Green-electricity/Demand-side-response/What-is-an-aggregator/.

[94] IRENA. *Aggregators - Innovation Landscape Brief*. 2019. URL: https://www.irena.org/-/media/Files/IRENA/Agency/Publication/2019/Feb/IRENA_Innovation_Aggregators_2019.PDF/.

[95] *German Aggregator Company*. URL: https://www.energymeteo.com/.

[96] J. Ferber. "Multi-Agent Systems: An Introduction to Distributed Artifical Intelligence, 1st". In: Addison-Wesley Longman Publishing Co. Inc., 1999. ISBN: 0201360489.

[97] P. G. Balaji and D. Srinivasan. "An Introduction to Multi-Agent Systems". In: *Innovations in Multi-Agent Systems and Applications - 1*. Ed. by D. Srinivasan and L. C. Jain. Springer Berlin Heidelberg, 2010, pp. 1–27. ISBN: 978-3-642-14435-6. DOI: 10.1007/978-3-642-14435-6_1. URL: https://doi.org/10.1007/978-3-642-14435-6_1.

[98] V. R. Lesser and L. D. Erman. "Distributed Interpretation: A Model and Experiment". In: *Readings in Distributed Artificial Intelligence*. Ed. by A. H. Bond and L. Gasser. Morgan Kaufmann, 1988, pp. 120–139. ISBN: 978-0-934613-63-7. DOI: https://doi.org/10.1016/B978-0-934613-63-7.50014-0. URL: https://www.sciencedirect.com/science/article/pii/B9780934613637500140.

[99] F. Klügl. *Agent based Simulation Engineering*. Habilitation. University of Würzburg, 2010.

[100] J. Hiry. "Agent-based Discrete Event Simulation Environment for Electric Power Distribution System Analysis". Dissertation. 2022. ISBN: 978-3-8440-8462-7.

[101] C. Macal. "Everything you need to know about agent-based modelling and simulation". In: *Journal of Simulation* 10 (May 2016), pp. 144–156. DOI: 10.1057/jos.2016.7.

[102] M. Woolridge. "An Introduction to Multi-Agent Systems, 2nd". In: Wiley Publishing, 2009. ISBN: 0470519460.

[103] S. Russel and P. Norvig. “Artifical Intelligence: A modern Approach, 4th”. In: Pearson, 2020. ISBN: 0134610997.

[104] Z. Wrona, W. Buchwald, M. Ganzha, M. Paprzycki, F. Leon, N. Noor, and C.-V. Pal. “Overview of Software Agent Platforms Available in 2023”. In: *Information, MDPI* 14.6 (2023), p. 348. ISSN: 2078-2489. DOI: 10.3390/info14060348. URL: http://dx.doi.org/10.3390/info14060348.

[105] D. Kafura and J. Briot. “Actors And Agents”. In: *IEEE Concurrency* 6.2 (1998), pp. 24–29. DOI: 10.1109/MCC.1998.678786.

[106] F. for Intelligent Physical Agents (FIPA). *Fifa Standard Specifications*. 2002. URL: https://en.energinet.dk/Electricity/Green-electricity/Demand-side-response/What-is-an-aggregator/.

[107] C. Rehtanz. “Autonomous Systems and Intelligent Agents in Power System Control and Operation”. In: Springer Berlin Heidelberg, 2003. DOI: 10.1007/978-3-662-05955-5.

[108] R. C. Cardoso and A. Ferrando. “A Review of Agent-Based Programming for Multi-Agent Systems”. In: *Computers* 10.2 (2021). DOI: 10.3390/computers10020016.

[109] P. Wegner. “Concepts and Paradigms of Object-Oriented Programming”. In: *SIGPLAN OOPS Mess.* 1.1 (1990), pp. 7–87. DOI: 10.1145/382192.383004.

[110] C. Hewitt, P. Bishop, and R. Steiger. “A Universal Modular ACTOR Formalism for Artificial Intelligence.” In: Jan. 1973, pp. 235–245.

[111] J. Kays. “Agent-based simulation environment for improving the planning of distribution grids”. Dissertation. 2014. ISBN: 9-783868-446623.

[112] A. Seack. “Time Series based distribution grid planning considering interaction of network participants with a multi-agent system”. Dissertation. 2016. ISBN: 9-783868-447965.

[113] C. Kittl. “Entwurf und Validierung eines individualitatszentrierten, interdisziplinaren Energiesystemsimulators basierend auf ereignisdiskreter Simulation und Agententheorie”. Dissertation. 2022. ISBN: 978-3-8440-8463-4.

[114] P. Palensky, A. A. van der Meer, C. D. Lopez, A. Joseph, and K. Pan. “Cosimulation of Intelligent Power Systems: Fundamentals, Software Architecture, Numerics, and Coupling”. In: *IEEE Industrial Electronics Magazine* 11.1 (2017), pp. 34–50. ISSN: 1932-4529. DOI: 10.1109/MIE.2016.2639825.

[115] I. Hafner and N. Popper. “On the terminology and structuring of co-simulation methods”. In: *Proceedings of the 8th International Workshop on Equation-Based Object-Oriented Modeling Languages and Tools*. Ed. by D. Zimmer and B. Bachmann. New York, NY, USA: ACM, 2017, pp. 67–76. ISBN: 9781450363730. DOI: 10.1145/3158191.3158203.

[116] J. Jewell, A. Cherp, and K. Riahi. “Energy security under de-carbonization scenarios: An assessment framework and evaluation under different technology and policy choices”. In: *Energy Policy* 65 (2014), pp. 743–760. ISSN: 03014215. DOI: 10.1016/j.enpol.2013.10.051.

[117] van Nguyen, Y. Besanger, Q. Tran, and T. Nguyen. “On Conceptual Structuration and Coupling Methods of Co-Simulation Frameworks in Cyber-Physical Energy System Validation”. In: *Energies* 10.12 (2017), p. 1977. DOI: 10.3390/en10121977.

[118] J. S. Schwarz, T. Witt, A. Nieße, J. Geldermann, S. Lehnhoff, and M. Sonnenschein. “Towards an Integrated Development and Sustainability Evaluation of Energy Scenarios Assisted by Automated Information Exchange”. In: *Smart Cities, Green Technologies, and Intelligent Transport Systems*. Ed. by B. Donnellan, C. Klein, M. Helfert, O. Gusikhin, and A. Pascoal. Vol. 921. Cham: Springer, 2019, pp. 3–26. ISBN: 978-3-030-02907-4. DOI: {10.1007/978-3-030-02907-4_1}.

[119] G Schweiger, C Gomes, G Engel, I Hafner, J Schoeggl, A Posch, and T Nouidui. “An empirical survey on co-simulation: Promising standards, challenges and research needs”. In: *Simulation Modelling Practice and Theory* 95 (2019), pp. 148–163. ISSN: 1569190X. DOI: 10.1016/j.simpat.2019.05.001.

[120] M. Vogt, F. Marten, and M. Braun. “A survey and statistical analysis of smart grid co-simulations”. In: *Applied Energy* 222 (2018), pp. 67–78. ISSN: 03062619. DOI: 10.1016/j.apenergy.2018.03.123.

[121] C. Steinbrink, M. Blank-Babazadeh, A. El-Ama, S. Holly, B. Lüers, M. Nebel-Wenner, R. Ramírez Acosta, T. Raub, J. S. Schwarz, S. Stark, A. Nieße, and S. Lehnhoff. “CPES Testing with mosaik: Co-Simulation Planning, Execution and Analysis”. In: *Applied Sciences* 9.5 (2019), p. 923. ISSN: 2076-3417. DOI: 10.3390/app9050923.

[122] U. Richter, M. Mnif, J. Branke, C Müller-Schloer, and H. Schmeck. "Towards a generic observer/controller architecture for organic computing". In: *GI Jahrestagung* 93 (2006), pp. 112–119.

[123] M. Barsanti, J. Schwarz, L. Constantin, P. Kasturi, C. Binder, and S. Lehnhoff. "Socio-technical modeling of smart energy systems: a co-simulation design for domestic energy demand". In: *Energy Informatics* 4 (Sept. 2021). DOI: 10.1186/s42162-021-00180-6.

[124] H. Hoops, T. Tjadenand, and K. Rösken. *RE-Lab-Projects/hplib: v1.9*. 2022. DOI: 10.5281/zenodo.6792486. URL: https://zenodo.org/records/6792486.

[125] M. Hajiaghapour-Moghimi, K. Azimi Hosseini, E. Hajipour, and M. Vakilian. "Residential Load Clustering Contribution to Accurate Distribution Transformer Sizing". In: Mar. 2020. DOI: 10.1109/PSC49016.2019.9081518.

[126] M. Uddin, M. F. Romlie, M. F. Abdullah, S. Abd Halim, A. H. Abu Bakar, and T. Chia Kwang. "A review on peak load shaving strategies". In: *Renewable and Sustainable Energy Reviews* 82 (2018). DOI: 10.1016/j.rser.2017.10.056.

[127] H. Shafique, L. B. Tjernberg, D.-E. Archer, and S. Wingstedt. "Energy Management System (EMS) of Battery Energy Storage System (BESS) – Providing Ancillary Services". In: *2021 IEEE Madrid PowerTech*. 2021, pp. 1–6. DOI: 10.1109/PowerTech46648.2021.9494781.

[128] P. Mouratidis, M. Schneider, and S. Rinderknecht. "Hybrid Energy Storage System for Peak Shaving Application in Industries". In: *16. Symposium Energieinnovation*. 2020.

[129] J. A. Saaravia-Guerrero and E. Espinosa-Juárez. "Optimal Sizing of BESS for Industrial Peak Shaving Applications Considering Different Electricity Billing Rates". In: *2021 Fourth International Conference on Electrical, Computer and Communication Technologies (ICECCT)*. 2021, pp. 1–6. DOI: 10.1109/ICECCT52121.2021.9616916.

[130] N. Collath, S. Englberger, A. Jossen, and H. Hesse. "Reduction of Battery Energy Storage Degradation in Peak Shaving Operation through Load Forecast Dependent Energy Management". In: *NEIS 2020; Conference on Sustainable Energy Supply and Energy Storage Systems*. 2020, pp. 1–6.

[131] H. C. Hesse, R. Martins, P. Musilek, M. Naumann, C. N. Truong, and A. Jossen. "Economic Optimization of Component Sizing for Residential Battery Storage Systems". In: *Energies* 10.7 (2017). DOI: 10.3390/en10070835.

[132] R. Martins, H. C. Hesse, J. Jungbauer, T. Vorbuchner, and P. Musilek. "Optimal Component Sizing for Peak Shaving in Battery Energy Storage System for Industrial Applications". In: *Energies* 11.8 (2018). DOI: 10.3390/en11082048.

[133] U. Langenmayr, W. Wang, and P. Jochem. "Unit commitment of photovoltaic-battery systems: An advanced approach considering uncertainties from load, electric vehicles, and photovoltaic". In: *Applied Energy* 280 (2020), p. 115972. DOI: 10.1016/j.apenergy.2020.115972.

[134] A. Arif, Z. Wang, J. Wang, B. Mather, H. Bashualdo, and D. Zhao. "Load Modeling—A Review". In: *IEEE Transactions on Smart Grid* 9.6 (2018), pp. 5986–5999. DOI: 10.1109/TSG.2017.2700436.

[135] M. S. Hossan, H. M. Mesbah Maruf, and B. Chowdhury. "Comparison of the ZIP load model and the exponential load model for CVR factor evaluation". In: *2017 IEEE Power & Energy Society General Meeting*. 2017, pp. 1–5. DOI: 10.1109/PESGM.2017.8274490.

[136] W. C. Schoonenberg and A. M. Farid. "A dynamic model for the energy management of microgrid-enabled production systems". In: *Journal of Cleaner Production* 164 (2017), pp. 816–830. DOI: 10.1016/j.jclepro.2017.06.119.

[137] D. Espín-Sarzosa, R. Palma-Behnke, and F. Valencia. "Modeling of Small Productive Processes for the Operation of a Microgrid". In: *Energies* 14.14 (2021). DOI: 10.3390/en14144162.

[138] X. Ma, Q. Zhang, G. Tian, J. Yang, and Z. Zhu. "On Tchebycheff Decomposition Approaches for Multiobjective Evolutionary Optimization". In: *IEEE Transactions on Evolutionary Computation* 22.2 (2018), pp. 226–244. DOI: 10.1109/TEVC.2017.2704118.

[139] D. Molzahn et al. "A Survey of Distributed Optimization and Control Algorithms for Electric Power Systems". In: *IEEE Transactions on Smart Grid* 8.6 (2017), pp. 2941–2962. DOI: 10.1109/TSG.2017.2720471.

[140] M. E. Baran and F. Wu. "Optimal sizing of capacitors placed on a radial distribution system". In: *IEEE Transactions on Power Delivery* 4.1 (1989), pp. 735–743. DOI: 10.1109/61.19266.

[141] M. Farivar and S. Low. "Branch Flow Model: Relaxations and Convexification—Part II". In: *IEEE Transactions on Power Systems* 28.3 (2013), pp. 2565–2572. DOI: 10.1109/TPWRS.2013.2255318.

[142] M. Baran and F. Wu. "Network reconfiguration in distribution systems for loss reduction and load balancing". In: *IEEE Transactions on Power Delivery* 4.2 (1989), pp. 1401–1407. DOI: 10.1109/61.25627.

[143] A. Aleman. *Proof of Implicit Function Theorem*. 2006. URL: https://sites.math.washington.edu/~morrow/334_15/IFT.pdf.

[144] Y. Tang, K. Dvijotham, and S. Low. "Real Time Optimal Power Flow". In: *IEEE Transactions on Smart Grid* 8.6 (2017), pp. 2963–2973. DOI: 10.1109/TSG.2017.2704922.

[145] P. Biswas, P. Suganthan, R. Mallipeddi, et al. "Multi-objective optimal power flow solutions using a constraint handling technique of evolutionary algorithms". In: *Soft Computing* 24 (2020), 2999–3023. DOI: 10.1007/s00500-019-04077-1.

[146] S. University. *Penalty Functions*. URL: https://web.stanford.edu/group/sisl/k12/optimization/MO-unit5-pdfs/5.6penaltyfunctions.pdf.

[147] R. Tibshirani. *Lecture 15: Log Barrier Method*. 2015. URL: https://www.stat.cmu.edu/~ryantibs/convexopt-S15/scribes/15-barr-method-scribed.pdf.

[148] L. Gan. "Distributed Load Control in Multiphase Radial Networks". Dissertation. 2015.

[149] S. University. *Pareto Optimality*. 2015. URL: https://web.stanford.edu/group/sisl/k12/optimization/MO-unit5-pdfs/5.8Pareto.pdf.

[150] K. Miettinen. "Nonlinear multiobjective optimization". In: *Springer Science & Business Media* 12 (2017).

[151] A. Santiago, H. Fraire-Huacuja, B. Dorronsoro, J. Pecero, C. Santillán, J. J. González B., and J. Soto Monterrubio. "A Survey of Decomposition Methods for Multi-objective Optimization". In: vol. 547. Mar. 2014, pp. 453–465. ISBN: 9783319051697. DOI: 10.1007/978-3-319-05170-3_31.

[152] R. Wang, Z. Zhou, H. Ishibuchi, T. Liao, and T. Zhang. "Localized Weighted Sum Method for Many-Objective Optimization". In: *IEEE Transactions on Evolutionary Computation* 22.1 (2018), pp. 3–18. DOI: 10.1109/TEVC.2016.2611642.

[153] J. Weyer, M. Philipp, and F. Adelt. "Agent-Based Modelling of Infrastructure Systems". In: *Metropolitan Research. Methods and Approaches*. Ed. by J. M. Gurr, R. Parr, and D. Hardt. Verlag, 2022, pp. 155–166. ISBN: 978-3-8394-6310-9. DOI: 10.14361/9783839463109-009. URL: https://doi.org/10.14361/9783839463109.

[154] R. D. Zimmerman, C. E. Murillo-Sánchez, and R. J. Thomas. "MATPOWER: Steady-State Operations, Planning, and Analysis Tools for Power Systems Research and Education". In: *IEEE Transactions on Power Systems* 26.1 (2011), pp. 12–19. DOI: 10.1109/TPWRS.2010.2051168.

[155] P. Biswas, R. Mallipeddi, P. Suganthan, and G. Amaratunga. "Optimal reconfiguration and distributed generator allocation in distribution network using an advanced adaptive differential evolution". In: Nov. 2017, pp. 1–7. DOI: 10.1109/SSCI.2017.8280824.

[156] G. Srinivasan and S. Venkat. "Application of AGPSO for Power loss minimization in Radial Distribution Network via DG units, Capacitors and NR". In: *Energy Procedia* 117 (June 2017), pp. 190–200. DOI: 10.1016/j.egypro.2017.05.122.

[157] ENTSO-E. *ENTSO-E Transparency Platform*. URL: https://www.entsoe.eu/data/transparency-platform/.

[158] M. Baran and F. Wu. "Network reconfiguration in distribution systems for loss reduction and load balancing". In: *IEEE Transactions on Power Delivery* 4.2 (1989), pp. 1401–1407. DOI: 10.1109/61.25627.

[159] F. I. for Solar Energy Systems. *Levelized Cost of Electricity Renewable Energy Technologies*. URL: file:///C:/Users/mdebsarm/Downloads/EN2021_Fraunhofer-ISE_LCOE_Renewable_Energy_Technologies.pdf.

[160] Bundesnetzagentur. *Anzulegende Werte für Solaranlagen August bis Oktober 2018*. http://www.bundesnetzagentur.de/SharedDocs/Downloads/. Accessed: 22 Sept. 2021. 2018.

[161] S. Bischof, H. Trittenbach, M. Vollmer, D. Werle, T. Blank, and K. Böhm. "HIPE – an Energy-Status-Data Set from Industrial Production". In: *Proceedings of ACM e-Energy (e-Energy 2018)*. 2018, pp. 599–603. DOI: 10.1145/3208903.3210278.

[162] *EPEX Spot Market Data*. https://www.epexspot.com/. Accessed: 01 Mar. 2021.

[163] *Renewables.ninja*. https://www.renewables.ninja/. Accessed: 11 Nov. 2021.

[164] B. Malika, V. Pattanaik, B. Sahu, et al. "Quasi-oppositional Forensic-Based Investigation for Optimal DG Selection for Power Loss Minimization". In: *Process Integration and Optimization for Sustainability* 7 (2023), pp. 73–106. DOI: 10.1007/s41660-022-00277-9.

[165] O. D. Montoya, E. Rivas-Trujillo, and J. C. Hernández. "A Two-Stage Approach to Locate and Size PV Sources in Distribution Networks for Annual Grid Operative Costs Minimization". In: *Electronics* 11.6 (2022). ISSN: 2079-9292. DOI: 10.3390/electronics11060961. URL: https://www.mdpi.com/2079-9292/11/6/961.

Scientific Publications

[self.1] J. Hiry, C. Kittl, D. S. Sarma, T. Oberließen, and C. Rehtanz. "Multi-voltage level distributed backward–forward sweep power flow algorithm in an agent-based discrete-event simulation framework". In: *Electric Power Systems Research* 213 (2022), p. 108365. ISSN: 0378-7796. DOI: https://doi.org/10.1016/j.epsr.2022.108365. URL: https://www.sciencedirect.com/science/article/pii/S0378779622005326.

[self.2] D. S. Sarma, S. Peter, and C. Rehtanz. "A Distributed Framework for Agent-based Optimal Energy Management of Distribution Systems". In: *2023 IEEE PES Innovative Smart Grid Technologies Europe (ISGT EUROPE)*. 2023, pp. 1–5. DOI: 10.1109/ISGTEUROPE56780.2023.10407568.

[self.3] F. Adelt, M. Barsanti, S. Hoffmann, D. S. Sarma, J. S. Schwarz, B. Vermeulen, T. Warendorf, C. Binder, B. Droste-Franke, S. Lehnhoff, J. Myrzik, C. Rehtanz, and J. Weyer. "Co-simulation of Socio-Technical Energy Systems: An Interdisciplinary Design Process". In: *Advances in Social Simulation*. Ed. by F. Squazzoni. Cham: Springer Nature Switzerland, 2023, pp. 477–488.

[self.4] D. S. Sarma, T. Warendorf, D. Espín-Sarzosa, F. Valencia-Arroyave, C. Rehtanz, J. Myrzik, and R. Palma-Behnke. "Multi-objective energy management for modern distribution power systems considering industrial flexibility mechanisms". In: *Sustainable Energy, Grids and Networks* 32 (2022), p. 100825. ISSN: 2352-4677. DOI: https://doi.org/10.1016/j.segan.2022.100825. URL: https://www.sciencedirect.com/science/article/pii/S2352467722001163.

[self.5] D. S. Sarma, T. Warendorf, J. Myrzik, and C. Rehtanz. "Energy Management using Industrial Flexibility with Multi-objective Distributed Optimization". In: *2021 International Conference on Smart Energy Systems and Technologies (SEST)*. 2021, pp. 1–6. DOI: 10.1109/SEST50973.2021.9543405.

[self.6] M. Barsanti, D. S. Sarma, C. R. Binder, and C. Rehtanz. "Impact of Heat Pump Electrification in Distribution Grids through a Socio-technical Approach". In: *2023 IEEE PES Innovative Smart Grid Technologies Europe (ISGT EUROPE)*. 2023, pp. 1–5. DOI: 10.1109/ISGTEUROPE56780.2023.10407465.

List of Abbreviations

Acronyms

DER Distributed Energy Resources

DG Distributed Generation

PV Photovoltaic

DERMS Distributed Energy Resource Management System

DR Demand Response

DSO Distribution System Operator

EMS Energy Management System

ICT Information and Communication Technologies

API Application Program Interface

MO-DOPF Multi-Objective Distributed Optimal Power Flow

OPF Optimal Power Flow

EM Energy Management

EV Electric Vehicles

EMA Energy Management Agent

GA Grid Agent

TSO Transmission System Operator

MAS Multi-Agent Systems

ABM Agent-Based Modeling

ABS Agent-Based Simulation

SPA System Participant Agent

KPI Key Performance Indicator

BESS Battery Energy Storage System

ZIP Constant Impedance, Current, Power

POC Point of Contact

IFT Implicit Function Theorem

GHG Greenhouse Gas Emissions

BFS Backward-Forward Sweep

MOP Multi-Objective Problem

PF Pareto Front

MV Medium-Voltage

WEC Wind Energy Converter

PDF Probability Density Function

PPF Point Percent Function

PCC Point of Common Contact

LV Low-Voltage

Notations

Chapter 2

N	Total Number of Grid Nodes
E	Total Number of Grid Lines
Y	Admittance Matrix
G	Branch Admittance
B	Branch Conductance
V	Nodal Voltage Magnitude
$\angle\theta$ or θ	Voltage Angle
P	Active Power
Q	Reactive Power
j	$\sqrt{-1}$
v	Squared Nodal Voltage Magnitude
x	State Variables
u	Control Variables
$F(x,u)$	Function of State and Control Variables
$G(x,u)$	Gradient of $F(x,u)$
t	time

Chapter 3

$\vec{i}$	Current Vector
$[Y]$	Nodal Admittance Matrix
.	Multiplication
X	Set of Input Events
Y	Set of Output Events
A	Agent States
S	Basic State
M	Physical Model State
$\delta_{int}, \delta_{ext}$	Change in State
λ	Possible Output Events
$\mathbb{R}$	Set of Real Numbers
P	Active Power Demand
V	Nodal Voltages
$\alpha_1, \alpha_2, \alpha_3$	Time-dependent ZIP Parameters
t	time step

Chapter 4

N^+	Total Number of Grid Nodes including Reference Node
E	Total Number of Grid Lines
$\cup$	Mathematical Union of Sets
N	Total Number of Grid Nodes
$\subseteq$	Mathematical Subset
V	Nodal Complex Voltage
v	Squared Nodal Voltage Magnitude
z	Branch Impedance
r	Branch Resistance
x	Branch Inductance
l	Branch Complex Current
I	Squared Branch Current Magnitude
V_0	Reference Node Voltage Magnitude
s	Apparent Power Injection
p	Active Power Injection
q	Reactive Power Injection

i	$\sqrt{-1}$
S	Apparent Power Flow
p	Active Power Flow
q	Reactive Power Flow
$\mathbb{P}$	Unique path between Nodes
p_0	Reference Node Active Power
q_0	Reference Node Reactive Power
v_0	Reference Node Squared Voltage Magnitude
$\in$	belongs in the set
$\rightarrow$	Direction of Flow
x	Control Variables
u	Dependent Variables
t	Single Time Instant
τ	Time Horizon
$F(x)$	Function of x
L	Objective Function
L_{Costs}	Objective Function for System Costs
a_0, b_0, c_0	Fuel Cost Coefficients
b_m	Market Price
N_{DG}	Nodes with Distributed Generation
$L_{Curtailment}$	Objective Function for Curtailment Costs
a_c, b_c	Curtailment Cost Coefficients
N_{ffg}	Nodes with Fossil Fuel Generation
L_{GHG}	Objective Function for Carbon Emissions
$\alpha_0, \beta_0, \gamma_0, \omega_0, \mu_0$	Carbon Emissions Coefficients
e	Exponential Function
$L_{p_{loss}}$	Objective Function for Active Power Losses
g	Branch Conductance
θ	Voltage Angle
$L_{V_{dev}}$	Objective Function for Voltage Deviation
v_{nom}	Squared Nominal Voltage Magnitude
$\bar{p}, \underline{p}$	Active Power Limits
$\bar{q}, \underline{q}$	Reactive Power Limits
$\bar{v}, \underline{v}$	Nodal Voltage Limits
ln	Logarithmic Function
μ	Penalty Function Coefficient

$L(x,\mu)$	Modified Objective Function
$P_{log}(x)$	Penalty Function
∂	Partial Differentiation
I	Identity Matrix
[.]	Matrix Multiplication
$\hat{P}, \hat{Q}, \hat{v}$	Estimated Values
R	Total Resistance in a Path
X	Total Inductance in a Path
$c_i, d_i, e_i, f_i, g_i, h_i$	BFS Gradient Coefficients
$\mathbb{J}$	Set of Nodes with Current Violations
$\mathbb{I}$	Set of Nodes with Voltage Violations
$\ll$	much smaller
η	Step Size
α, β, ϵ	Distributed OPF Parameters
Δ	Change in Value
$\forall$	for all
p^{new}, q^{new}	Intermediate Control Signals
p^*, q^*	Optimal Control Signals
R_M	Objective Space
Ω	Decision Vector Space
x^*	Pareto Optimal Point
N	Population Size for the MOP
C	Mathematical Combination
H	Weight Resolution
λ	Weight Vector
z^*	Minimum Value for Objective Function
€	European Currency Symbol

Chapter 5

p_0	Active Power for Reference Node
p_i	Active Power for Generator Node
a_0, b_0	Fuel Cost Coefficients
b_i	Renewable Cost Coefficient
v_i	Squared Nodal Voltage Magnitude
ln	Logarithmic Function

μ	Penalty Coefficient
α, β, ϵ	Distributed OPF Parameters
hr	hour
s	seconds
E_{bat}^{nom}	Optimum BESS Capacity
$P_{peak_{shave}}$	Peak Shaving Limit

Indices

i, j, k	Denoting Variables
i, j, k	Counting Variables
n	Last Element of a Set

List of Figures

List of Tables

Appendix

Step-by-Step Gradient Computation

For Carbon Emissions

The objective function for carbon emissions is given by:

$$L_{GHG}(x) = \alpha_0 p_0(x)^2 + \beta_0 p_0(x) + \gamma_0 + \omega_0 e^{\mu_0 p_0(x)}$$

The following steps compute the derivative of the objective function w.r.t. the control variables:

- w.r.t. real power injections, p_i

$$\begin{aligned}\frac{\partial L_{GHG}(x)}{\partial p_i} &= 2\alpha_0 p_0 \frac{\partial p_0}{\partial p_i} + \beta_0 \frac{\partial p_0}{\partial p_i} + \gamma_0 + \omega_0 e^{\mu_0 p_0} \frac{\partial p_0}{\partial p_i} \\ &= \left(2\alpha_0 p_0 + \beta_0 + \omega_0 e^{\mu_0 p_0}\right) \frac{\partial p_0}{\partial p_i}\end{aligned}$$

- w.r.t. reactive power injections, q_i

$$\begin{aligned}\frac{\partial L_{GHG}(x)}{\partial q_i} &= 2\alpha_0 p_0 \frac{\partial p_0}{\partial q_i} + \beta_0 \frac{\partial p_0}{\partial q_i} + \gamma_0 + \omega_0 e^{\mu_0 p_0} \frac{\partial p_0}{\partial q_i} \\ &= \left(2\alpha_0 p_0 + \beta_0 + \omega_0 e^{\mu_0 p_0}\right) \frac{\partial p_0}{\partial q_i}\end{aligned}$$

where the derivative of $\gamma_0 = 0$ because it is a constant.

For Active Power Losses

The objective function for active power losses is given by:

$$L_{p_{loss}}(x) = \sum_{i \in E} g_{ij} \left[v_i(x)^2 + v_j(x)^2 - 2 v_i(x) v_j(x) \cos\theta_{ij}(x) \right]$$

The derivative of the trigonometric term is of special importance. Let,

$$\omega = \cos\theta_{ij}(x) = \cos\theta_i(x)\cos\theta_j(x) - \sin\theta_i(x)\sin\theta_i(x)$$

Therefore:

$$\frac{\partial\omega}{\partial x_i} = \cos\theta_j(x)\left[-\sin\theta_i(x)\frac{\partial\theta_i}{\partial x_i}\right] + \cos\theta_i(x)\left[-\sin\theta_j(x)\frac{\partial\theta_j}{\partial x_i}\right] - \sin\theta_j(x)\left[-\cos\theta_i(x)\frac{\partial\theta_i}{\partial x_i}\right] - \sin\theta_i(x)\left[-\cos\theta_j(x)\frac{\partial\theta_j}{\partial x_i}\right]$$

Expanding the equation:

$$= \left[\cos\theta_j(x)\sin\theta_i(x) - \sin\theta_j(x)\cos\theta_i(x)\right]\frac{\partial\theta_i}{\partial x_i} - \left[\cos\theta_i(x)\sin\theta_j(x) - \sin\theta_i(x)\cos\theta_j(x)\right]\frac{\partial\theta_j}{\partial x_i}$$

$$= \sin\theta_{ij}(x)\frac{\partial\theta_j}{\partial x_i} - \sin\theta_{ij}(x)\frac{\partial\theta_i}{\partial x_i}$$

$$= \sin\theta_{ij}\left(\frac{\partial\theta_j}{\partial x_i} - \frac{\partial\theta_i}{\partial x_i}\right)$$

Finally, the derivative of the objective function results in:

- w.r.t. real power injections, p_i

$$\frac{\partial L_{p_{loss}}(x)}{\partial p_i} = g_{ij}\left(2v_i\frac{\partial v_i}{\partial p_i} + 2v_j\frac{\partial v_j}{\partial p_i} - 2v_j\omega\frac{\partial v_i}{\partial p_i} - 2v_i\omega\frac{\partial v_j}{\partial p_i} - 2v_iv_j\frac{\partial\omega}{\partial p_i}\right)$$

- w.r.t. reactive power injections, q_i

$$\frac{\partial L_{p_{loss}}(x)}{\partial q_i} = g_{ij}\left(2v_i\frac{\partial v_i}{\partial q_i} + 2v_j\frac{\partial v_j}{\partial q_i} - 2v_j\omega\frac{\partial v_i}{\partial q_i} - 2v_i\omega\frac{\partial v_j}{\partial q_i} - 2v_iv_j\frac{\partial\omega}{\partial q_i}\right)$$

For Total Voltage Deviation

The objective function for the total voltage deviation is given by:

$$L_{V_{dev}}(x) = \sum_{i=1}^{N} |v_i(x) - v_{nom}(x)|$$

The derivative is:

- w.r.t. real power injections, p_i

$$\frac{\partial L_{V_{dev}}(x)}{\partial p_i} = \frac{\partial v_i}{\partial p_i} - \frac{\partial v_{nom}}{\partial p_i}$$

$$\frac{\partial L_{V_{dev}}(x)}{\partial p_i} = \frac{\partial v_i}{\partial p_i}$$

- w.r.t. reactive power injections, q_i

$$\frac{\partial L_{V_{dev}}(x)}{\partial q_i} = \frac{\partial v_i}{\partial q_i} - \frac{\partial v_{nom}}{\partial q_i}$$

$$\frac{\partial L_{V_{dev}}(x)}{\partial q_i} = \frac{\partial v_i}{\partial q_i}$$

where the derivative of $v_{nom} = 0$ because the nominal voltage is a constant.